

**Synthesis, Characterization and Optical Properties of
a Bay-Substituted Perylene Dye: N,N'-Didodecyl-1,7-
di(2-Decyl-1-tetradecanoyl)- perylene-3,4:9,10-
tetracarboxylic Acid Bisimide**

Karar Tawfeeq Jawad Shukur

Submitted to the
Institute of Graduate Studies and Research
in partial fulfillment of the requirements for the Degree of

Master of Science
in
Chemistry

Eastern Mediterranean University
February 2014
Gazimağusa, North Cyprus

Approval of the Institute of Graduate Studies and Research

Prof. Dr. Elvan Yılmaz
Director

I certify that this thesis satisfies the requirements as a thesis for the degree of Master of Science in Chemistry.

Prof. Dr. Mustafa Halilsoy
Chair, Department of Chemistry

We certify that we have read this thesis and that in our opinion it is fully adequate in scope and quality as a thesis for the degree of Master of Science in Chemistry

Prof. Dr. Huriye İcil
Supervisor

Examining Committee

1. Prof. Dr. Huriye İcil

2. Asst. Prof. Dr. Mustafa E. Özser

3. Asst. Prof. Dr. Nur P. Aydınlık

ABSTRACT

Functionalization of perylene chromophore to result in a wide variety of perylene derivatives is a renowned strategy. Functionalization can be achieved by the substitution of corresponding groups at bay and imide positions of the conjugated aromatic perylene chromophore.

In the current work, we have synthesized a new bay-substituted perylene diimide in three steps. We have selected the long aliphatic and branched aliphatic chains to substitute at imide and bay- positions, respectively, to promote the solubility as well as the electrical and optical characteristics. In the first step the raw compound perylene dianhydride was brominated at 1,7-positions of the perylene chromophore to result in brominated dianhydride (BrPDA). Subsequently, BrPDA was imidized at the imide positions of BrPDA with dodecyl amine to yield brominated perylene diimide (BrPDI). In the final step, the designed bay-substituted perylene diimide (PDI-Decanol) was synthesized upon substituting 2-decyl-1-tetradecanol at the bay positions of perylene core. The final compound was purified and the resulting PDI-Decanol was characterized by FTIR, UV-vis and fluorescence measurements. A detailed comparison on optical properties was made especially by studying the photophysics of the intermediate products along with the PDI-Decanol.

The UV-vis absorption spectra of the three synthesized perylene derivatives in nonpolar aprotic solvents show regular characteristic π - π^* absorption bands. Contrarily, absorption in dipolar aprotic solvents shows weak additional absorption bands (BrPDA in NMP; BrPDI in DMF; and PDI-Decanol in DMF and NMP; and

methanol) at higher wavelengths which were remained after microfiltering the solution.

Interestingly, the emission spectra of the three perylene derivatives have shown traditional three characteristic emission peaks and were not influenced by additional weak absorption bands.

Keywords: Perylene, bay-substitution, brominated dianhydride, brominated diimide, aliphatic substituent.

ÖZ

Perilen boyaları fonksiyonelleştirilerek çok çeşitli perilen türevlerinin elde edilmesi, bilinen bir stratejidir. Fonksiyonelleşme konjüge aromatik perilen boyalarının körfez ve imid pozisyonlarına ilgili grupların süstitüe edilmesi ile elde gerçekleşir.

Bu çalışmada, üç basamaklı sentez yöntemiyle körfez pozisyonunda süstitüe yeni bir perilen diimid sentezlenmiştir. Çözünürlük yanında elektrik ve optik özellikleri geliştirmek amacı ile uzun alifatik ve dallı alifatik zincir süstitüentler seçilerek sırası ile imid ve körfez pozisyonlarına bağlanmıştır. Birinci adımda, başlangıç maddesi olan perilen dianhidrit, bromlu dianhidrit (BrPDA) elde edebilmek için perilen yapısının 1,7-pozisyonlarında brominleştirildi. Daha sonra, BrPDA dodesil amin ile imid pozisyonunda imidize edilerek bromlu perilen diimid (BrPDI) elde edildi. Son aşamada ise tasarlanan diimid (PDI-Dekanol) perilen yapısının körfez pozisyonuna 2-desil-1-tetradekanol bağlanması ile sentezlendi. Sentezlenen bileşik saflandırılmış ve elde edilen PDI-Dekanol FTIR, UV-vis ve floresans ölçümleri ile karakterize edilmiştir. Özellikle ara ürünler ile PDI-Dekanol'un fotofiziksel özellikleri incelenerek optik özellikleri üzerinde ayrıntılı bir karşılaştırma yapılmıştır.

Sentezlenen üç perilen türevinin apolar aprotik çözücülerdeki UV-vis absorpsiyon spektrumları normal karakteristik $\pi-\pi^*$ absorpsiyon bantları göstermiştir. Buna karşılık, dipolar aprotik çözücülerde solüsyonlar mikrofilterden geçirildikten sonra dahi uzun dalga boylarında ek zayıf absorpsiyon bantları göstermiştir (BrPDA NMP'de; BrPDI DMF'te; ve PDI-Dekanol DMF, NMP ile metanol'da).

İlginç olarak, üç perilen türevlerinin emisyon spektrumları ek zayıf absorpsiyon bandlarından etkilenmeden geleneksel üç karakteristik emisyon pikleri göstermiştir.

Anahtar kelimeler: Perilen, körfez pozisyonu, bromlu dianhidrit, bromlu diimid, alifatik sübstütie.

To My Supervisor

ACKNOWLEDGMENTS

I would like to express my special appreciation and thanks to my supervisor Professor Dr. Huriye Icil, you have been a tremendous mentor for me. I would like to thank you for encouraging my research and for allowing me to grow as a research scientist. Your advice on both research as well as on my career have been priceless. I also want to thank my committee members for letting my defense be an enjoyable moment, and for your brilliant comments and suggestions, thanks to you. I would especially like to thank the organic group members for everything they gave me. I would like to thank Dr. Duygu Uzun which also helped me in doing a lot of Research and I came to know about so many new things I am really thankful. I am giving a special thanks to the brother that I had here, He never stop advised me through my work even if he is far away from me so thanks a lot Dr. Jagadeesh Babu Bodapati. Special thanks to my lab partner who help me to assemble the parts and gave suggestion about the thesis, thanks a lot Basma Alkhateeb. I would like to offer my special thanks to Melika Mostafanejad who helped me a lot in finalizing this project within the limited time frame.

A special thanks to my family. Words cannot express how grateful I am to my mother, my father, my brothers (Ziyad, Awse) and my lovely sister (Esraa). Special thanks for all of the sacrifices that you've made on my behalf. Your prayer for me was what sustained me thus far. I would also like to thank all of my friends who supported me in writing, and incented me to strive towards my goal.

TABLE OF CONTENTS

ABSTRACT.....	iii
ÖZ	v
ACKNOWLEDGMENTS	viii
LIST OF FIGURES	xi
LIST OF TABLES	xvi
LIST OF SYMBOLS/ABBREVIATIONS	xviii
1 INTRODUCTION.....	1
2 THEORETICAL	10
2.1 Properties of Perylene Diimides Dyes.....	10
2.1.1 Optical Characteristics of Perylene Diimide Dyes	11
2.1.2 Perylene Diimide Dyes; Bay-Substituted Derivatives.....	12
2.1.3 Electron Acceptor Properties of Perylene Diimide Dyes for Photovoltaic application.....	13
2.1.4 Perylene Diimide Dyes; Conversion Efficiency of Solar Energy into Electrical Energy.....	14
2.2 The Future and Commercialization of Dye Sensitized Solar Cells.....	15
3 EXPERIMENTAL	16
3.1 Materials	16
3.2 Instruments	17
3.3 Methods of Synthesis	17
3.4 Synthesis of Brominated Perylene Bisanhydride (BrPDA)	18
3.5 Synthesis of N, N' -Didodecyl-1, 7-dibromoperylene-3, 4, 9, 10- tetracarboxylic Acid Bisimide (BrPDI).....	18

3.6	Synthesis of N,N'-Didodecyl-1,7-di(2-Decyl-1-tetradecanoyl)- perylene-3,4:9,10-tetracarboxylic acid bisimide (PDI-Decanol)	19
3.7	General reaction mechanism of Perylene Dyes.....	19
4	DATA AND CALCULATIONS.....	22
4.1	Calculations of Maximum Extinction Co-efficient (ϵ_{\max})	22
4.2	Calculations of Half-width of the selected Absorption ($\Delta\nu^{1/2}$)	26
4.3	Calculations of Theoretical Radiative Lifetimes (τ_0)	28
4.4	Calculations of Fluorescence Rate Constant (k_f)	30
4.5	Calculations of oscillator strength (f)	31
4.7	Calculations of Optical Band Gap Energies.....	34
5	RESULTS AND DISCUSSION	65
5.1	Synthesis of the Designed Bay-substituted Perylene Dye Derivatives	65
5.2	Solubility of the Designed Bay-substituted Perylene Dye Derivatives.....	67
5.3	Analysis of FTIR Spectra	69
5.4	Interpretation of UV-vis Spectra	70
5.5	Interpretation of Emission Spectra	74
6	CONCLUSION	77
	REFERENCES.....	79

LIST OF FIGURES

Figure 1-1: The chemical structures for PTCDA (from left) and perylene diimides without bay- positions.	1
Figure1-2: Structures of 1,7 Dibromoperylene-3,4,9,10-tetra carboxylic dianhydride	5
Figure1-3: N,N' -Didodecy 1-1, 7-dibromoperylene-3, 4, 9, 10-tetracarboxylic acid bisimide.....	6
Figure1-4: N,N-Didodecy 1-1, 7-di (2-Decyl-1-tetradecanoyl) -perylene -3, 4:9,10-tetracarboxylic acid bisimide (BDPDI).....	7
Figure1-5: N,N' -Didodecy 1-1, 7-di (2-Decyl-1-tetradecanoyl) -perylene-3, 4: 9,10-tetracarboxylic acid bisimide (BDPDI) in 2 dimensions.....	8
Figure1-6: N,N' -Didodecy 1-1, 7-di (2-Decyl-1-tetradecanoyl)-perylene-3, 4:9, 10-tetracarboxylic acid bisimide (BDPDI) in 3 dimensions.....	9
Figure2-1: Photoinduced charge transfer between donor and acceptor of Perylene diimide in creating D^+ - PDI: (A) Electron transfer from excited donor to Perylene diimide; (B) Electron transfer from donor to excited PDI. (Blue balls refer to denote electrons).	14
Figure4-1: Absorption spectrum of PDI-Decanol in chloroform at $1 \times 10^{-5} M$ Concentration	23
Figure4-2: Absorption spectrum of PDI-Decanol in chloroform and half-width.	26
Figure4-3: Absorption spectrum of PDI-Decanol and the cut-off wavelength.....	35
Figure 4-4: FTIR spectrum of BrPDA	2
Figure 4-5: FTIR spectrum of BrPDI.....	3
Figure 4-6: FTIR Spectrum of PDI-Decanol	4
Figure 4-7: UV-vis absorption spectrum of BrPDA in DMF	5

Figure 4-8: UV-vis absorption spectrum of BrPDA in DMF after micro filtration.....	6
Figure 4-9: UV-vis absorption spectrum of BrPDA in NMP	7
Figure 4-10: UV-vis absorption spectrum of BrPDA in NMP after micro filtration...	8
Figure 4-11: Overlap UV-vis absorption of BrPDA in DMF, in DMF after Micro filtration	9
Figure 4-12: Overlap of UV-vis absorption of BrPDA in NMP, NMP after M.F	10
Figure 4-13: Overlap of UV-vis absorption of BrPDA in DMF, NMP	11
Figure 4-14: UV-vis absorption spectrum of BrPDI in DMF	12
Figure 4-15: UV-vis absorption spectrum of BrPDI in DMF after M.F.....	13
Figure 4-16: UV-vis absorption spectrum of BrPDI in NMP	14
Figure 4-17: UV-vis absorption spectrum of BrPDI in CHL.....	15
Figure 4-18: UV-vis absorption spectrum of BrPDI in DMF and DMF after micro filtration	16
Figure 4-19: UV-vis absorption spectrum of BrPDI in DMF, NMP and CHL.....	17
Figure 4-20: UV-vis absorption spectrum of PDI-Decanol in DMF	18
Figure 4-21: UV-vis absorption spectrum of PDI-Decanol in NMP	19
Figure 4-22: UV-vis absorption spectrum of PDI-Decanol in NMP after micro filtration	20
Figure 4-23: UV-vis absorption spectrum of PDI-Decanol in NMP after micro filtration	21
Figure 4-24: UV-vis absorption spectrum of PDI-Decanol in DMF after Micro Filtration	22
Figure 4-25: UV-vis absorption spectrum overlap of PDI-Decanol in DMF/DMF after Micro Filtration	23

Figure 4-26: UV-vis absorption spectrum overlap of PDI-Decanol in NMP/NMP after Micro Filtration	24
Figure 4-27: UV-vis absorption spectrum of PDI-Decanol in CHL	25
Figure 4-28: UV-vis absorption spectrum of PDI-Decanol in EtOH.....	26
Figure 4-29: UV-vis absorption spectrum of PDI-Decanol in EtOH after Micro filtration	27
Figure 4-30: UV-vis absorption spectrum overlap of PDI-Decanol in EtOH/EtOH after Micro Filtration	28
Figure 4-31: UV-Visible absorption spectrum of PDI-Decanol in Acetone.....	29
Figure 4-32: UV-Visible absorption spectrum of PDI-Decanol in Acetone after Micro Filtration	30
Figure 4-33: UV-Visible absorption spectrum of PDI-Decanol in DMF, NMP, CHL, EtOH AND Acetone	31
Figure 4-34: UV-Visible absorption spectrum of PDI-Decanol, BrPDI and BrPDA in DMF.....	32
Figure 4-35: UV-Visible absorption spectrum of PDI-Decanol, BrPDI and BrPDA in NMP.....	33
Figure 4-36: UV-Visible absorption spectrum of PDI-Decanol, BrPDI in CHL.....	34
Figure 4-37: Emission spectrum ($\lambda_{exc}=485nm$) of BrPDA in DMF.....	35
Figure 4-38: Emission spectrum ($\lambda_{exc}=485nm$) of BrPDA in DMF after micro filtration	36
Figure 4-39: Emission spectrum ($\lambda_{exc}=485nm$) of BrPDA in DMF and in DMF after micro filtration	37
Figure 4-40: Emission spectrum ($\lambda_{exc}=485nm$) of BrPDA in NMP.....	38

Figure 4-41: Emission spectrum ($\lambda_{exc}=485nm$) of BrPDA in NMP after micro filtration	39
Figure 4-42: Emission spectrum ($\lambda_{exc}=485nm$) of BrPDA in NMP and in NMP after micro filtration	40
Figure 4-43: Emission spectrum ($\lambda_{exc}=485nm$) of BrPDA in NMP and in DMF	41
Figure 4-44: Emission spectrum ($\lambda_{exc}=485nm$) of BrPDI in DMF	42
Figure 4-45: Emission spectrum ($\lambda_{exc}=485nm$) of BrPDI in DMF after micro-filtratio	43
Figure 4-46: Emission spectrum ($\lambda_{exc}=485nm$) of BrPDI in DMF and in DMF after micro filtration.....	44
Figure 4-47: Emission spectrum ($\lambda_{exc}=485nm$) of BrPDI in NMP	45
Figure 4-48: Emission spectrum ($\lambda_{exc}=485nm$) of BrPDI in CHL.....	46
Figure 4-49: Emission spectrum ($\lambda_{exc}=485nm$) of BrPDI in DMF, NMP and CHL	47
Figure 4-50: Emission spectrum ($\lambda_{exc}=485nm$) of PDI-Decanol in DMF.....	48
Figure 4-51: Emission spectrum ($\lambda_{exc}=485nm$) of PDI-Decanol in DMF after Micro Filtration.....	49
Figure 4-52: Emission spectrum ($\lambda_{exc}=485nm$) of overlap of PDI-Decanol in DMF/DMF Micro Filtration.....	50
Figure 4-53: Emission spectrum ($\lambda_{exc}=485nm$) of PDI-Decanol in NMP.....	51
Figure 4-54: Emission spectrum ($\lambda_{exc}=485nm$) of PDI-Decanol in NMP after Micro Filtration.....	52
Figure 4-55: Emission spectrum ($\lambda_{exc}=485nm$) of PDI-Decanol overlap in NMP/NMP after Micro Filtration.....	53
Figure 4-56: Emission spectrum ($\lambda_{exc}=485nm$) of PDI-Decanol in CHL	54
Figure 4-57: Emission spectrum ($\lambda_{exc}=485nm$) of PDI-Decanol in EtOH.....	55

Figure 4-58: Emission spectrum ($\lambda_{exc}=485nm$) of PDI- Decanol in EtOH after Micro Filtration	56
Figure 4-59: Emission spectrum ($\lambda_{exc}=485nm$) of overlap of PDI-Decanol in EtOH/EtOH after Micro Filtration	57
Figure 4-60: Emission spectrum ($\lambda_{exc}=485nm$) of PDI-Decanol in Acetone.....	58
Figure 4-61: Emission spectrum ($\lambda_{exc}=485nm$) of PDI-Decanol in Acetone after Micro Filtration	59
Figure 4-62: Emission spectrum ($\lambda_{exc}=485nm$) of PDI-Decanol overlap in Acetone/Acetone after Micro Filtration	60
Figure 4-63: Emission spectrum ($\lambda_{exc}=485nm$) of PDI-Decanol in DMF, NMP, CHL, EtOH and Acetone.....	61
Figure 4-64: Emission spectrum ($\lambda_{exc}=485nm$) overlap of Br-PDI, Br-PDA and PDI-Decanol in DMF	62
Figure 4-65: Emission spectrum ($\lambda_{exc}=485nm$) overlap of Br-PDI, Br-PDA and PDI-Decanol in NMP	63
Figure 4-66: Emission spectrum ($\lambda_{exc}=485nm$) overlap of Br-PDI and PDI-Decanol in CHL	64

LIST OF TABLES

Table 4-1: Molar absorptivity data of BrPDA, BrPDI and PDI-Decanol in CHL.....	24
Table 4-2: Molar absorptivity data of BrPDA, BrPDI and PDI-Decanol in DMF	24
Table 4-3: Molar absorptivity data of BrPDA, BrPDI and PDI-Decanol in NMP	24
Table 4-4: Molar absorptivity data of BrPDA, BrPDI and PDI-Decanol in EtOH.....	25
Table 4-5: Molar absorptivity data of BrPDA, BrPDI and PDI-Decanol in Acetone.....	25
Table 4-6: Half width of the selected absorptions of PDI-Decanol and measured in different solvents	27
Table 4-7: Half width of the selected absorptions of BrPDI and measured in different solvents	28
Table 4-8: Half width of the selected absorptions of BrPDA and measured in different solvents	28
Table 4-9: Theoretical radiative lifetimes of PDI-Decanol measured in different solvents.....	29
Table 4-10: Theoretical radiative lifetimes of BrPDI measured in different solvents	30
Table 4-11: Theoretical radiative lifetimes of BrPDA measured in different solvents ...	30
Table 4-12: Fluorescence rate constants data of PDI-Decanol in different solvents	31
Table 4-13: Fluorescence rate constants data of BrPDI in different solvents.....	31
Table 4-14: Fluorescence rate constants data of BrPDA in different solvents	31
Table 4-15: Oscillator strength data of PDI-Decanol measured in different solvents	32
Table 4-16: Oscillator strength data of BrPDI measured in different solvents.....	32
Table 4-17: Oscillator strength data of BrPDA measured in different solvents	32
Table 4-18: Singlet Energies data of PDI-Decanol in Different Solvents	33
Table 4-19: Singlet Energies Data of BrPDI in Different Solvents.....	33

Table 4-20: Singlet Energies Data of BrPDA in Different Solvents	33
Table 4-21: Band Gap Energies of PDI-Decanol were calculated in Different Solvents.....	35
Table 4-22: Band Gap Energies of BrPDI were calculated in Different Solvents.....	36
Table 4-23: Band Gap Energies of BrPDA were Calculated in Different Solvents	36
Table 5-1: Solubility of the synthesized Perylene derivatives	68

LIST OF SYMBOLS/ABBREVIATIONS

\AA	Armstrong
Cm	Centimeter
$^{\circ}\text{C}$	Degrees Celsius
$\Delta\nu_{1/2}$	Half-width of the selected absorption
ϵ_{max}	Maximum extinction coefficient
E_s	Singlet energy
F	Oscillator strength
λ_{exc}	Excitation wavelength
λ_{max}	Absorption wavelength maximum
Δ	Chemical shift (ppm)
τ_0	Theoretical radiative lifetime
τ_f	Fluorescence lifetime
Φ_f	Fluorescence quantum yield
Nm	Nanometer
A.nitrile	Acetonitrile
CDCl_3	Deutero-Chloroform
CF_3COOD	Deutero-Trifloroaceticacid

CH ₂ Cl ₂	Dichloromethane
CHCl ₃	Chloroform
CHL	Chloroform
CH ₃ CN	Acetonitrile
CV	Cyclic Voltammetry
DMF	N,N'-dimethylformamide
DMSO	N,N'-dimethyl sulfoxide
DNA	Deoxyribonucleic acid
DSC	Differential Scanning Calorimetry
Et.Acetate	Ethylacetate
EtOH	Ethanol
FT-IR	Fourier Transform Infrared Spectroscopy
HCl	Hydrochloric acid
KBr	Potassium bromide
K _d	Rate constant of Radiationless deactivation
K _f	Theoretical fluorescence rate constant
KOH	Potassium hydroxide
M	molar concentration

MeOH	Methanol
NaOH	Sodium hydroxide
NMR	Nuclear Magnetic Resonance Spectroscopy
RNA	Ribonucleic acid
TGA	Thermo gravimetric Analysis
UV-vis	Ultraviolet visible absorption spectroscopy

Chapter 1

INTRODUCTION

Perylene Diimides are colorant materials which are widely studied as industrial dyes and pigments. PDIs mostly regarded as the main compound of this kind of dyes has been studied around 1912[1]. Figure 1.1 demonstrates different Perylene Diimide dyes with various physical and chemical features can be gained by change of the substituents on the position of the imide (R groups) or bay (1,6,7,12 on the central aromatic support) positions.

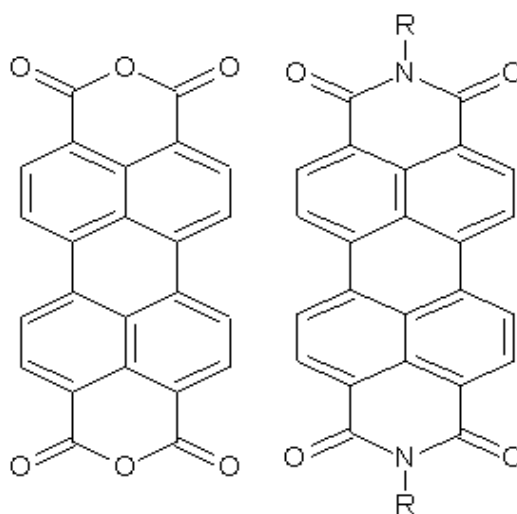


Figure 1-1: The chemical structures for PTCDA (from left) and perylene diimides without bay- positions.

Perylene diimides (PDIs) are optoelectronic pigments that are mostly encouraging materials for applications in organic solar cells, photovoltaic instruments and for dye lasers as molecular semiconductor. PDI products have great fluorescence quantum

yields of photoluminescence, high absorption and emission, positive semiconductor [2,3].

High degree of photochemical and thermal stability, and absorptivity with highly molar. That makes them model for many organic optoelectronic or electronic products such as solar cells and light emitting diodes. PDI molecules are extremely significant in photoelectronic devices. PDIs are defined as n-type semiconductors that are the main charge transports through conduction band when most of the materials' organic conducting could be defined as p-type semiconductors [4]. PDIs display two changeable electrochemical reductions. It gives steady anions and di-anions. This characteristic of PDIs creates them gravitate materials in chemiluminescence electrochromic tools. The study of Perylene diimides began with study of Kardos in 1913 [5,6]. These compounds observed their application in tank dyes and several products are still formed now a day for red dyes. Perylene diimides characterized by relatively short reduction potential, that can be used as n-type semiconductors and an electron acceptor in photoinduced charge transfer reactions [7,8]. The economic part of assessment, the practice of Perylene diimide established dyes in these one-use articles is a bit restricted, in line for to the moderately big price of tools by means of dyes [9,10]. Now a day, Perylene diimides are established dyes observed especially in fiber uses or in additional high-quality manufacturing dyes, the price of them is overbalance by great type and resistance of the colors, especially in carpeting fibers and vehicle industry [11,12]. Perylene diimide dyes, in general, are bright florescent compounds with high fluorescence quantum yields near to unity. The fluorophores like Perylene bisimide derivatives offer excellent photostability and emit green to red colors. It depends mainly on the bay-/core- substituents attached at the respective bay areas of Perylene chromphore [13]. Derivatization at 1, 6, 7, 12

positions by a suitable substituent will greatly alter the optoelectronic properties. The properties such as electron transporting ability and n-type semiconducting property are also rely on various conformational transitions and non-covalent interactions such as self-assembly, π - π staking interactions [14].

Photovoltaic is an appealing technology to create the environmental clean energy from the common renewable reference which is the sun. Surrounded by photovoltaic technologies, dye sensitized solar cells (DSSCs) be an appealing one and that cause theoretically little price [15]. Organic electronic compounds are motivating for working in solar cells for next years. Even though product for single layer organic compounds has been undesirable, great photocurrent quantum proficiencies can be succeeded in complex structures with electron donating and electron accepting ingredients [16]. The core features OPV hold by the comparing with further kinds of PV are less weight, appealing system factor, scalability, elasticity and cheap fabrication. Though, as OPV still giving little efficiency proportions and little lifetimes, the rated market entrance of OPV-based uses have been seen in the mobile off-network uses. The organic photovoltaic components are conjugated solids wherever both optical absorption and charge transfer are controlled by π and π^* orbitals. Organic materials are appealing to the photovoltaic in order to the probability of great productivity by spray deposition [17].

Electrical energy storage systems are advanced [18], and solar cells are one of the important safety energy applications and that is because no carbon dioxide will produce and will not cause global warming [19,20]. Even though, silicon solar cells have a great conversion efficiency and big lifetime, the production of silicon solar cells are complex with high cost. Energy and fuel squeeze is the main attention

worldwide. Fossil fuels are confronting quick resource exhaustion; on the other hand, the request for energy is developing every day and most of the countries around the world have no alternative but to raise local oil procedure [21]. As a result there is a critical necessity of permanent energy resources like solar energy. Solar energy well-thought-out as an environmentally friend, super alternative and promising nominate to solve this problem [22]. Nevertheless, solar energy has an incomplete application that in a direct way refer to its great cost of per watt electricity generated. In these days, technology of solar cells established on crystalline silicon is facing difficulties of silicon based raw resources. Thus, little cost replacements and then new types of little cost solar cells in an urgent case. Dye compounds are the basic unit of DSSC to get a big amount of the efficiency over their abilities to absorb solar energy [22].

The aim of this thesis is to develop a novel bay-substituted perylene diimide namely N,N'-Didodecyl-1,7-di(2-Decyl-1-tetradecanoyl)- perylene-3,4:9,10-tetracarboxylic acid bisimide (BDPDI). The main product was obtained from Perylene-3,4,9,10-tetracarboxylic dianhydride (PTCDA) in a three-step synthesis according to the route shown in Scheme (1-2). In the first reaction step, 1,7-dibromo perylene tetracarboxylic anhydride was prepared by the bromination of Perylene-3,4,9,10-tetracarboxylic dianhydride. N,N'-Didodecyl-1,7-dibromoperylene-3,4,9,10-tetracarboxylic Acid bisimide was formed via imidization reaction mechanism in the second step. Finally, N,N'-Didodecyl-1,7-dibromoperylene-3,4,9,10-tetracarboxylic Acid bisimide was reacted with 2-Decyl-1-tetradecanol to produce N,N'-Didodecyl-1,7-di(2-Decyl-1-tetradecanoyl)- perylene-3,4:9,10-tetracarboxylic acid bisimide (BDPDI) by the nucleophilic substitution of both bromine atoms as shown in Scheme (1-4). All three products were purified and characterized by spectroscopic

techniques. The photophysical and photochemical properties of these compounds have been investigated and discussed in detail.

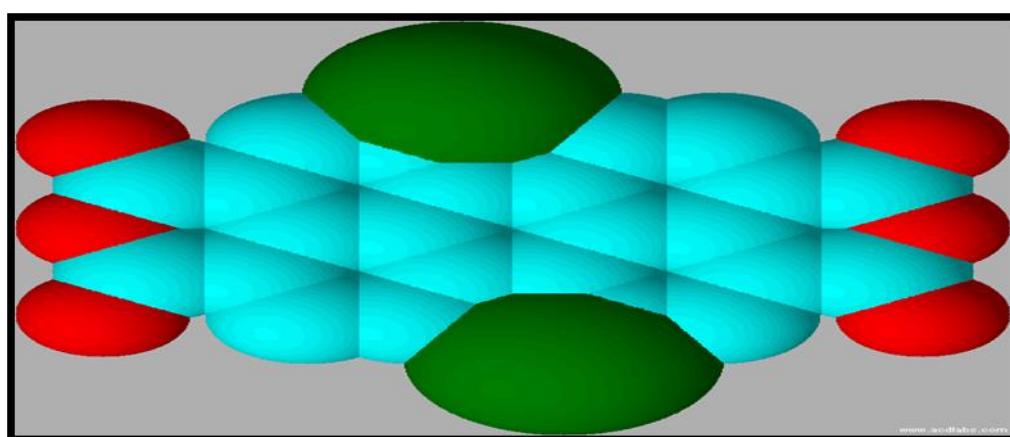
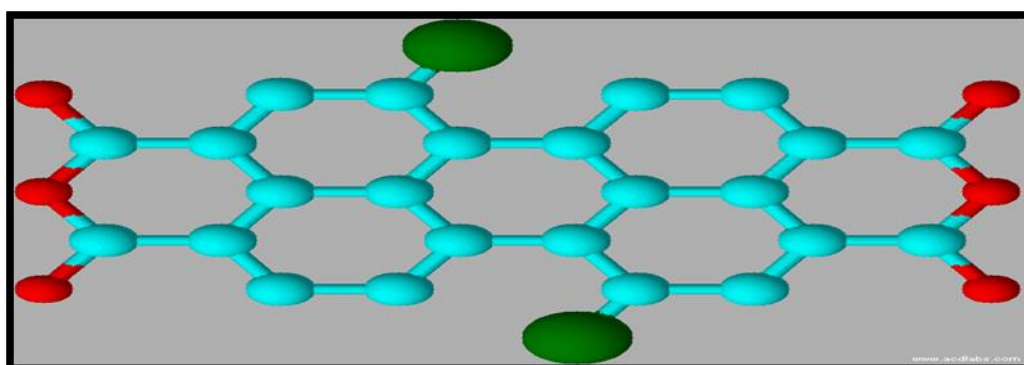
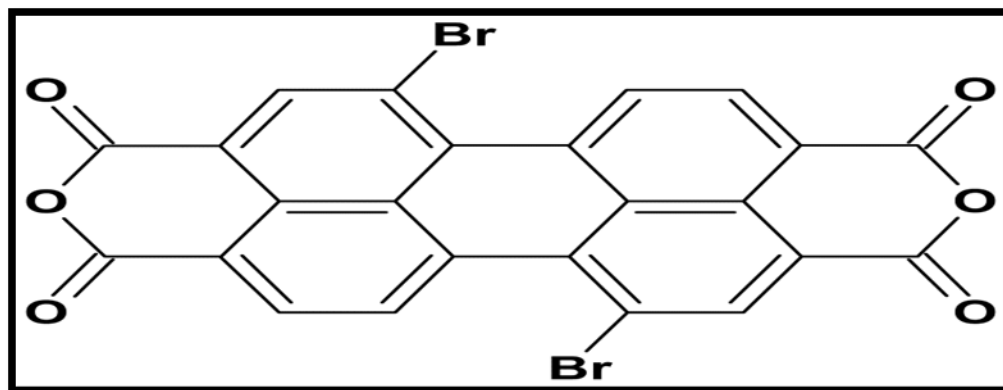


Figure1-2: Structures of 1,7 Dibromoperylene-3,4,9,10-tetra carboxylic dianhydride

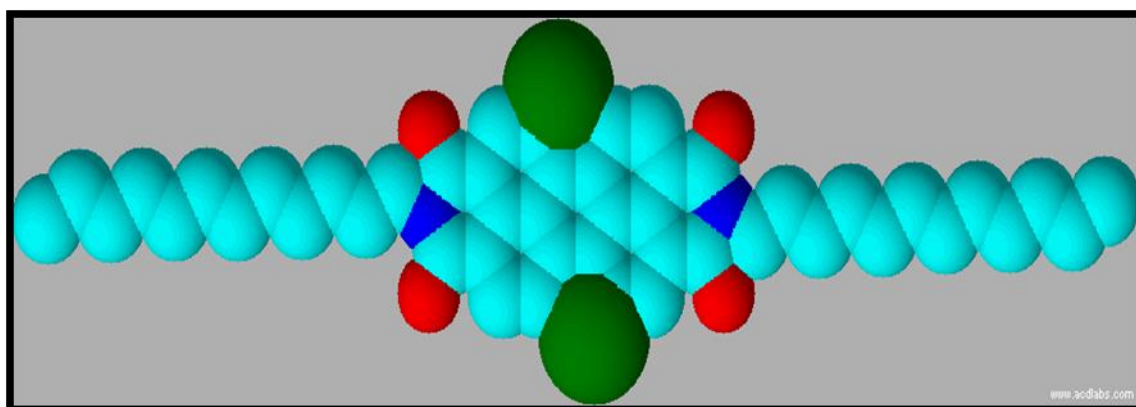
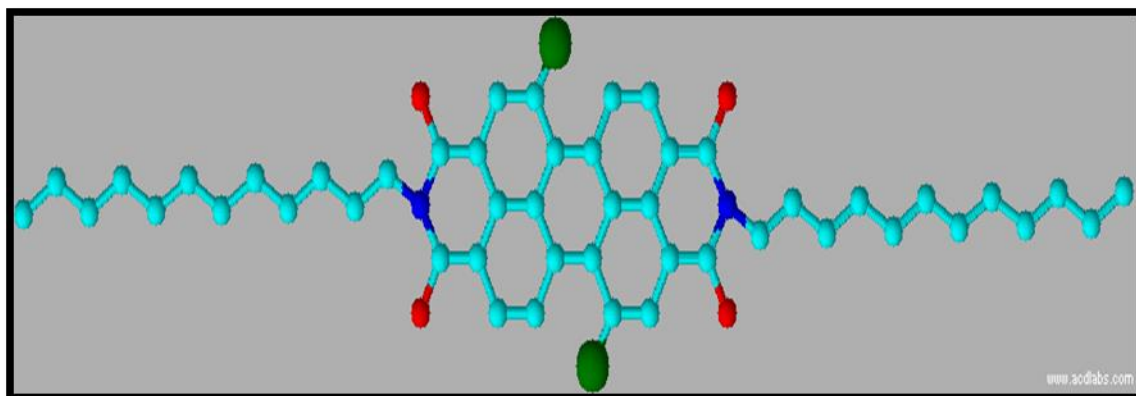
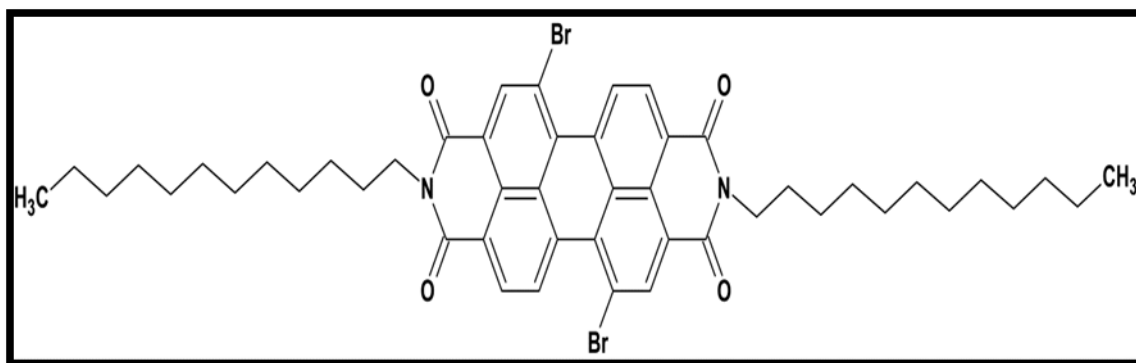


Figure1-3: N,N'-Didodecyl-1,7-dibromoperylene-3,4,9,10-tetracarboxylic acid bisimide.

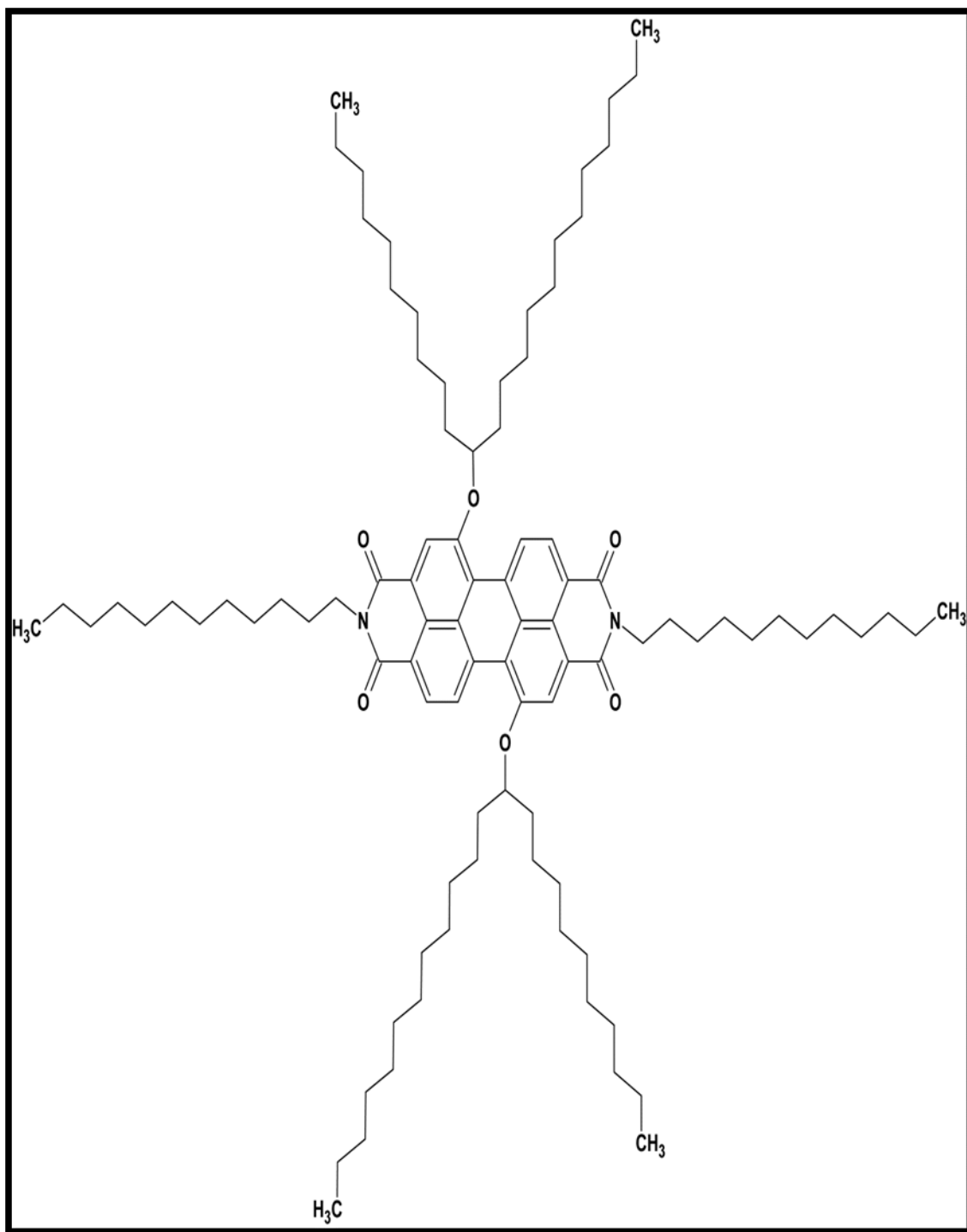


Figure1-4: N,N'-Didodecyl-1,7-di(2-Decyl-1-tetradecanoyl)-perylene-3,4:9,10-tetracarboxylic acid bisimide (BDPDI).

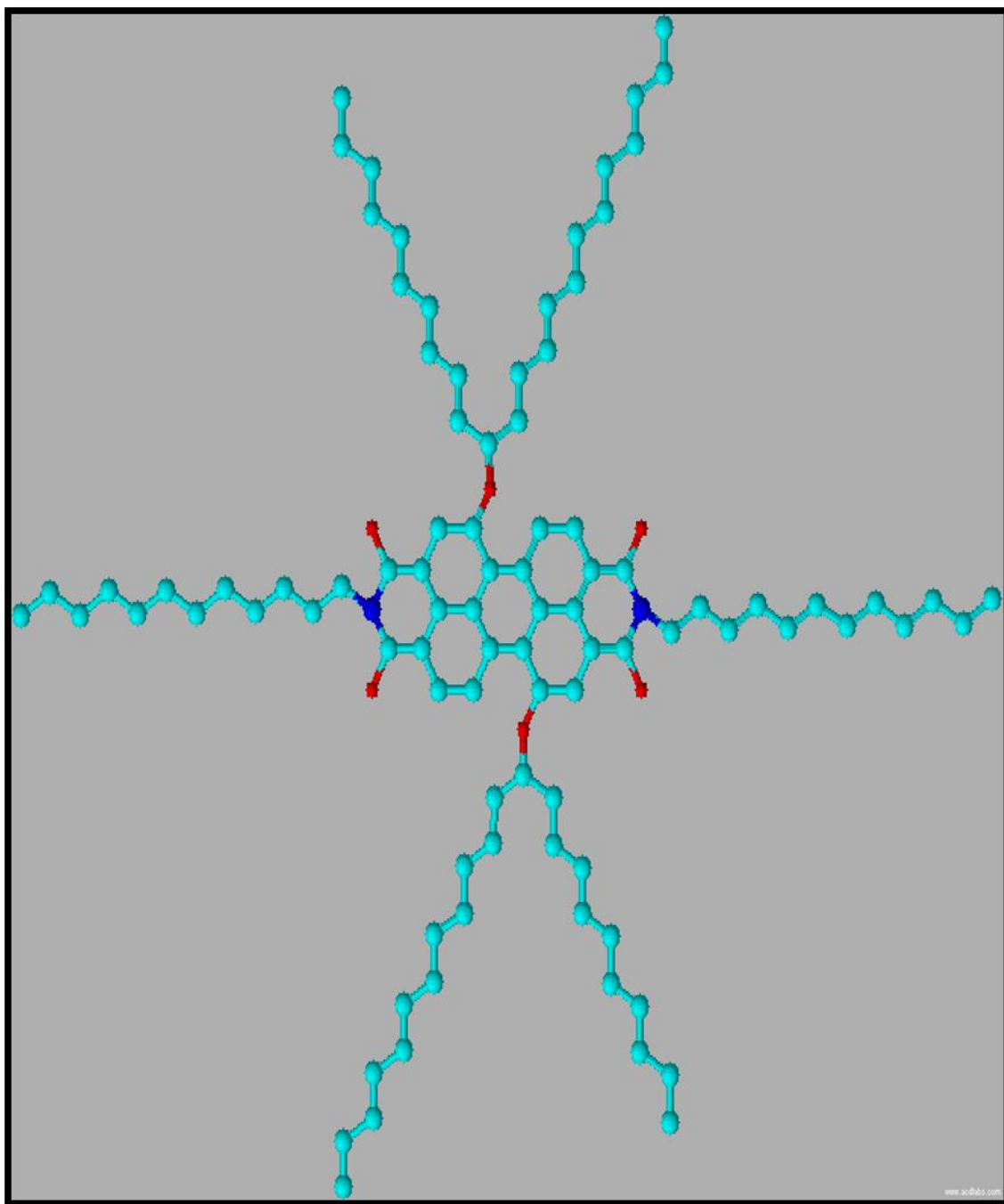


Figure1-5: N,N'-Didodecyl-1,7-di(2-Decyl-1-tetradecanoyl)-perylene-3,4:9,10-tetracarboxylic acid bisimide (BDPDI) in 2 dimensions.

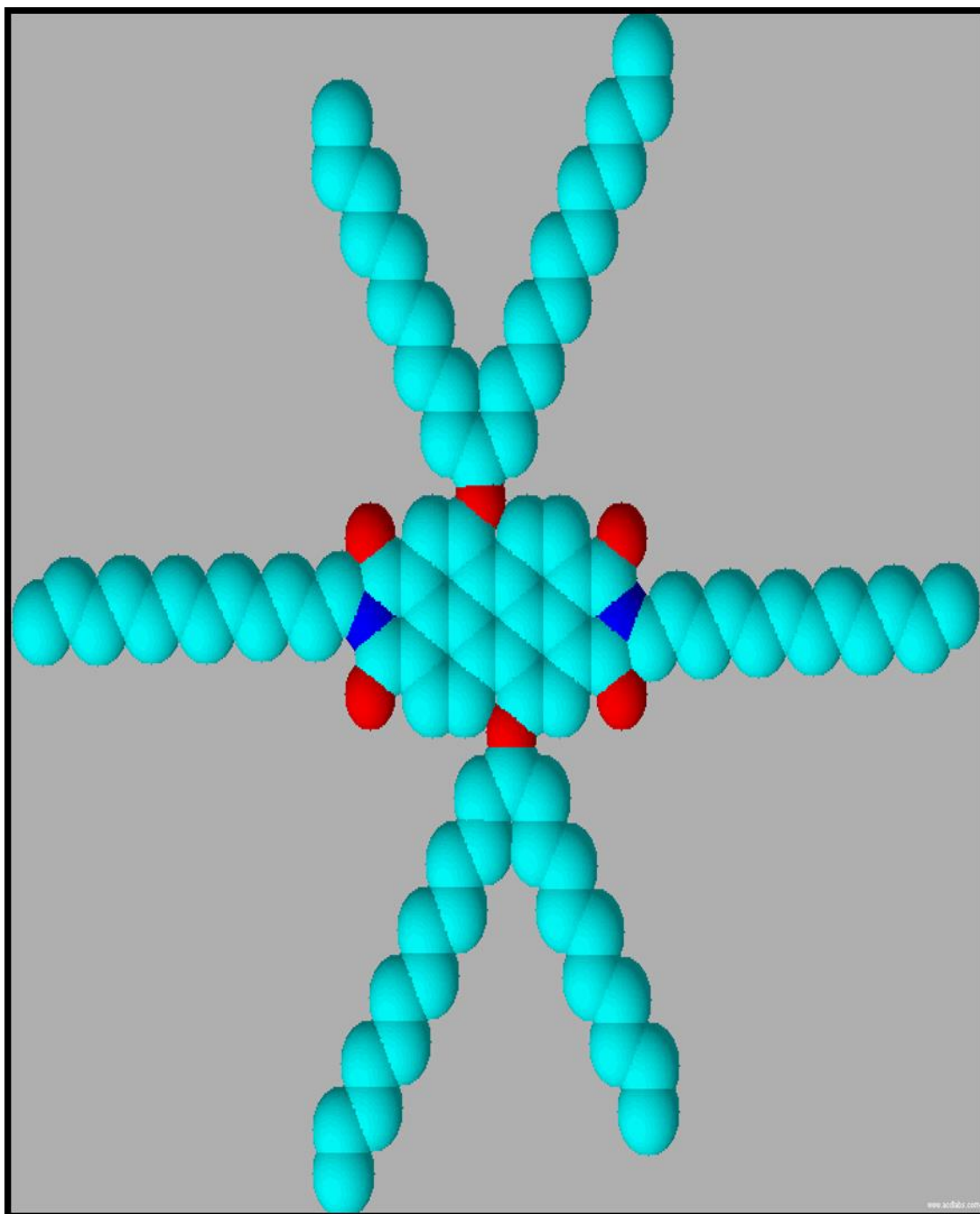


Figure1-6: N,N'-Didodecyl-1,7-di(2-Decyl-1-tetradecanoyl)-perylene-3,4:9,10-tetracarboxylic acid bisimide (BDPDI) in 3 dimensions.

Chapter 2

THEORETICAL

2.1 Properties of Perylene Diimides Dyes

PDI's refer to the greatest captivating useful molecular compounds. Perylene diimides are possibly stimulating electron accepting compounds and with greatest n-type molecular semi-conductors obtainable to date, as long as hopeful materials for implementation in electronic tools [13]. PDIs occur in an extensive variety of colors starting from red to violet, also shadows of black [14]. Additionally, PDIs molecules display exceptional migration stability especially in plastics, also showing great amount of light and excellent stability up on the weather [7,8]. Perylene diimides are essential compounds in industrial dyes, furthermore; these compounds syndicate a sturdy absorption in the visible area together with nearly fluorescence quantum yields, the stability of photochemical property is great, and several motivating chemical and physical features that permit Perylene diimides to be used in new multiple implementations[8,15]. Perylene diimides on the hand are electron accepting materials with four carbonyl groups present in the structure.

2.1.1 Optical Characteristics of Perylene Diimide Dyes

Perylene diimides are extremely versatile compounds. PDIs appeal a big attention in order to their uses in different areas of physical organic chemistry, like dye lasers [23], light harvesting arrays [24], and organic electronic tools [25, 26, 27]. The property of an attractive Perylene diimides is the steady under precinct conditions and great intensities, like solvent polarity and temperature [28,30]. The melting points of greatest PDI-based chromophores are high, red solids and great with photo-stability and thermal stability. Nevertheless, PDI-based dyes with orange, maroon, bluish black and black color are similarly due to, in nearly issues very noticeable aggregation effects, leads to the detected difference in solid absorption spectra [29,30]. Generally, PDIs are deliberated as a set of great organic pigments with high absorption extinction coefficients at visible wavelength (400-600nm), nearly unity fluorescence quantum yields, and extended singlet-excited-state life-times [30,31,32].

In general, Perylene diimides are described by a vibronically structured band and strong absorption in the visible area (400-550nm), they give a tough yellow-green fluorescent as a mirror image of the absorption in public organic solvents. The studies have been mentioned that the electronic transitions for Perylene diimides without substitutions are mainly HOMO to LUMO transitions [30]. PDIs are frequently used for important photo- induced charge-transfer studies and that due to the effortlessly recognized Perylene diimides radical anions absorption spectra in the visible-NIR area [34].

2.1.2 Perylene Diimide Dyes; Bay-Substituted Derivatives

One of the procedures for creating Perylene diimides having great solubility are to give the effective groups in the “bay-region” of Perylene diimide aromatic centers [30,38].

The replacement in the bay area of Perylene diimide between carbon atoms or between carbon atoms to N coupling is the basic retreat to alter the highest occupied molecular orbital-lowest unoccupied molecular orbital level reduces to shield the complete (vis-near IR) area when we compare it with unsubstitution Perylene diimide [39]. PDIs devoid of alteration of the core bay region are worthy electron accepters, and they are pretty simply reduced and slightly hard oxidized in solution. Substituents on the bay positions give a greatly further clear effect on the absorption and emission spectra for PDIs, in line for the sturdier electronic coupling from the π -orbital of PDIs to the substituents on the bay positions [30,33]. Derivatization at 1,6,7,12 positions by a suitable substituent will greatly alter the optoelectronic properties. The properties such as electron transporting ability and n-type semiconducting property are also rely on various conformational transitions and non-covalent interactions such as self-assembly, π - π stacking interactions.

2.1.3 Electron Acceptor Properties of Perylene Diimide Dyes for Photovoltaic application

Molecular structures which have electron and energy donor-accepter couples are of specific importance together with affection to the probability to regulator the energy or electron transfer. Struggles are particularly motivated to synthesis fake donor-accepter structural design in a try to impressionist the light that converts to chemical energy or electrical energy [40]. Novel improvement in the domain of Perylene diimide-based effective resources in these days are dedicated on the way to the create of donor – Perylene diimide molecular associations together with the purpose of endorsing an effective PIET reaction among the two energetic units with redox and high lived charge in separated states[41,42]. Perylene diimide-based compounds can occupy in range of excited state with electron transfer reactions, principally by means of accepter, such as demonstrated in figure 2.1 functionalized (D-A) kind Perylene diimide products have appealed on their photoinduced charge transfer progressions[43].

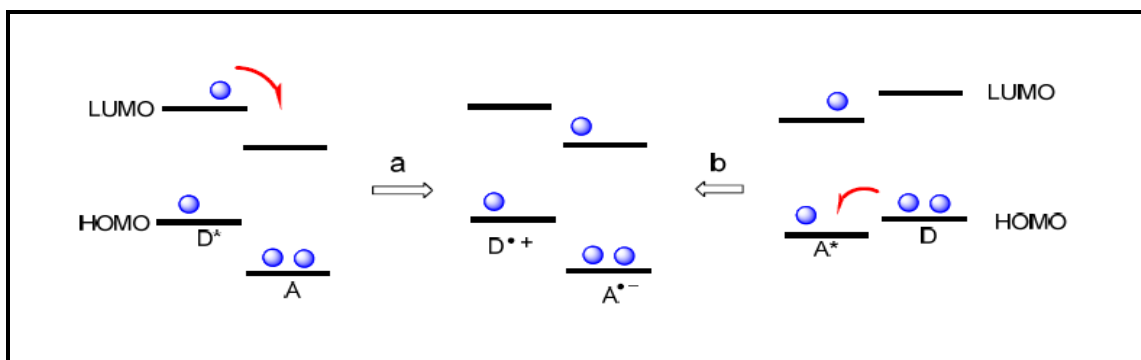


Figure2-1: Photoinduced charge transfer between donor and acceptor of Perylene diimide in creating D^+ - PDI: (A) Electron transfer from excited donor to Perylene diimide; (B) Electron transfer from donor to excited PDI. (Blue balls refer to denote electrons).

2.1.4 Perylene Diimide Dyes; Conversion Efficiency of Solar Energy into Electrical Energy

Photons coming from dissimilar energy in the light of sun attack on the cell, piercing obsessed by the film of the dye subsequently together the ITO film together with glass Pivot and the TiO_2 nanocrystals are limpid to vis-light. When the photon energy is very near to the energy gap in the dye molecule, specifically, the differences that found in energy from the HOMO and LUMO, so the dye will be absorb it, by sponsoring from HOMO to LUMO one electron. In order to be active, commonly it needs highest occupied molecular orbital of the dye to exist in the band gap of the semiconductor, and also the lowest unoccupied molecular orbital to locate inside the conduction band of the semiconductor. Even though, electrons could be inserted from the part of cyanin dyes to the part of TiO_2 nano-wire contained by fifty immediately afterward the excitation process, even though the dye in the part LUMO is initially less than the TiO_2 conduction band least possible[44]. The excited state must equal to the energy level of the conduction band advantage of the oxide. The light of the excitation part must be related with electron current beginning from the light reaping moiety of the pigment on the way to the superficial of the

semiconductor part superficial given for the effective electron transfer from the excited pigment to the TiO₂ conduction band, a sturdy conjugation through the donor and attaching groups, also great electronic coupling among the LUMO of the dye and TiO₂ conduction band. The main issue for the less of the efficiency conversion for the most of organic dyes in SDSC is the creation of pigment aggregates taking place in the semiconductor superficial. This aggregation event will touch the light absorption via filtering result [45, 46].

2.2 The Future and Commercialization of Dye Sensitized Solar Cells

Dye sensitized solar cell demonstrated it's prospective like a low-cost different to costly silicon solar cells. It is a price actual knowledge in order to types that associated with great efficiency, high stability and relaxed fabrication. Additionally, dye sensitized solar cells extra sensitive than the cells of crystalline silicon to vis-light, and also light event at a narrow angle. Like these properties in dye sensitized solar cells permit it to be trustworthy power source in the environment that having less light intensity. Presently, dye sensitized solar cells are yet below laboratory studies and improvement level. Abundant effort residues as conducted to additional develop the energy conversion efficiency in order to theoretical implementation. Pigments are the basic unit of DSSCs, have been drawn a great attention in researches, that is because the conversion of the light to electrical in DSSCs sturdily be influenced by the light absorption in the dyes of the sensitized [46].

Chapter 3

EXPERIMENTAL

3.1 Materials

Perylene-3, 4, 9, 10-tetracarboxylic dianhydride, isoquinoline, dodecylamine, 2-decyl-1-tetradecanol, acetic acid, iodine, bromine and m-cresol were obtained from Sigma Aldrich and used without further purification, potassium carbonate obtained from MERCK, dimethyl formamide supplied by fluka, solvents like methanol, acetone and chloroform which obtained from Aldrich purified by distillation, m-cresol and isoquinoline stored over 4Å molecular sieves.

Molecular sieves of size 4Å (4-8 mesh) which supplied by sigma Aldrich were activated at 500°C and used for drying liquid reagents.

For spectroscopic analysis, pure spectroscopic grade solvents were used without further purification.

All the reactions were controlled by Thin Layer Chromatography (TLC aluminum sheets 5×10 cm silica gel 60 F254) which visualize by UV light and/or placing the plate in acidic vanillin solution.

3.2 Instruments

Infrared spectra were recorded with potassium bromide pellets using JASCO FT/IR-6200 (Fourier transform infrared spectrometer).

Ultraviolet Absorption spectra (UV) were measured with Cary-100 UV-Visible spectrophotometer.

Emission spectra and fluorescence Quantum yield were measured by Varian Cary Eclipse fluorescence spectrophotometer.

3.3 Methods of Synthesis

The aim of this thesis is to synthesize a bay substituted perylene diimide which is N,N'-Didodecyl-1,7-diphenoxy- perylene-3,4:9,10-tetracarboxylic acid bisimide (BPPDI). This synthesis was achieved by three steps .

These three steps were explained in this section, step one represent the synthesis of Brominated Perylene Bisanhydride (BASF patent procedure), step two illustrate the Synthesis of N, N'-Didodecyl-1, 7-dibromoperylene-3, 4, 9, 10-tetracarboxylic Acid Bisimide and the final step perform the synthesis of N, N'-Didodecyl-1, 7-bis (2-decyl-1-tetradecanol) perylene-3, 4, 9, 10-tetracarboxylic Acid Bisimide (N, N'-Didodecyl-1, 7-bis (m-cresol) perylene-3, 4, 9, 10-tetracarboxylic Acid Bisimide).

3.4 Synthesis of Brominated Perylene Bisanhydride (BrPDA)

A mixture of 7.8503g (20.00mmol) of perylene-3, 4:9, 10-tetra carboxylic acid di anhydride and 64 ml of 95-97% sulfuric acid (density =1.84 g/cm³) . And subsequently Iodine (I₂) 0.1925 g 0.75mmol was added. The reaction mixture was heated to 35°C for 1 hour, 45°C for 1 hour then 55°C for 16 hours. 2.26 ml (44 mmol, density 3.119 g/ml) of bromine was added drop wise over a time period of 2 hour at room temperature. The reaction mixture (we used isopropanol condenser at 5°C) was stirred 48h at room temperature then heated to 40 °C for 24h and 85°C for 6h, then cooled to room temperature. The excess of bromine was removed by passing a gentle stream of argon gas. The reaction mixture was added into a beaker contain 500 ml of water (ratio 1:5) and kept overnight in the fridge. The mixture was filtered by a suction filtration. The precipitate was washed with a mixture of (500 ml water and 75 ml 86% sulfuric acid) and kept overnight in a fridge. For purification, the precipitate was purified by water soxhlet for 24 h.

3.5 Synthesis of N, N'-Didodecyl-1, 7-dibromoperylene-3, 4, 9, 10-tetracarboxylic Acid Bisimide (BrPDI)

A mixture of 1,7-Dibromoperylene-3,4,9,10-tetracarboxylic dianhydride (2 g ,3.6mmol) and dodecyl amine (1.5g, 8.1mmol) and isoquinoline (40 mL) under argon gas . Heat the up mixture to 60°C for 2hours, 80°C 2hours, and 100°C for 4hours and 160°C for 6hours. The temperature was raised to 180°C around 8hours then, Complete the reaction with continuous stirring at 200°C for more than 10 hours. 400 mL of methanol was refrigerated for 30 minutes then the reaction mixture was poured into it, covered with foil paper, refrigerated for 1 day for complete precipitation. The resulting precipitate was filtered by suction filtration, and then the

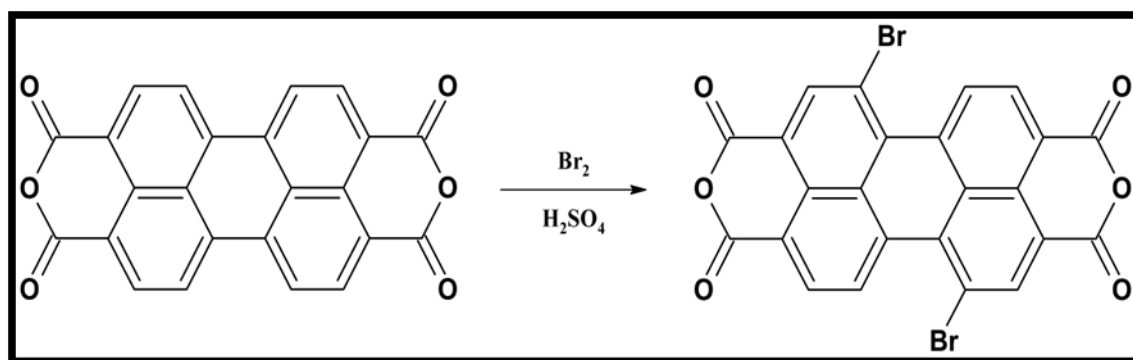
precipitate was purified by methanol soxhlet around 24hours. Then it was dried by a vacuum oven.

3.6 Synthesis of N,N'-Didodecyl-1,7-di(2-Decyl-1-tetradecanoyl)-perylene-3,4:9,10-tetracarboxylic acid bisimide (PDI-Decanol)

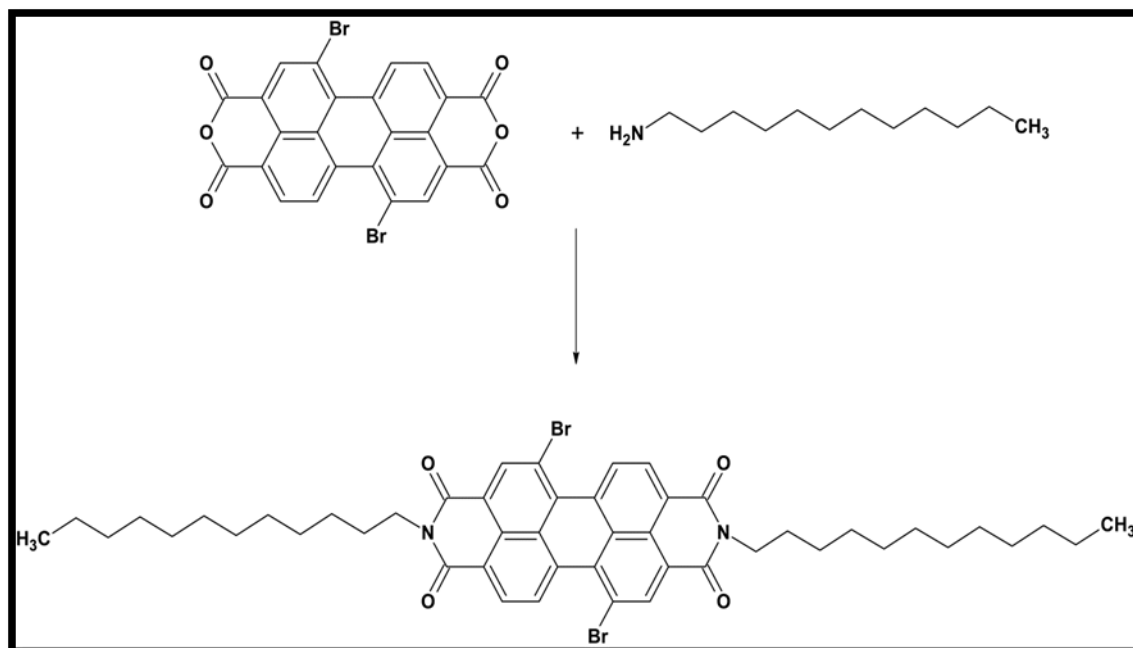
A solution of BrPDI (0.5 g, 0.56 mmol), 0.5896ml (0.4965g, 1.4mmol) 2-decyl-1-tetradecanol and K_2CO_3 (0.1972 g, 1.427mmol) in 100 mL DMF were brought to reflux for 30 h under argon gas with stirring. The reaction mixture was then poured into a mixture of 20 mL cold acetic acid and 50 mL cold water and kept in the fridge overnight. The mixture was filtered by using vacuum filtration; then the precipitate was purified by a water soxhlet for 24 h, and then dried with vacuum oven.

3.7 General reaction mechanism of Perylene Dyes

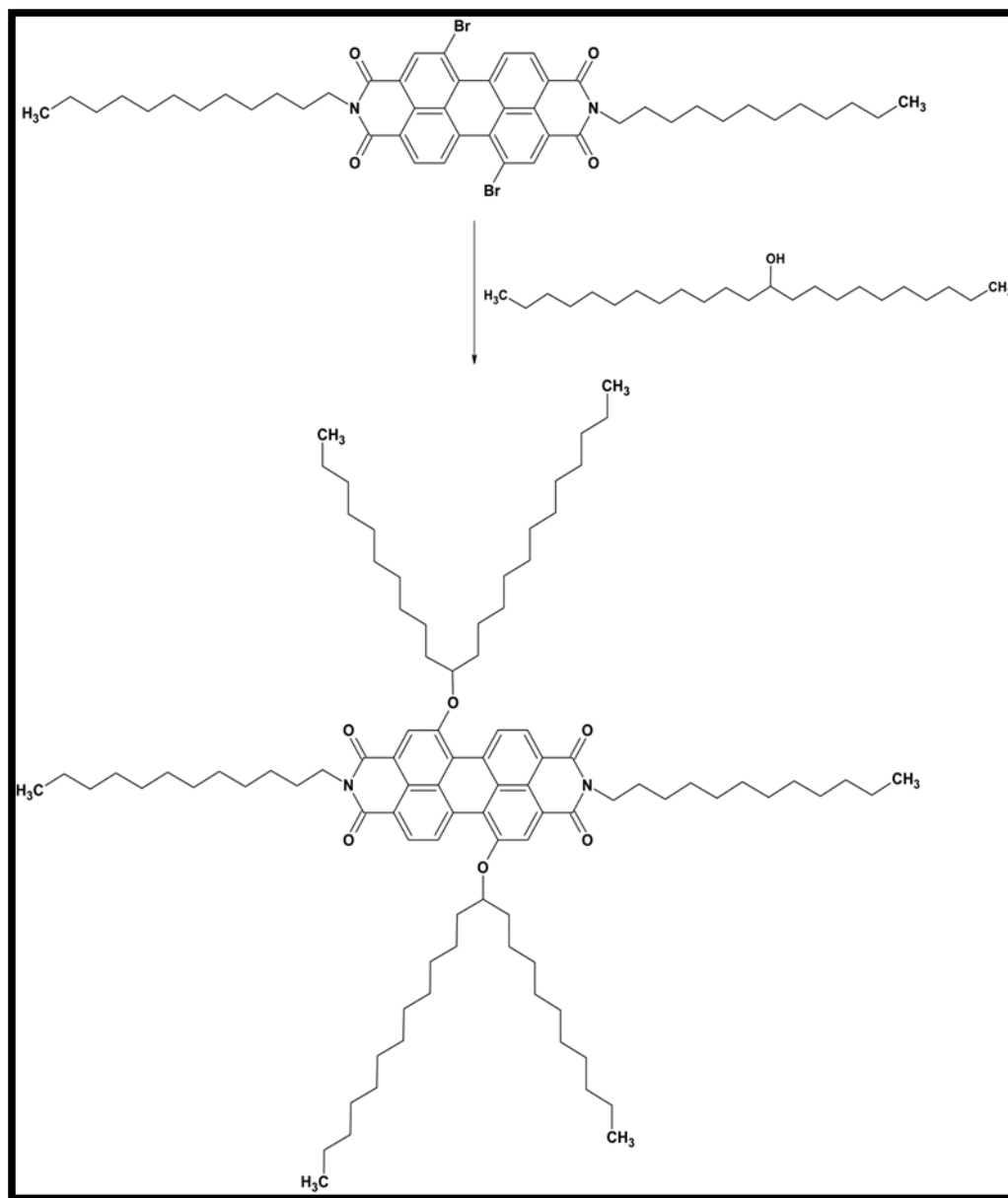
Step 1: Synthesis of BrPDA



Step 2: Synthesis of Dodecyl BrPDI:



Step 3: Synthesis of PDI-Decanol



Chapter 4

DATA AND CALCULATIONS

4.1 Calculations of Maximum Extinction Co-efficient (ϵ_{\max})

According to Beer-Lambert law extinction coefficient can be calculated by

$$\epsilon_{\max} = A/cl$$

ϵ_{\max} : maximum absorption coefficient in $\text{L.mol}^{-1}.\text{cm}^{-1}$ at λ_{\max}

A: Absorption

C: concentration

l: length of the cell

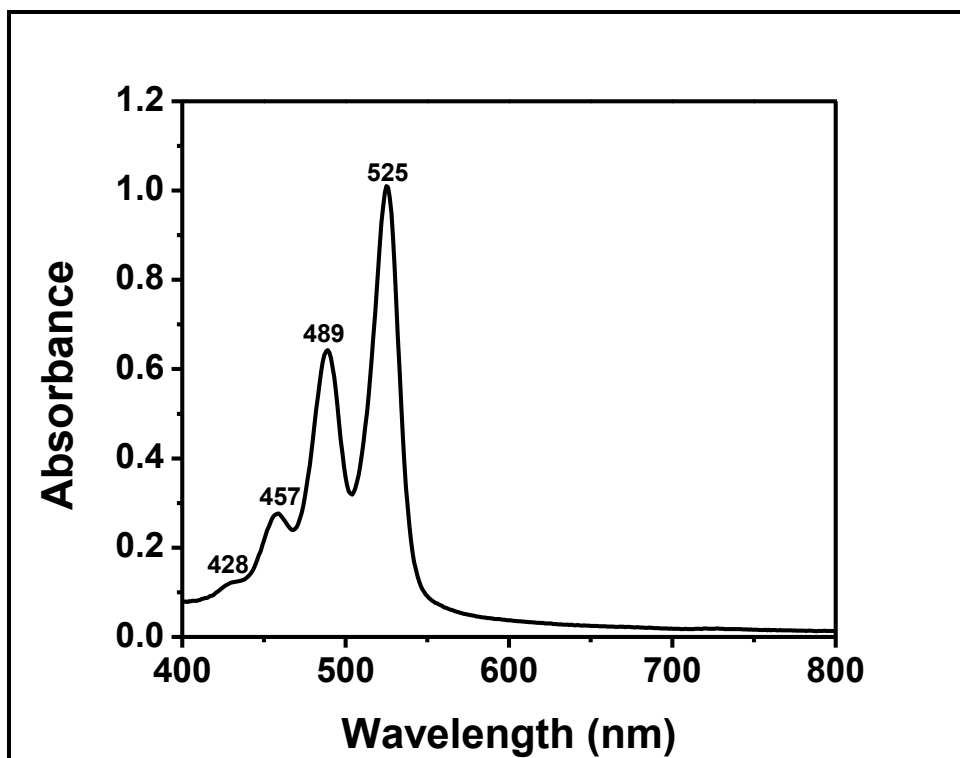


Figure4-1: Absorption spectrum of PDI-Decanol in chloroform at 1×10^{-5} M Concentration

According to the absorption spectrum of PDI-Decanol (figure 4.1) the absorption is 1.01 for the concentration of 1×10^{-5} M at the wavelength, $\lambda_{\text{max}}=525\text{nm}$.

$$\epsilon_{\text{max}} = \frac{1.01}{1 \times 10^{-5}}$$

$$\epsilon_{\text{max}} \text{ of PDI-Decanol} = 101000 \text{ L.mole}^{-1}.\text{cm}^{-1}$$

The molar absorptivities of the synthesized compounds were calculated in the similar method and listed below in (Table 4.1).

Table 4-1: Molar absorptivity data of BrPDA, BrPDI and PDI-Decanol in CHL

Compound	Concentration	Absorbance	λ_{\max}	$\varepsilon_{\max}(\text{L.M}^{-1} \text{cm}^{-1})$
BrPDA	-----	-----	-----	-----
BrPDI	$1 \times 10^{-5} \text{ M}$	1.2	526	120000
PDI-Decanol	$1 \times 10^{-5} \text{ M}$	1.01	525	101000

Table 4-2: Molar absorptivity data of BrPDA, BrPDI and PDI-Decanol in DMF

Compound	Concentration	Absorbance	$\lambda_{\max} \text{ (nm)}$	$\varepsilon_{\max}(\text{L.M}^{-1} \text{cm}^{-1})$
BrPDA	$1 \times 10^{-5} \text{ M}$	0.8	518	80000
BrPDI	$1 \times 10^{-5} \text{ M}$	0.9	523	90000
PDI-Decanol	$1 \times 10^{-5} \text{ M}$	0.5	522	51900

Table 4-3: Molar absorptivity data of BrPDA, BrPDI and PDI-Decanol in NMP

Compound	Concentration	Absorbance	$\lambda_{\max} \text{ (nm)}$	$\varepsilon_{\max}(\text{L.M}^{-1} \text{cm}^{-1})$
BrPDA	$1 \times 10^{-5} \text{ M}$	0.3	515	30000
BrPDI	$1 \times 10^{-5} \text{ M}$	0.2	523	20000
PDI-Decanol	$1 \times 10^{-5} \text{ M}$	1.11	525	111000

Table 4-4: Molar absorptivity data of BrPDA, BrPDI and PDI-Decanol in EtOH

Compound	Concentration	Absorbance	λ_{\max} (nm)	$\epsilon_{\max}(\text{M}^{-1} \text{cm}^{-1})$
BrPDA	-----	-----	-----	-----
BrPDI	-----	-----	-----	-----
PDI-Decanol	1×10^{-5} M	0.68	525	68000

Table 4-5: Molar absorptivity data of BrPDA, BrPDI and PDI-Decanol in Acetone

Compound	Concentration	Absorbance	λ_{\max} (nm)	$\epsilon_{\max}(\text{M}^{-1} \text{cm}^{-1})$
BrPDA	-----	-----	-----	-----
BrPDI	-----	-----	-----	-----
PDI-Decanol	1×10^{-5} M	0.38	517	38000

4.2 Calculations of Half-width of the selected Absorption ($\Delta\nu^{1/2}$)

The half-width of the selected maximum absorption is the full width at half maximum and can be calculated from the following equation.

$$\Delta\nu^{1/2} = \nu_I - \nu_{II}$$

Where, ν_I, ν_{II} : The frequencies from the absorption spectrum in cm^{-1}

$\Delta\nu^{1/2}$: Half-width of the selected maximum absorption in cm^{-1}

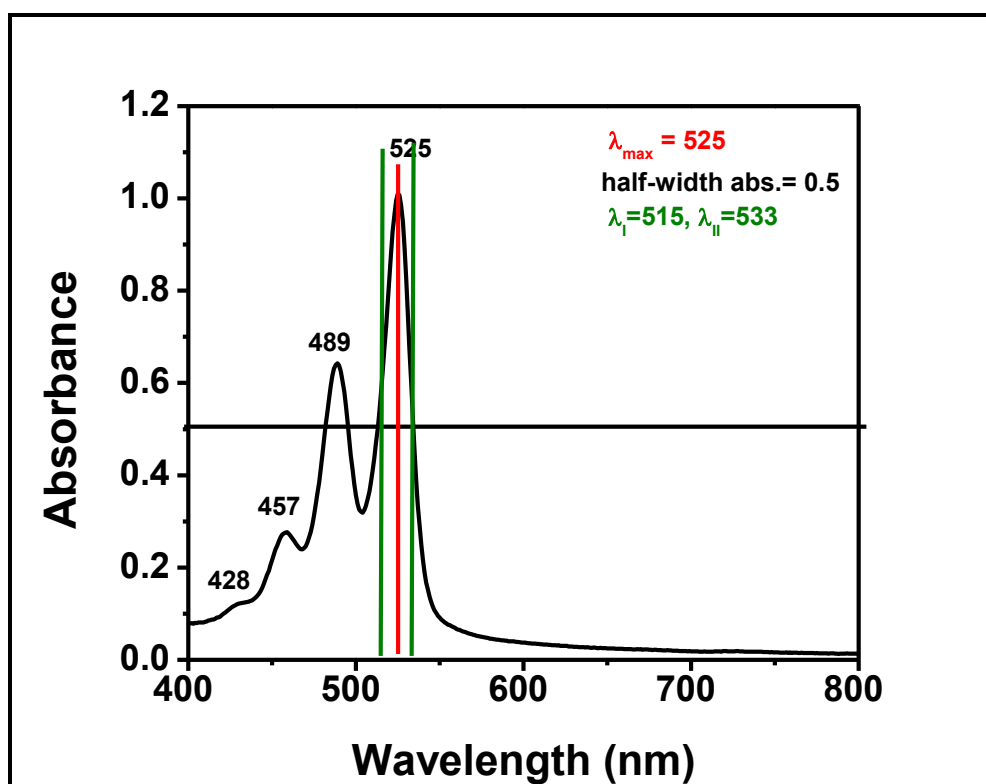


Figure4-2: Absorption spectrum of PDI-Decanol in chloroform and half-width.

From the Figure 4.2,

$$\lambda_{\text{I}} = 515 \times \frac{10\text{m}^{-9}}{1\text{nm}} \times \frac{1\text{cm}}{10\text{m}^{-2}} = 5.15 \times 10^{-5} \text{ cm}$$

$$\lambda_{\text{II}} = 533\text{nm} \times \frac{10\text{m}^{-9}}{1\text{nm}} \times \frac{1\text{cm}}{10\text{m}^{-2}} = 5.33 \times 10^{-5} \text{ cm}$$

$$\nu_1 = \frac{1}{5.15 \times 10\text{cm}^{-5}} = 19417.47 \text{ cm}^{-1}$$

$$\nu_2 = \frac{1}{5.33 \times 10^{-5}} = 18761.72 \text{ cm}^{-1}$$

$$\Delta\nu^{1/2} = \nu_1 - \nu_2$$

$$\Delta\nu^{1/2} = 19417.47 - 18761.72 = 655.7 \text{ cm}^{-1}$$

It is required to estimate the half-width of the compounds in order to calculate the theoretical radiative lifetimes of the compounds. In the similar manner shown above, the half-width were calculated and presented below in Table 4.6

Table 4-6: Half width of the selected absorptions of PDI-Decanol and measured in different solvents

Solvent	$\lambda_{\text{I}}(\text{nm})$	$\lambda_{\text{II}}(\text{nm})$	$\Delta\nu^{1/2} (\text{cm}^{-1})$
DMF	511	535	877.88
NMP	507	539	1170.98
Acetone	502	529	1016.72
Ethanol	509	556	1660.74

Table4-7: Half width of the selected absorptions of BrPDI and measured in different solvents

Solvent	$\lambda_I(\text{nm})$	$\lambda_{II}(\text{nm})$	$\Delta\nu_{1/2}(\text{cm}^{-1})$
DMF	503	537	1258.73
DMF/M.F	503	537	1258.73
NMP	500	534	1273.41
CHL	502	531	1087.91

Table 4-8: Half width of the selected absorptions of BrPDA and measured in different solvents

Solvent	$\lambda_I(\text{nm})$	$\lambda_{II}(\text{nm})$	$\Delta\nu_{1/2}(\text{cm}^{-1})$
DMF	495	533	1440.32
DMF/M.F	498	529	1176.7
NMP	498	527	1104.96
NMP/M.F	498	532	1283.1

4.3 Calculations of Theoretical Radiative Lifetimes (τ_0)

The theoretical radiative lifetime of a molecule refers to the lifetime of an excited molecule theoretically measured in the absence of non-radiative transitions.

$$\tau_0 = \frac{3.5 \times 10^8}{\nu_{max}^2 \times \epsilon_{max} \times \Delta\nu_{1/2}}$$

Where, τ_0 : Theoretical radiative lifetime in ns

ν_{max} : Mean frequency of the maximum absorption band in cm^{-1}

ϵ_{max} : The maximum extinction coefficient in $\text{L. mol}^{-1} \cdot \text{cm}^{-1}$ at the maximum absorption wavelength, λ_{max}

$\Delta\nu_{1/2}$ = Half-width of the selected absorption in units of cm^{-1} .

Theoretical radiative lifetime of PDI-Decanol in chloroform

With the help of calculated molar absorptivity and half-width of selected absorptions of PDI-Decanol:

From the Figure 4.1 and 4.2, $\lambda_{\text{max}}=525\text{nm}$

$$\lambda_{\text{max}} = 525\text{nm} \times \frac{10^{-9}\text{m}}{1\text{nm}} \times \frac{1\text{cm}}{10^{-2}\text{m}} = 5.25 \times 10^{-5}\text{cm}$$

$$\nu_{\text{max}} = \frac{1}{5.25 \times 10^{-5}} = 19047.6 \text{ cm}^{-1}$$

$$\nu_{\text{max}}^2 = 3.63 \times 10^8 (\text{cm}^{-1})^2$$

$$\tau_0 = \frac{3.5 \times 10^8}{3.63 \times 10^8 \times 101000 \times 655.7} = 1.45 \times 10^{-8} \text{ s} = 14.5 \text{ ns}$$

With similar method of calculation, theoretical radiative lifetimes were calculated for the other synthesized compounds in chloroform and the data was presented below.

Table 4-9: Theoretical radiative lifetimes of PDI-Decanol measured in different solvents

Solvent	λ_{max} (nm)	ϵ_{max} ($\text{M}^{-1} \cdot \text{cm}^{-1}$)	ν_{max}^2 (cm^{-1}) ²	$\Delta\nu_{1/2}$ cm^{-1}	τ_0 ns
DMF	522	80000	3.67×10^8	877.88	13.58
NMP	525	111000	3.6×10^8	1170.98	7.48
CHL	525	101000	3.63×10^8	655.7	14.5
Acetone	517	38000	3.7×10^8	1016.72	24.5
Ethanol	525	68000	3.66×10^8	1660.74	8.6

Table 4-10: Theoretical radiative lifetimes of BrPDI measured in different solvents

Solvent	λ_{\max} (nm)	$E_{\max}(M^{-1}.cm^{-1})$	$\nu^2_{\max}(cm^{-1})^2$	$\Delta\nu_{1/2}(cm^{-1})$	τ_0 (ns)
DMF	523	25200	3.65×10^8	1258.73	30.2
NMP	523	20000	3.65×10^8	1273.41	37.6
CHL	526	120000	3.65×10^8	1087.91	7.54

Table 4-11: Theoretical radiative lifetimes of BrPDA measured in different solvents

Solvent	λ_{\max} (nm)	$E_{\max}(M^{-1}.cm^{-1})$	$\nu^2_{\max}(cm^{-1})^2$	$\Delta\nu_{1/2}(cm^{-1})$	τ_0 (ns)
DMF	515	40000	3.77×10^8	1440.32	18.2
NMP	515	30000	3.77×10^8	1104.96	28

4.4 Calculations of Fluorescence Rate Constant (k_f)

The theoretical fluorescence rate constants for the synthesized perylene derivatives are calculated by the equation given below.

$$K_f = \frac{1}{\tau_0}$$

Where, K_f : Fluorescence rate constant in s^{-1}

τ_0 : theoretical radiative lifetime in s

Fluorescence Rate constant of PDI-Decanol

$$K_f = \frac{1}{1.45 \times 10^{-8}} = 6.8 \times 10^7 s^{-1}$$

Table 4-12: Fluorescence rate constants data of PDI-Decanol in different solvents

Solvent	τ_0 (s)	k_f (s^{-1})
CHL	1.45×10^{-8}	6.8×10^7
DMF	1.358×10^{-8}	7.36×10^7
NMP	7.479×10^{-9}	13.3×10^7
Acetone	2.45×10^{-8}	4.08×10^7
ETOH	8.6×10^{-9}	11.6×10^7

Table 4-13: Fluorescence rate constants data of BrPDI in different solvents

Solvent	τ_0 (s)	K_f (s^{-1})
DMF	3.02×10^{-8}	3.3×10^7
NMP	3.7×10^{-8}	2.7×10^7
CHL	7.45×10^{-9}	1.3×10^8

Table 4-14: Fluorescence rate constants data of BrPDA in different solvents

Solvent	τ_0 (s)	K_f (s^{-1})
DMF	1.82×10^{-8}	5.5×10^7
NMP	2.8×10^{-8}	3.5×10^7

4.5 Calculations of oscillator strength (f)

The oscillator strength is a dimensionless quantity infers the strength of an electronic transition. It can be estimated by the equation below.

$$f = 4.32 \times 10^{-9} \cdot \Delta\nu_{1/2} \cdot \epsilon_{max}$$

Where, f : Oscillator strength

$\Delta\nu_{1/2}$: Half-width of the selected absorption in units of cm^{-1}

ϵ_{max} : The maximum extinction coefficient in $\text{L} \cdot \text{mol}^{-1} \cdot \text{cm}^{-1}$ at the maximum absorption wavelength, λ_{max}

Oscillator strength of PDI-Decanol in DMF:

$$f = 4.32 \times 10^{-9} \times 101000 \times 655.7 = 0.286$$

The following Table 4.15 presents the calculated rate constants of the radiationless deactivation for PDI-Decanol

Table 4-15: Oscillator strength data of PDI-Decanol measured in different solvents

Solvent	$\Delta\nu_{1/2}$ (cm ⁻¹)	E_{\max} (M ⁻¹ .cm ⁻¹)	f
DMF	877.88	80000	0.3
NMP	1170.98	111000	0.56
CHL	655.7	101000	0.286
Acetone	1016.72	38000	0.167
EtOH	1660.74	68000	0.487

Table 4-16: Oscillator strength data of BrPDI measured in different solvents

Solvent	$\Delta\nu_{1/2}$ (cm ⁻¹)	ϵ_{\max} (M ⁻¹ .cm ⁻¹)	F
DMF	1258.7	25200	0.14
NMP	1273.4	20000	0.11
CHL	1087.91	120000	0.56

Table 4-17: Oscillator strength data of BrPDA measured in different solvents

Solvent	$\Delta\nu_{1/2}$ (cm ⁻¹)	ϵ_{\max} (M ⁻¹ .cm ⁻¹)	f
DMF	1440.32	40000	0.25
NMP	1104.96	30000	0.14

4.6 Calculations of Singlet Energy Singlet energy is the required amount of energy for the electronic transitions of a chromophore from ground state to an excited state.

$$E_s = \frac{2.86 \times 10^5}{\lambda_{\max}}$$

Where, E_s : singlet energy in kcal mol⁻¹

λ_{\max} : the maximum absorption wavelength in Å

Singlet energy of PDI-Decanol:

$$E_s = \frac{2.86 \times 10^5}{5250} = 54.47 \text{ kcal.mol}^{-1}$$

Similarly, the singlet energies of PDI-Decanol were calculated and listed in the following table.

Table 4-18: Singlet Energies Data of PDI-Decanol in Different Solvents

Solvent	λ_{\max} (Å)	E_s (kcal mol ⁻¹)
CHL	5250	54.47
DMF	5220	54.7
NMP	5250	54.47
Acetone	5170	55.31
EtOH	5250	54.47

Table 4-19: Singlet Energies Data of BrPDI in Different Solvents

Solvent	λ_{\max} (Å)	E_s (kcal mol ⁻¹)
DMF	5230	54.6
NMP	5230	54.6
CHL	5260	54.3

Table 4-20: Singlet Energies Data of BrPDA in Different Solvents

Solvent	λ_{\max} (Å)	E_s (kcal mol ⁻¹)
DMF	5150	55.5
NMP	5150	55.5

4.7 Calculations of Optical Band Gap Energies

The optical band gap energy gives important information relating to its HOMO and LUMO energy states to be applicable in solar cells and can be calculated from the following equation

$$E_g = \frac{1240 \text{ eV nm}}{\lambda}$$

Where, E_g : Band gap energy in eV

λ : cut-off wavelength of the absorption band can be estimated from the maximum absorption band in nm

Band gap energy of PDI-Decanol:

The cut-off wavelength of the absorption band can be estimated from the maximum absorption band (0→0 absorption band) by extrapolating it to zero absorbance as shown below (Figure 4.3)

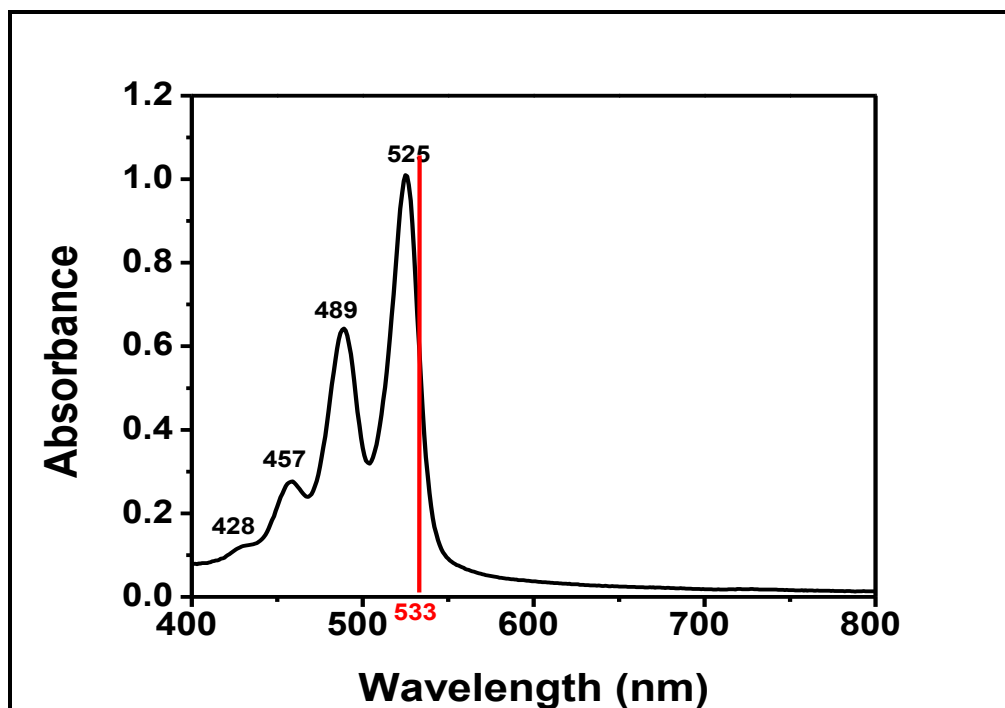


Figure 4-3: Absorption spectrum of PDI-Decanol and the cut-off wavelength

$$E_g = \frac{1240 \text{ eVnm}}{533 \text{ nm}} = 2.3 \text{ eV}$$

Similarly, the band gap energies of PDI-M-Decanol were calculated in different solvents and listed in the following Table 4.21

Table 4-21: Band Gap Energies of PDI-Decanol were calculated in Different Solvents

Solvents	λ (nm)	E_g (eV)
DMF	530	2.34
NMP	533	2.3
Acetone	523	2.37
EtOH	540	2.29
CHL	533	2.3

Table 4-22: Band Gap Energies of BrPDI were calculated in Different Solvents

Solvent	λ (nm)	E_g (eV)
DMF	552	2.24
NMP	550	2.25
CHL	542	2.28

Table 4-23: Band Gap Energies of BrPDA were Calculated in Different Solvents

Solvent	λ (nm)	E_g (eV)
DMF	579	2.14
NMP	553.8	2.24

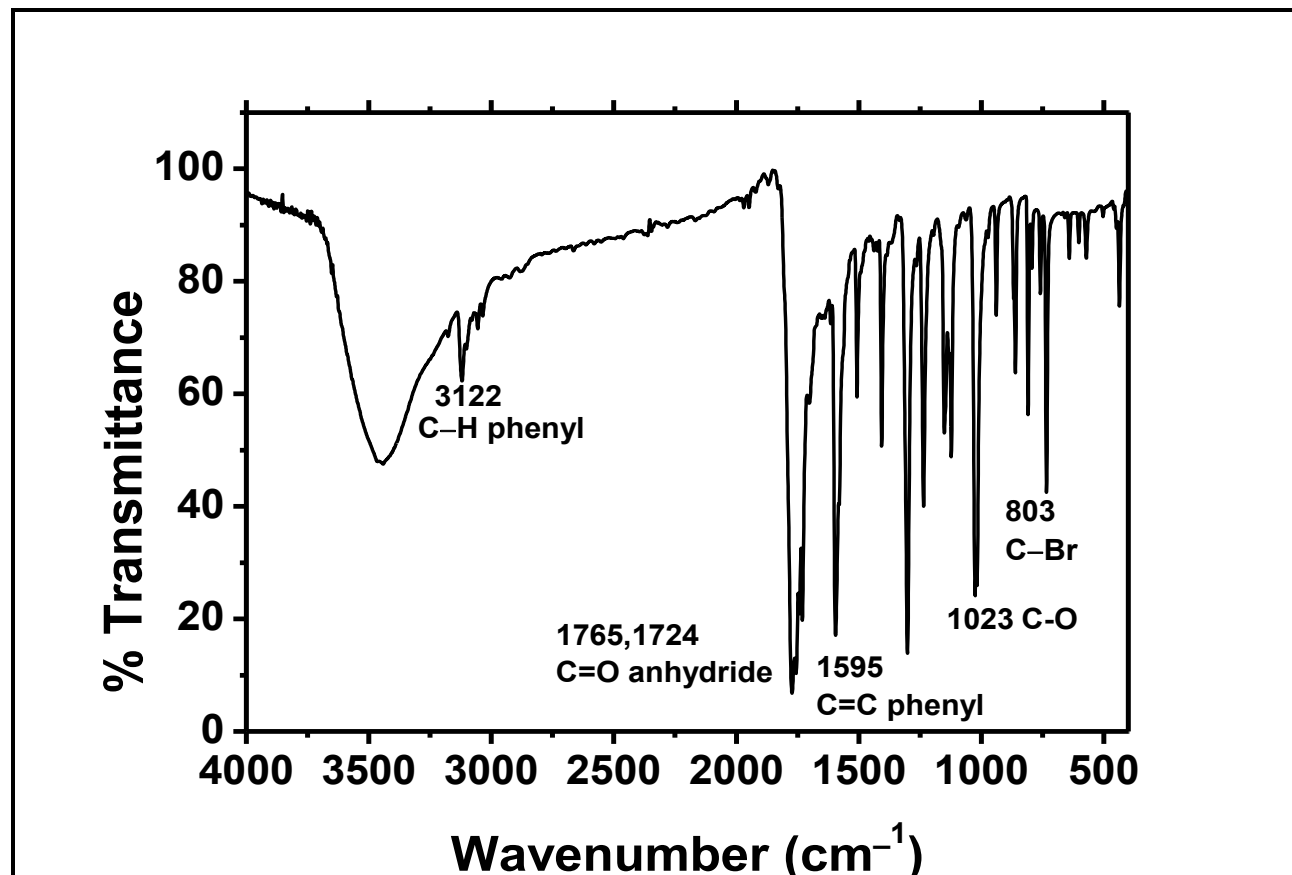


Figure 4-4: FTIR spectrum of BrPDA

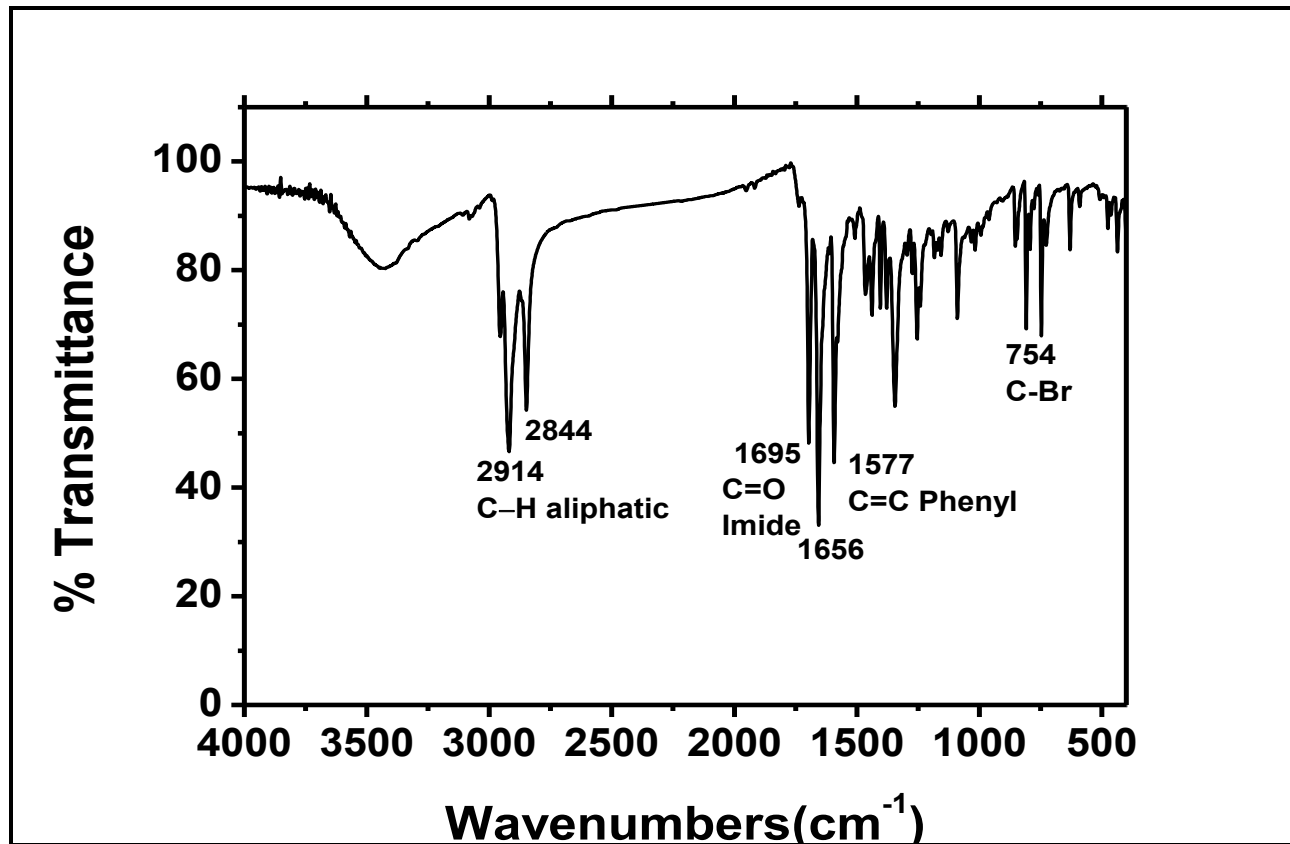


Figure 4-5: FTIR spectrum of BrPDI

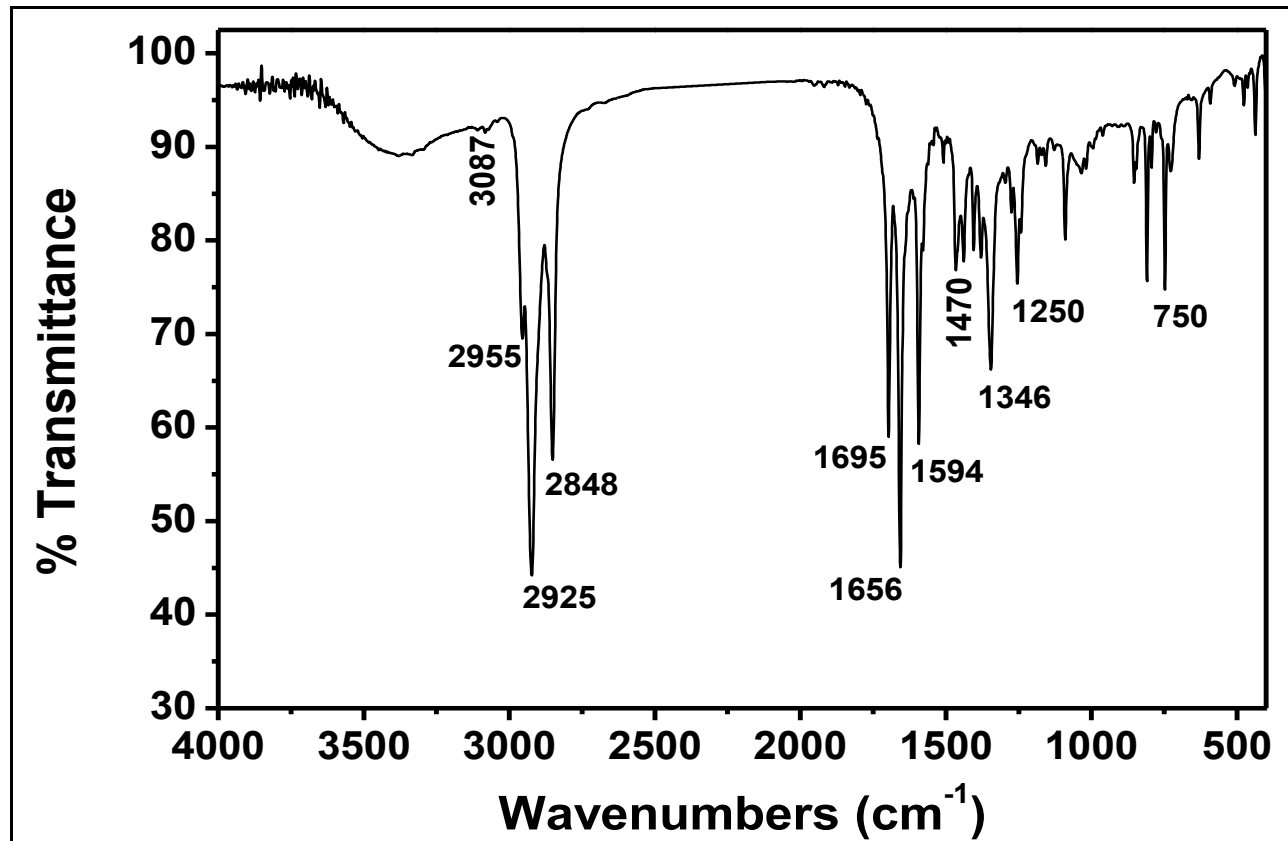


Figure 4-6: FTIR Spectrum of PDI-Decanol

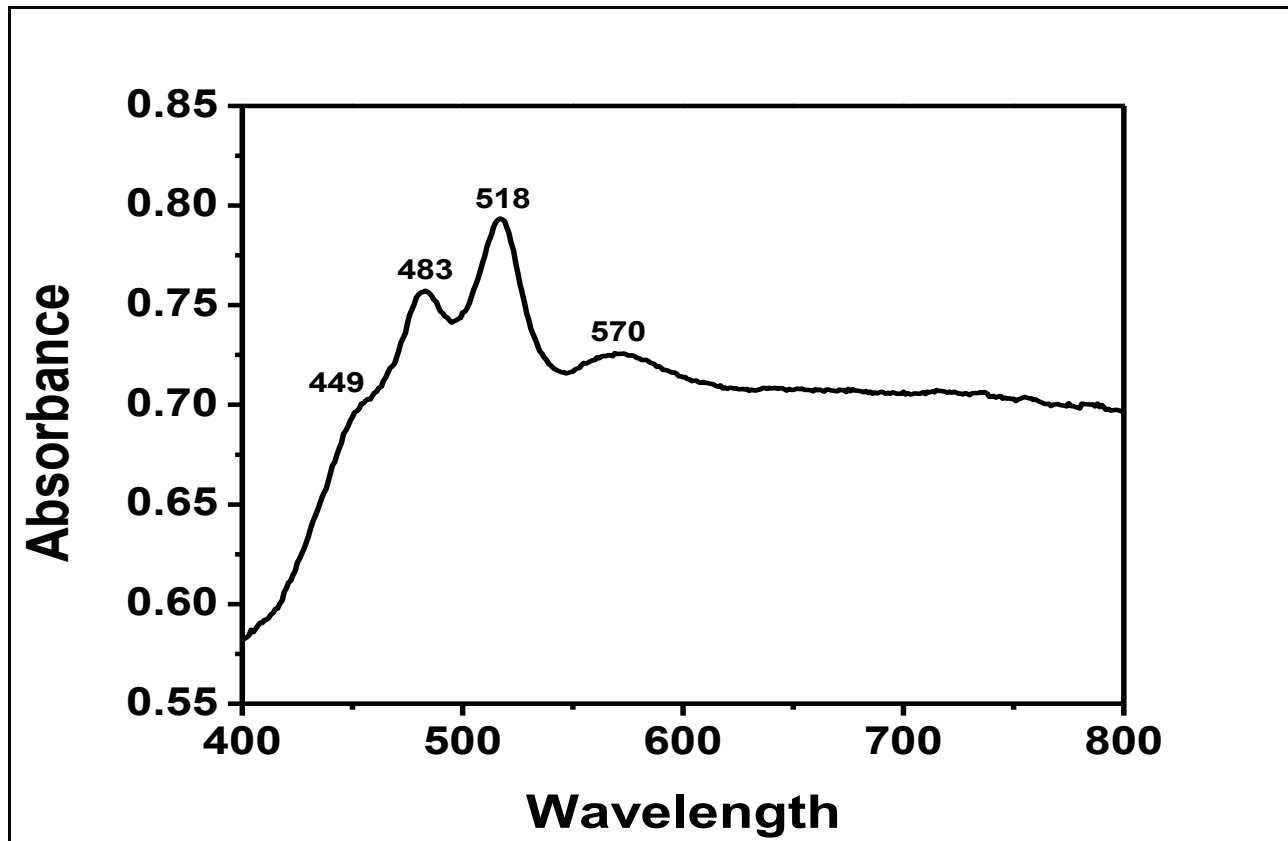


Figure 4-7: UV-vis absorption spectrum of BrPDA in DMF

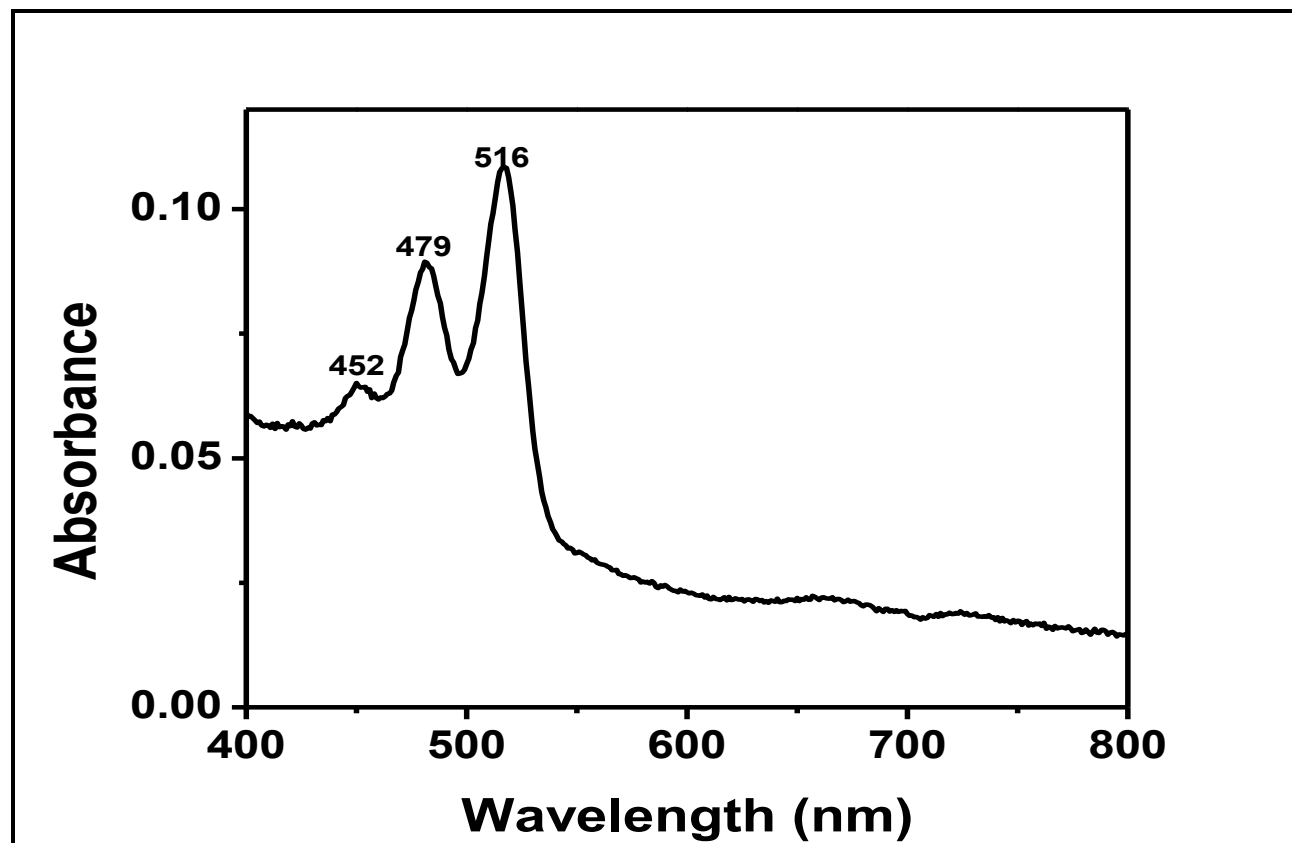


Figure 4-8: UV-vis absorption spectrum of BrPDA in DMF after micro filtration

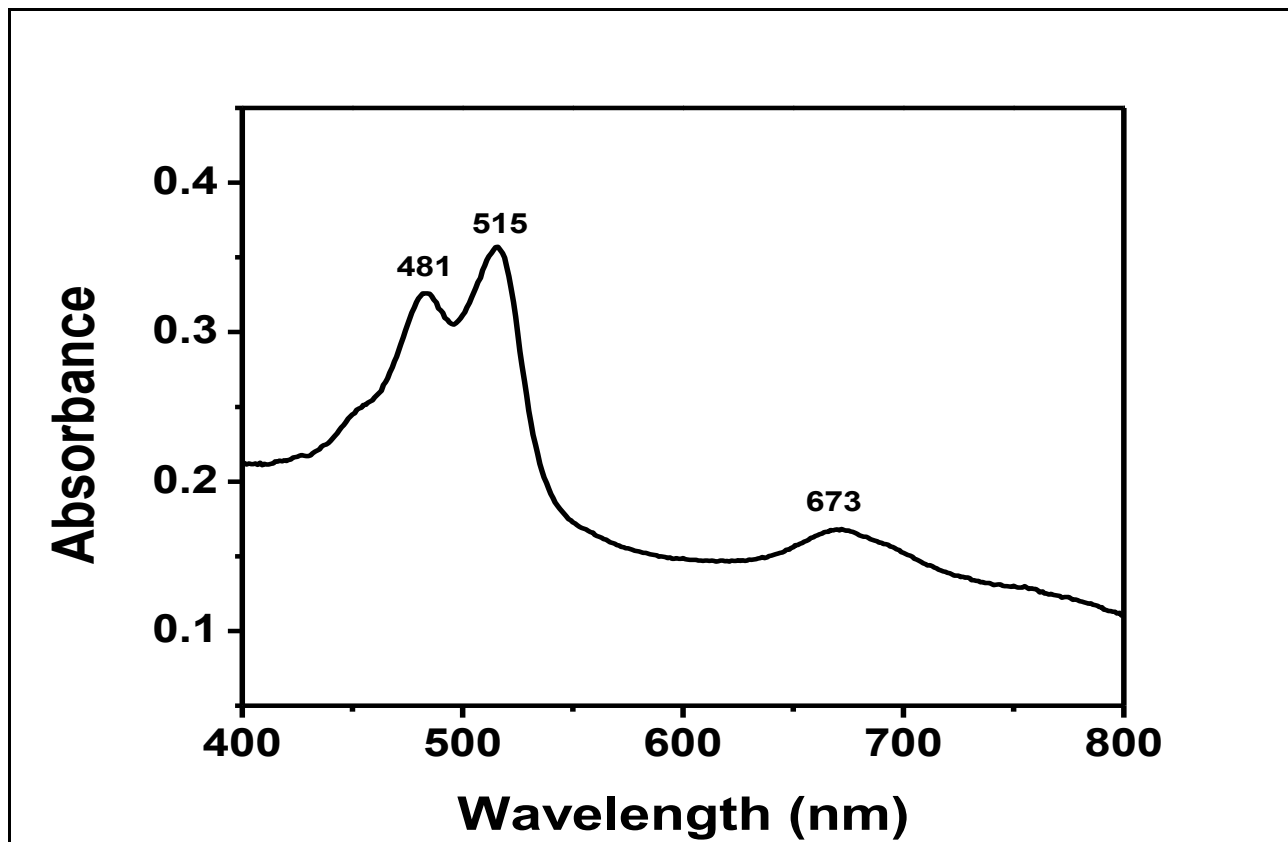


Figure 4-9: UV-vis absorption spectrum of BrPDA in NMP

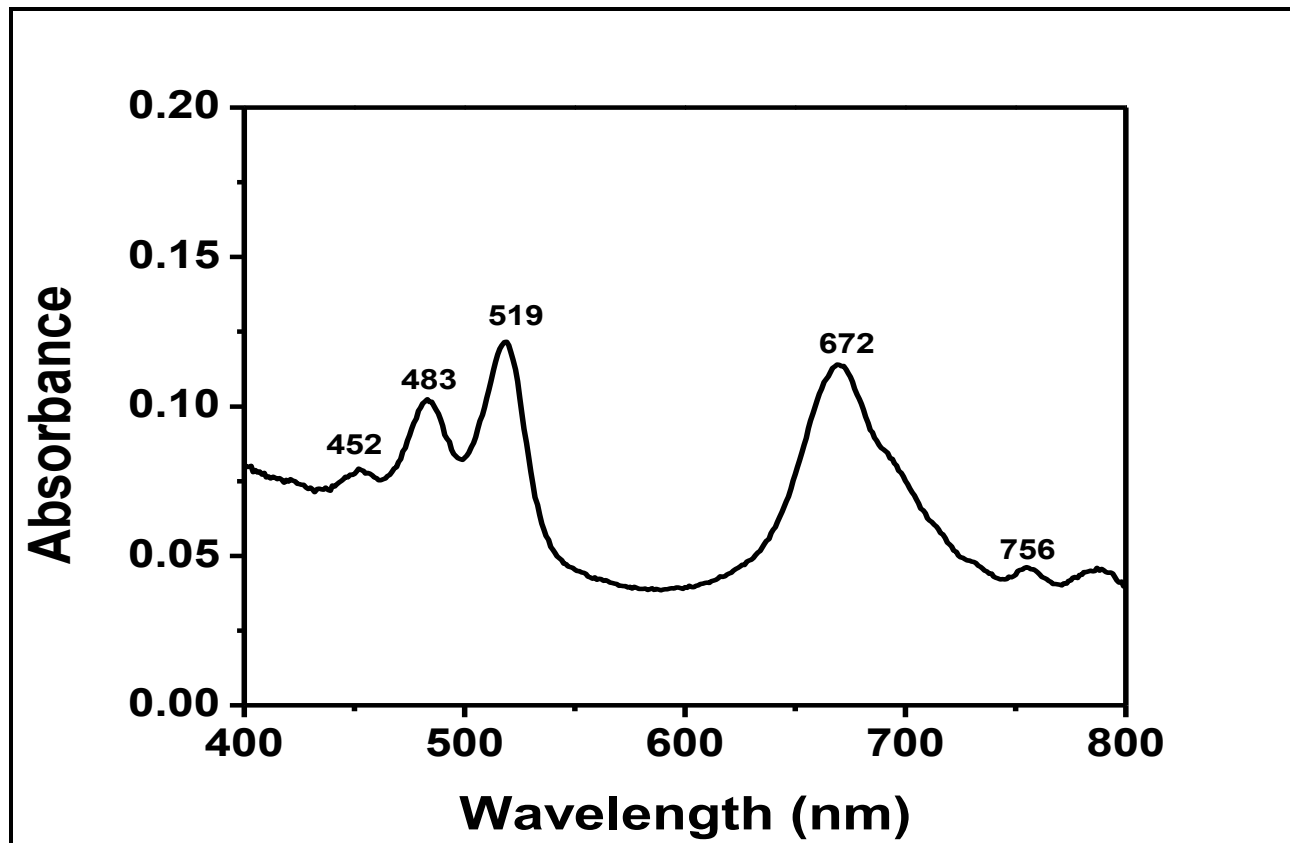


Figure 4-10: UV-vis absorption spectrum of BrPDA in NMP after micro filtration

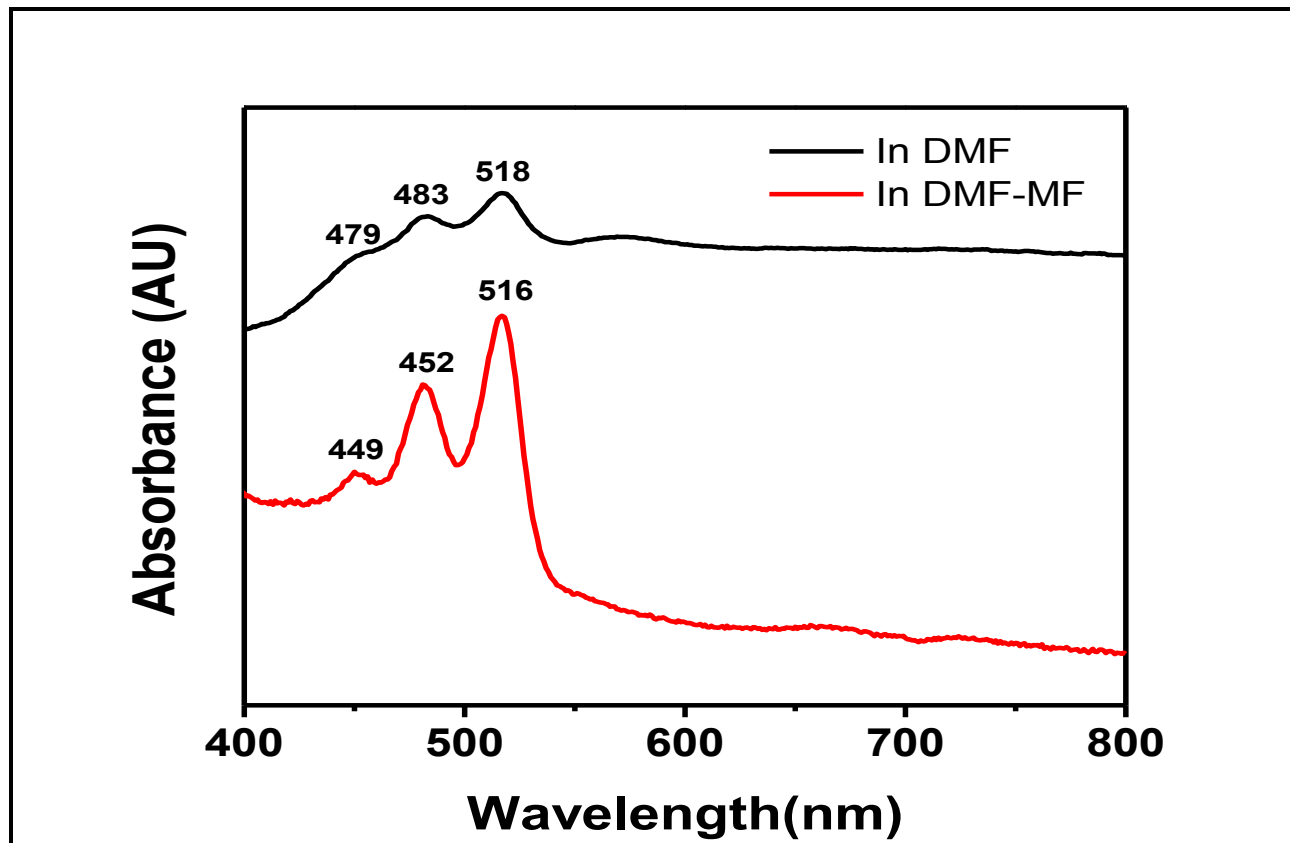


Figure 4-11: overlap UV-vis absorption of BrPDA in DMF, in DMF after Micro filtration

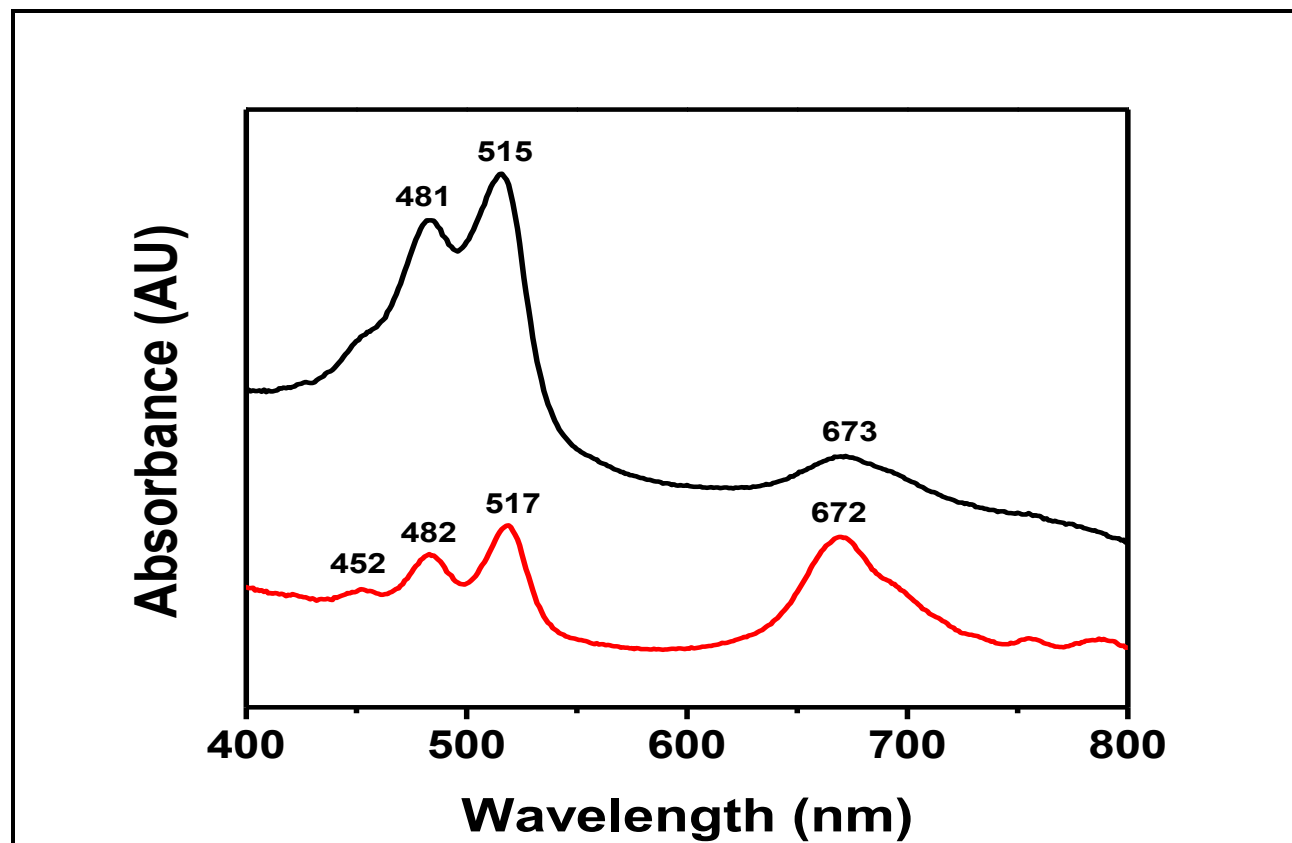


Figure 4-12: overlap of UV-vis absorption of BrPDA in NMP, NMP after M.F

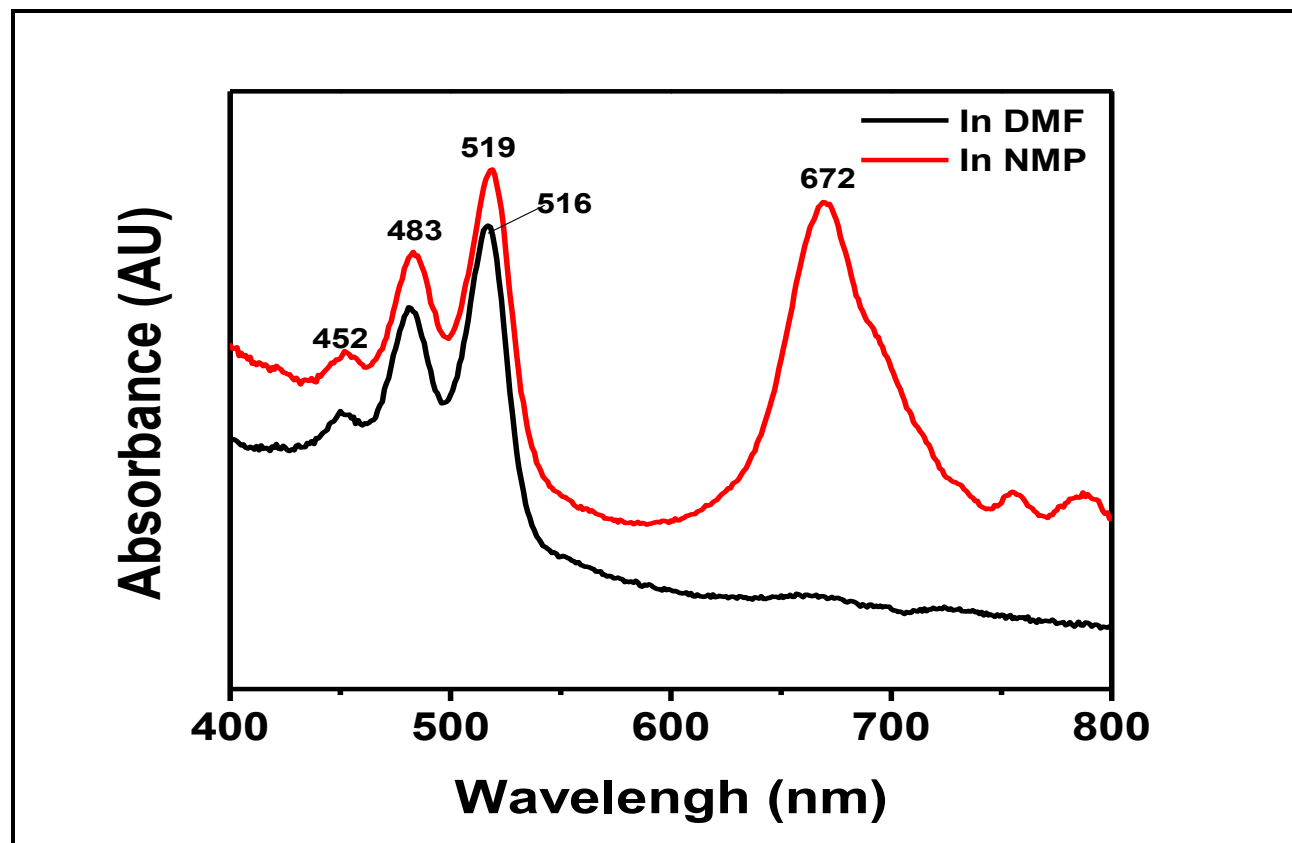


Figure 4-13: overlap of UV-vis absorption of BrPDA in DMF, NMP

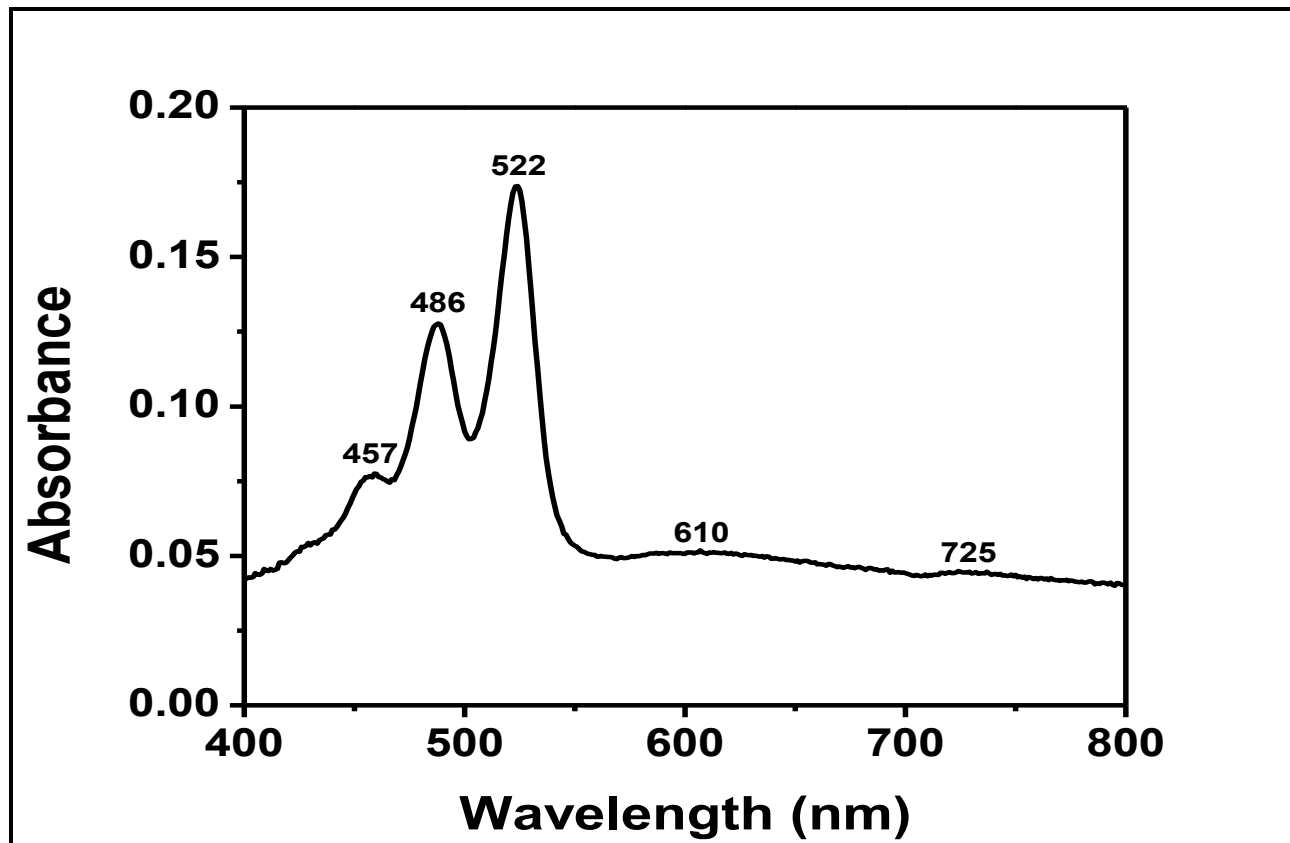


Figure 4-14: UV-vis absorption spectrum of BrPDI in DMF

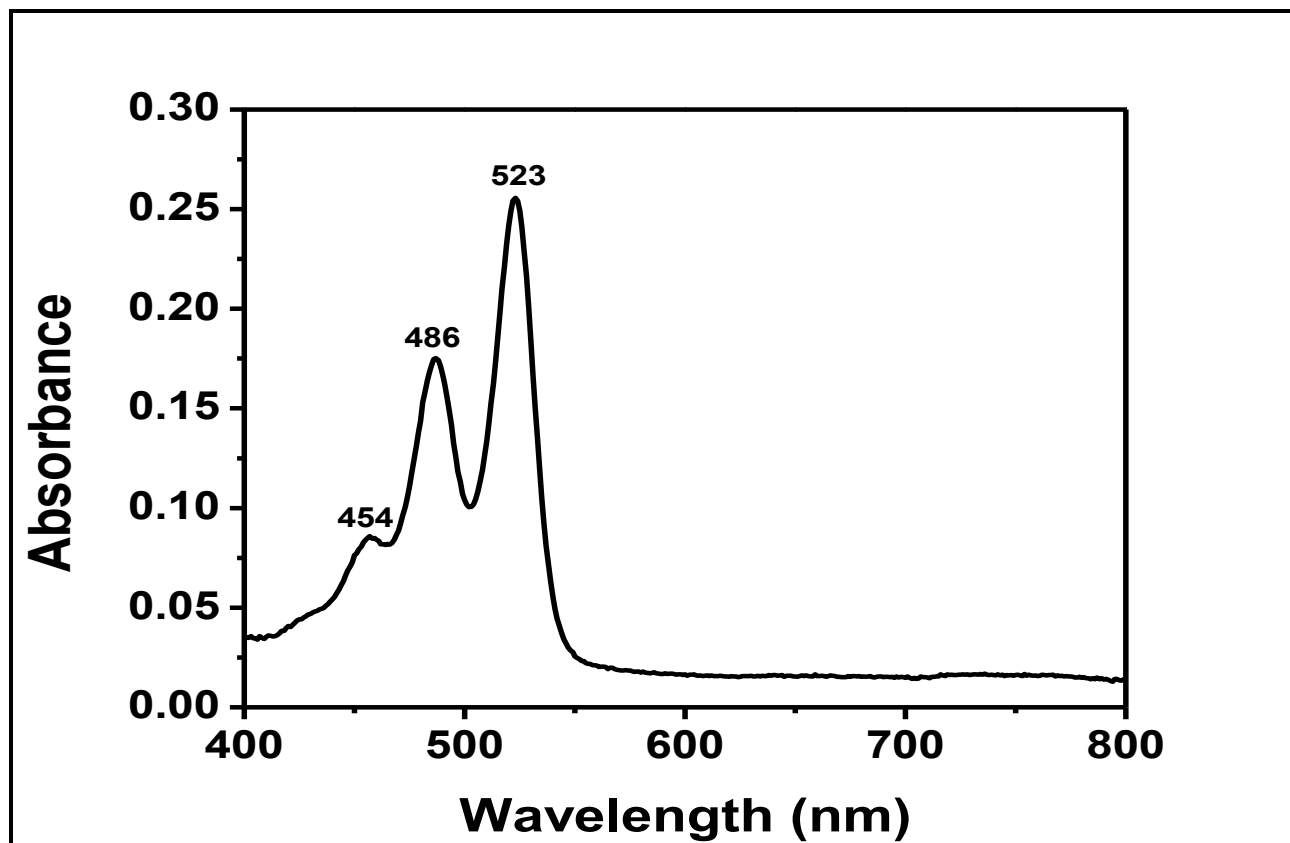


Figure 4-15: UV-vis absorption spectrum of BrPDI in DMF after M.F.

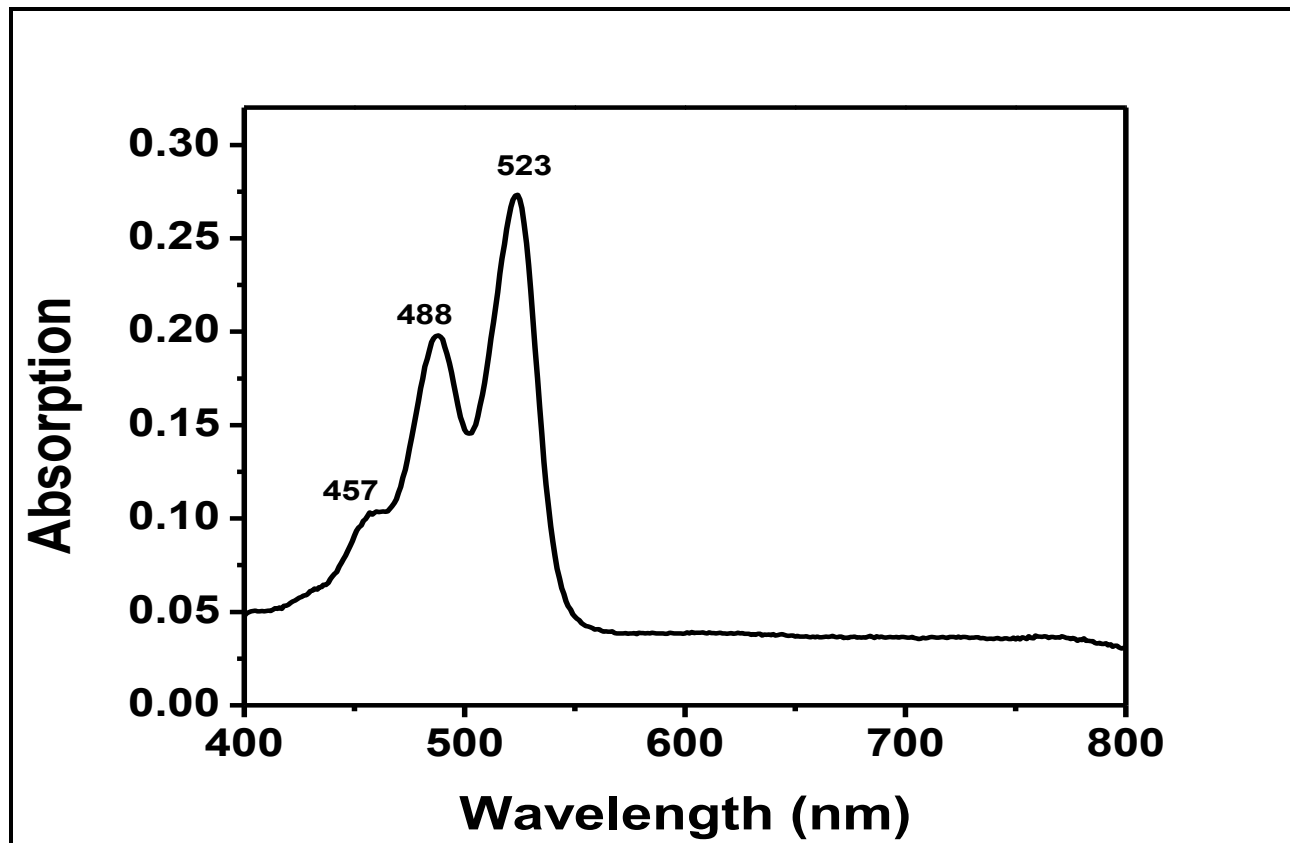


Figure 4-16: UV-vis absorption spectrum of BrPDI in NMP

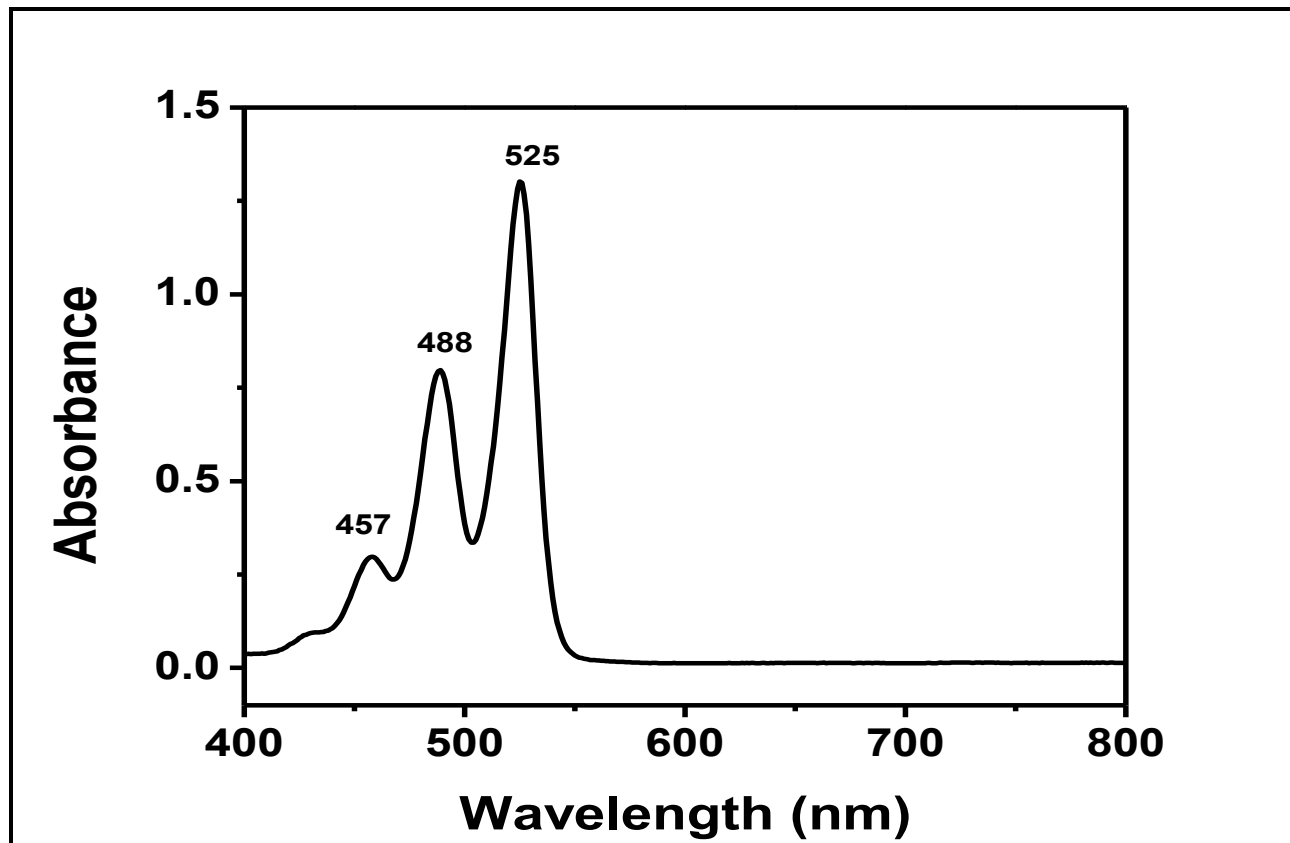


Figure 4-17: UV-vis absorption spectrum of BrPDI in CHL

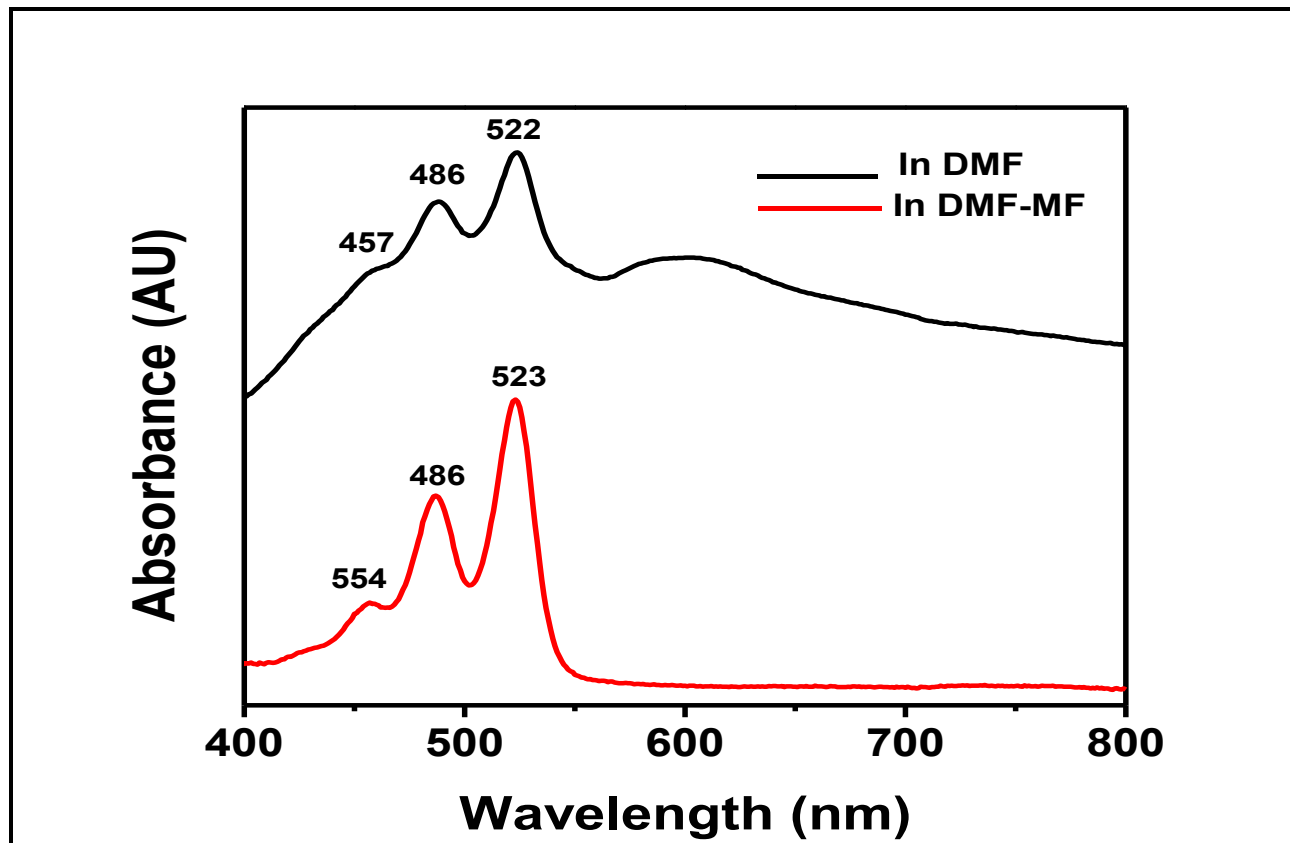


Figure 4-18: UV-vis absorption spectrum of BrPDI in DMF and DMF after micro filtration

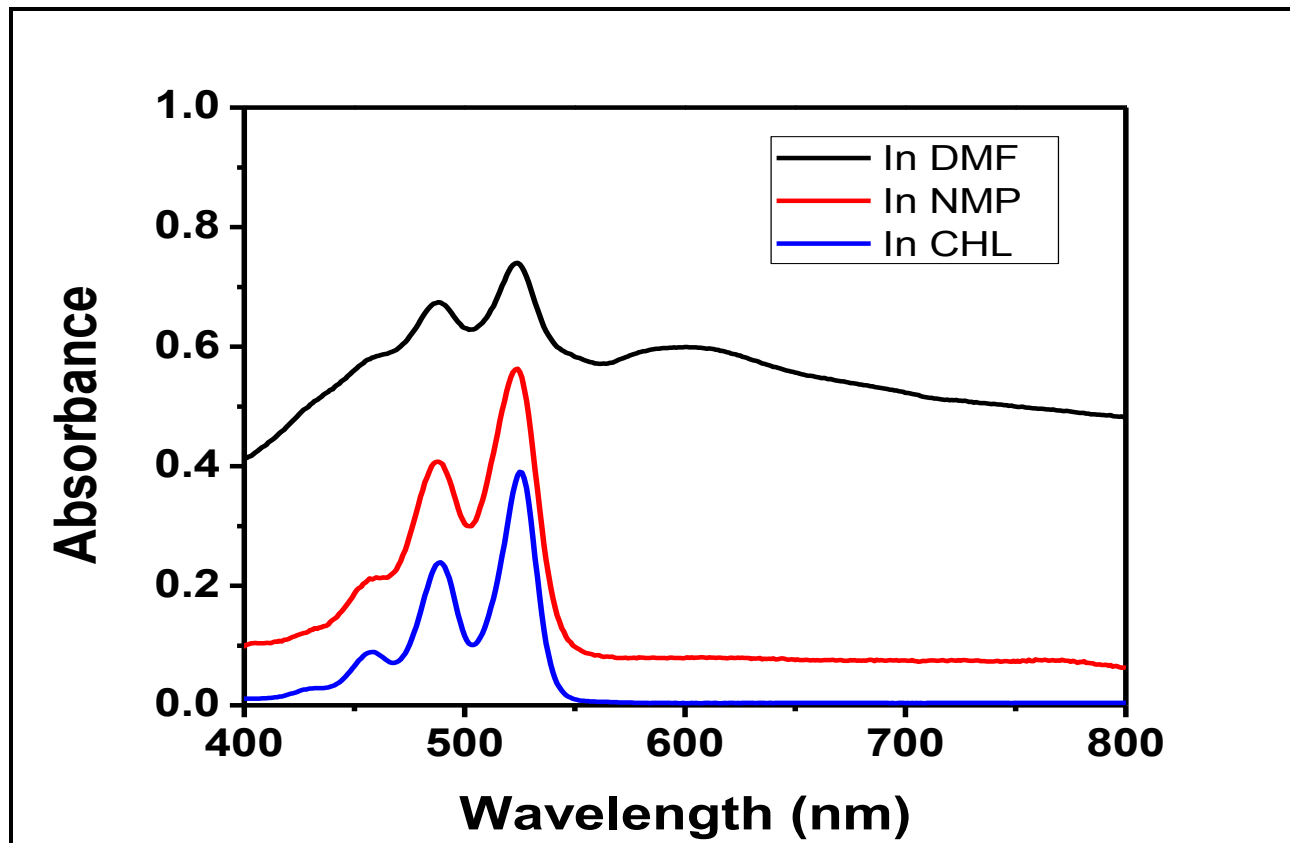


Figure 4-19: UV-vis absorption spectrum of BrPDI in DMF, NMP and CHL

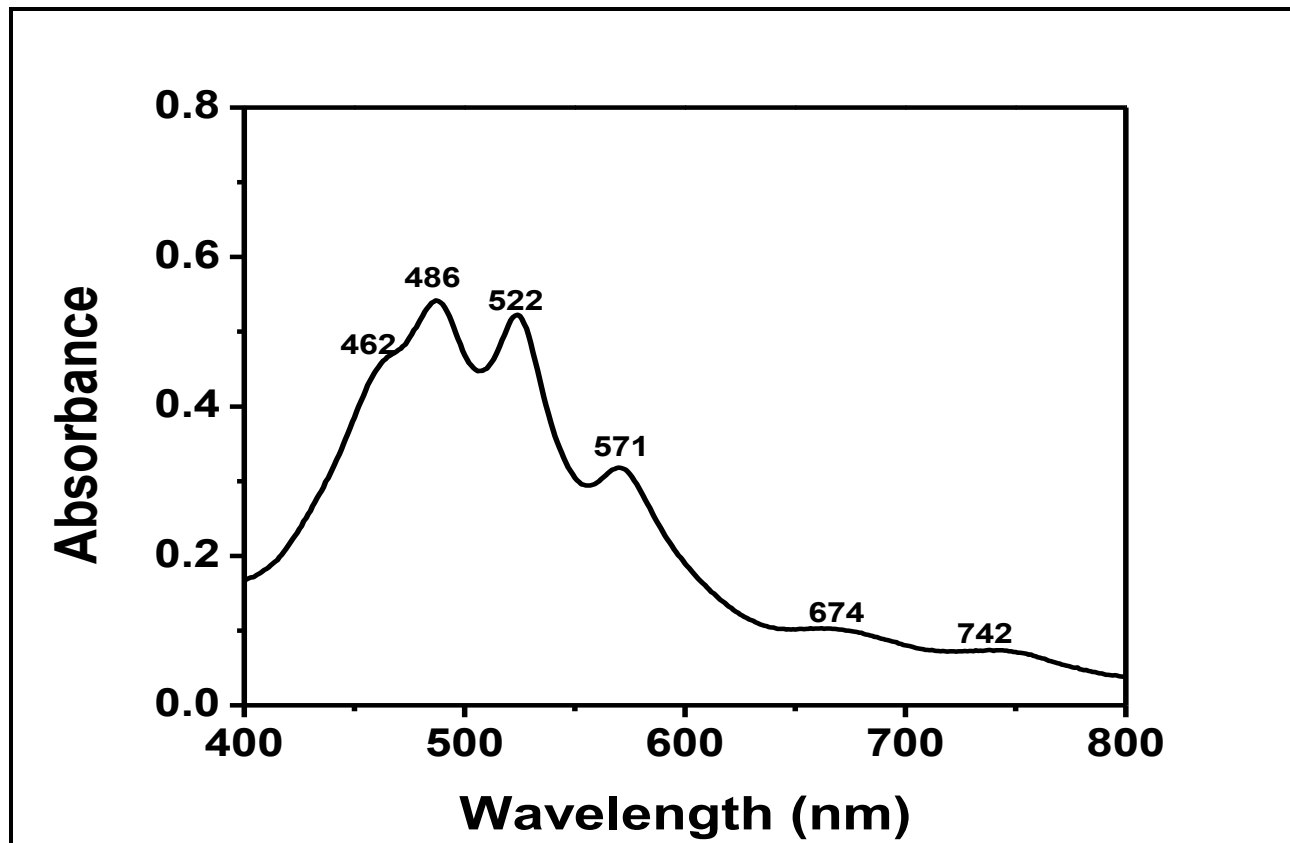


Figure 4-20: UV-vis absorption spectrum of PDI-Decanol in DMF

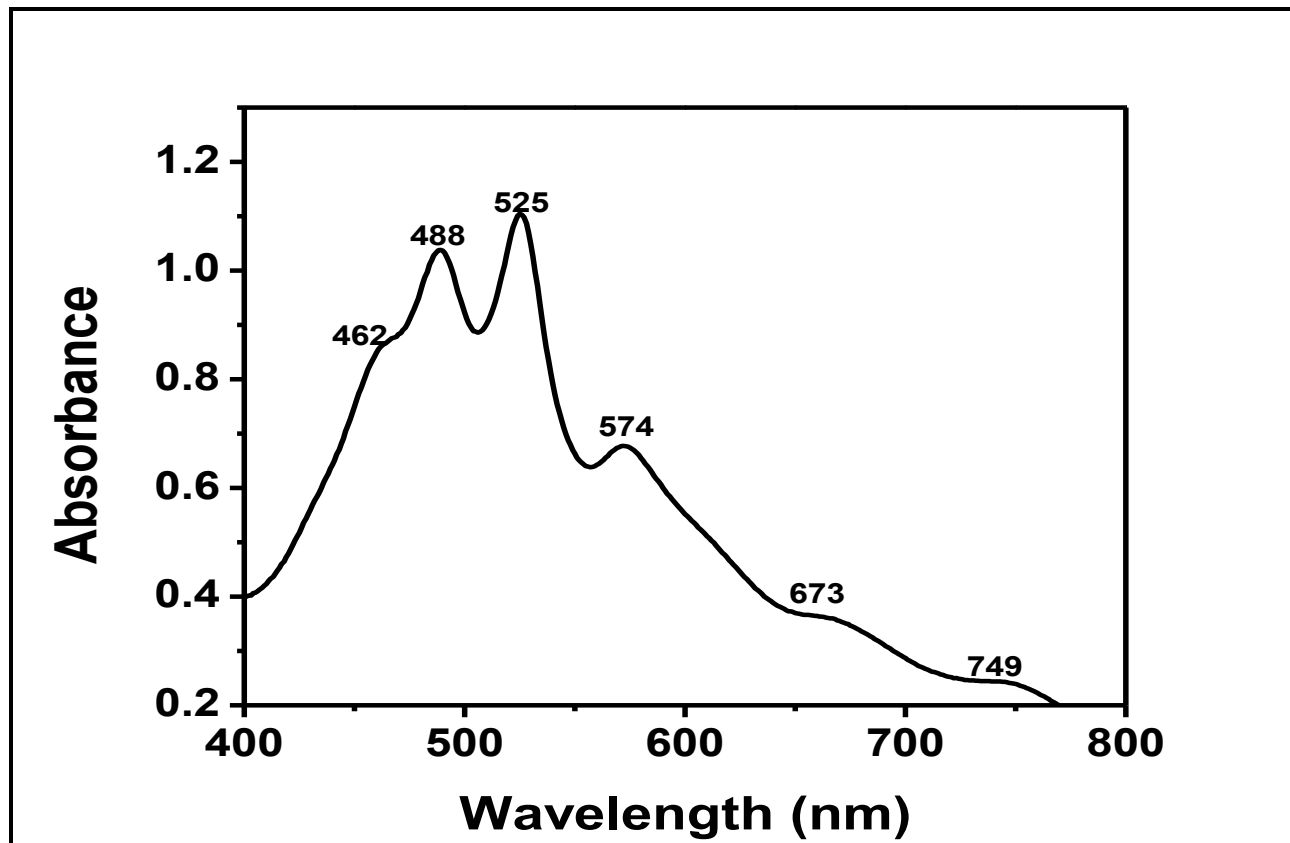


Figure 4-21: UV-vis absorption spectrum of PDI-Decanol in NMP

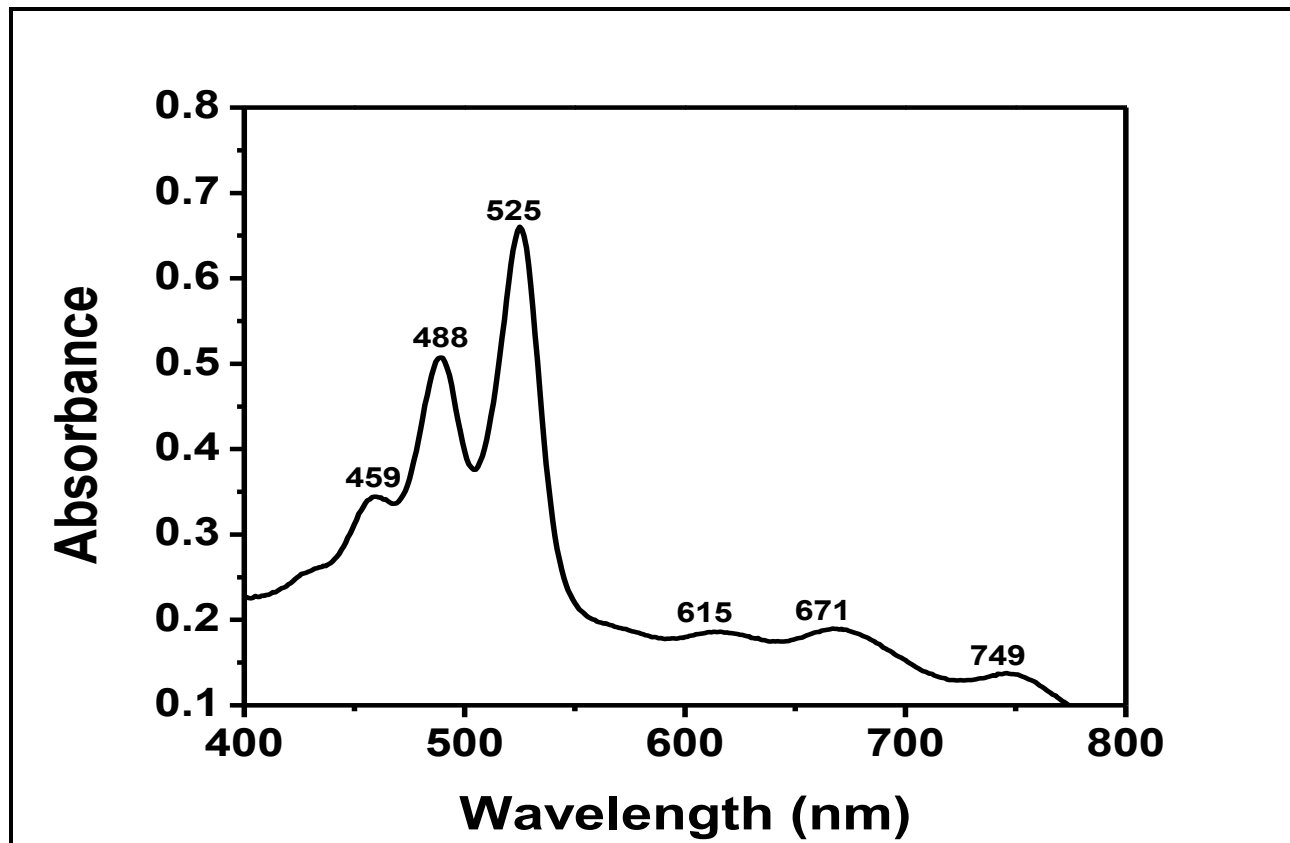


Figure 4-22: UV-vis absorption spectrum of PDI-Decanol in NMP after micro filtration

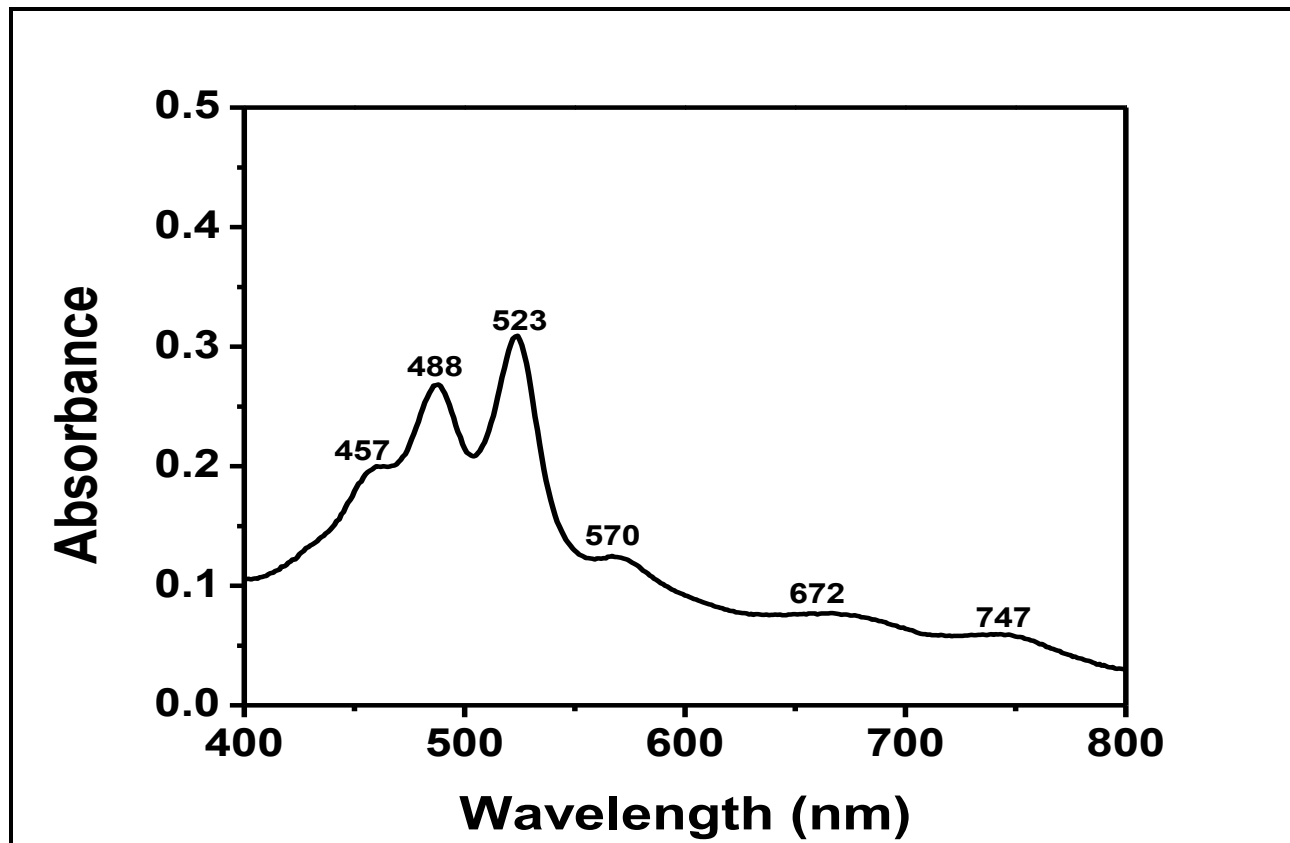


Figure 4-23: UV-vis absorption spectrum of PDI-Decanol in NMP after micro filtration

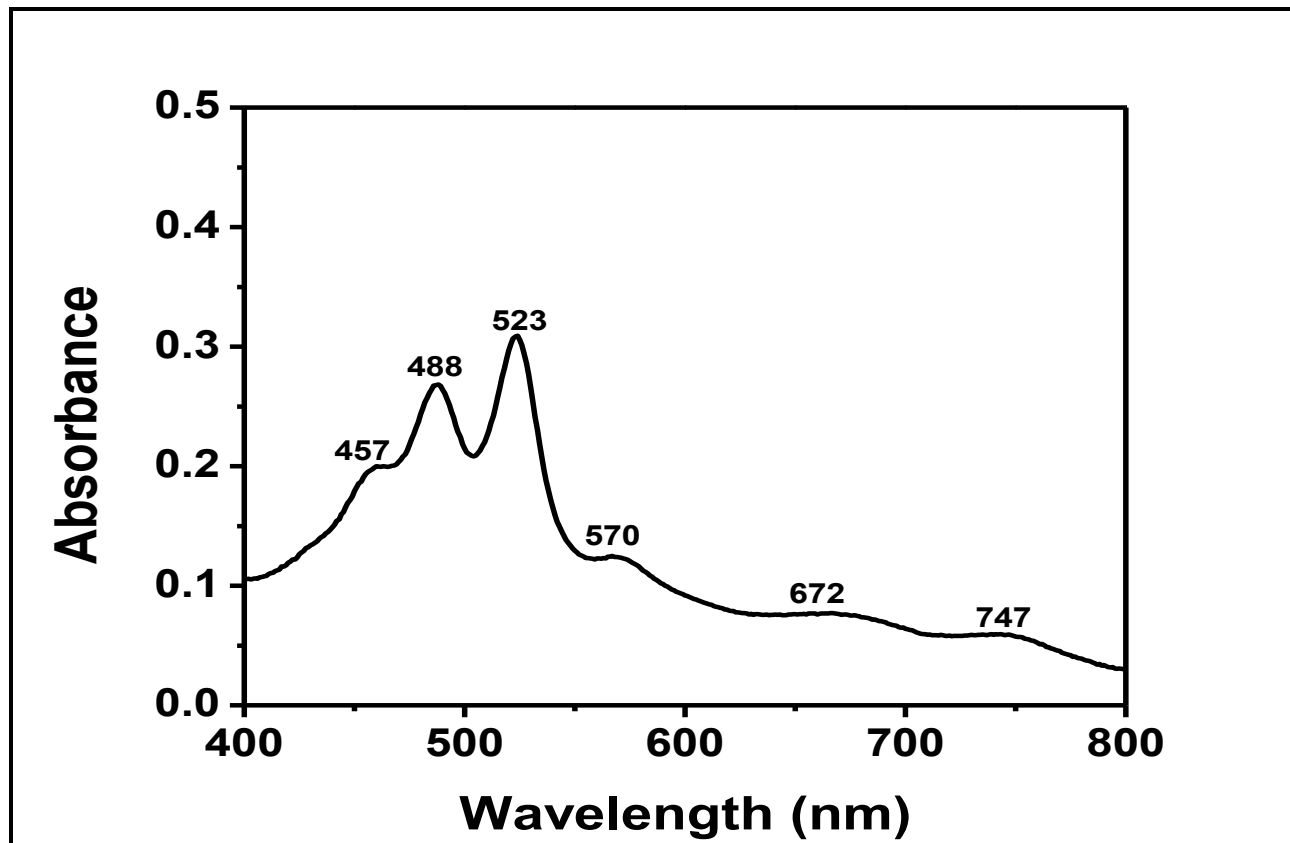


Figure 4-24: UV-vis absorption spectrum of PDI-Decanol in DMF after Micro Filtration

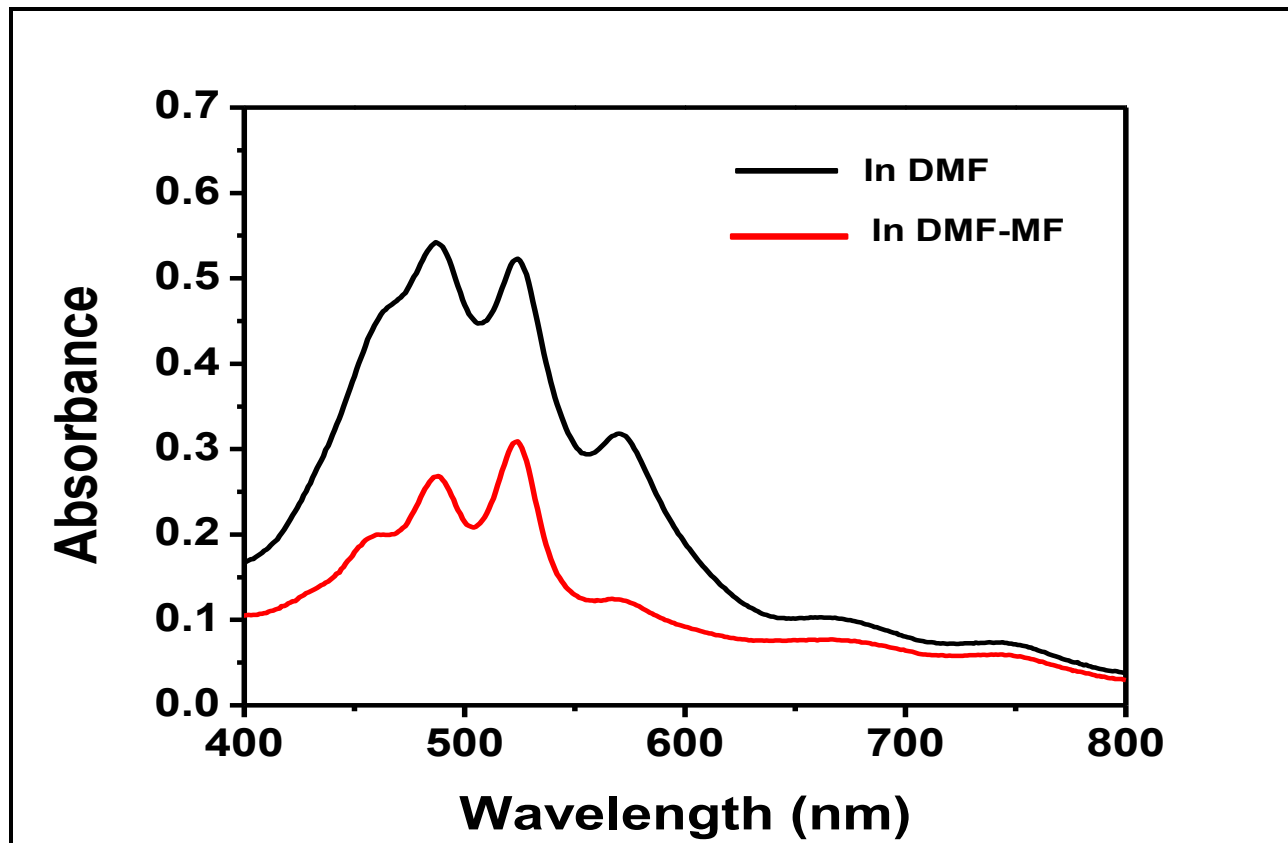


Figure 4-25: UV-vis absorption spectrum overlap of PDI-Decanol in DMF/DMF after Micro Filtration

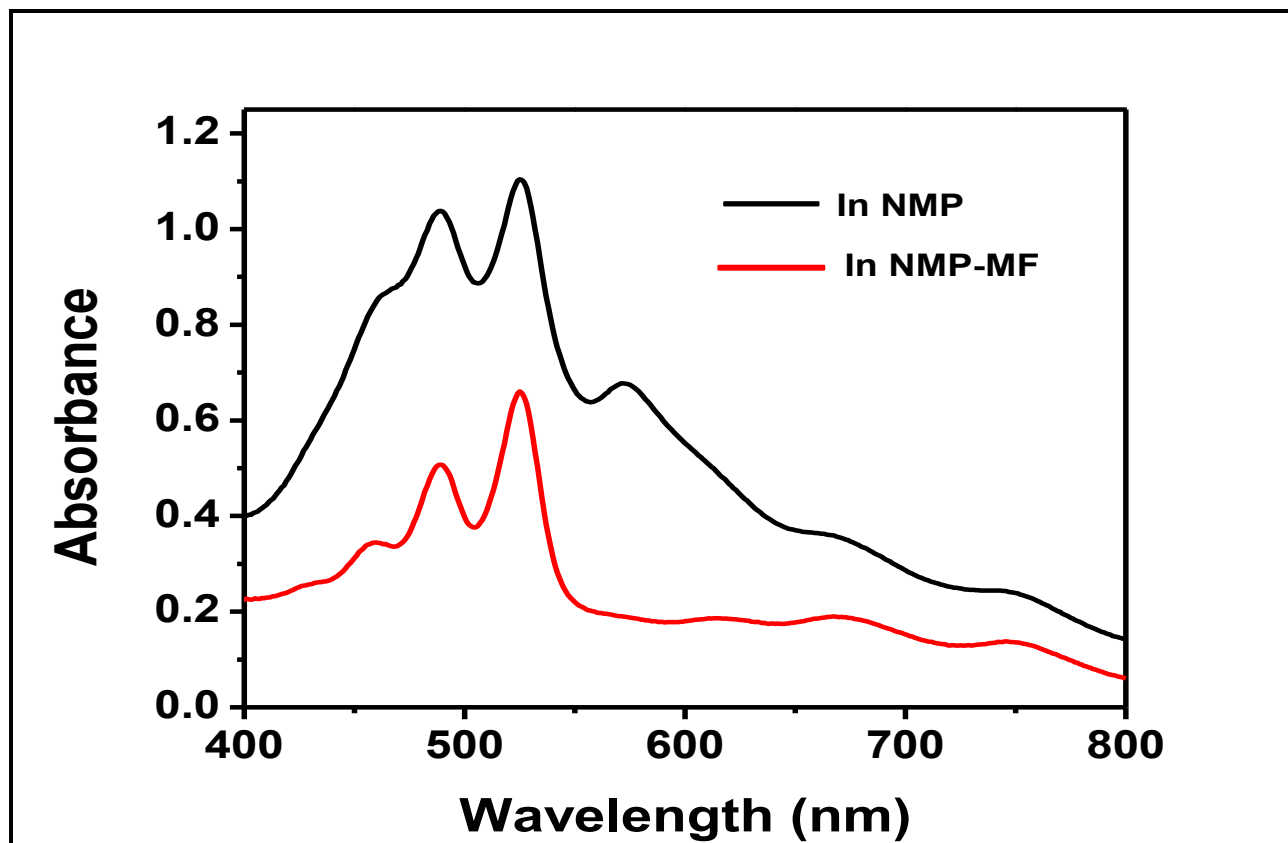


Figure 4-26: UV-vis absorption spectrum overlap of PDI-Decanol in NMP/NMP after Micro Filtration

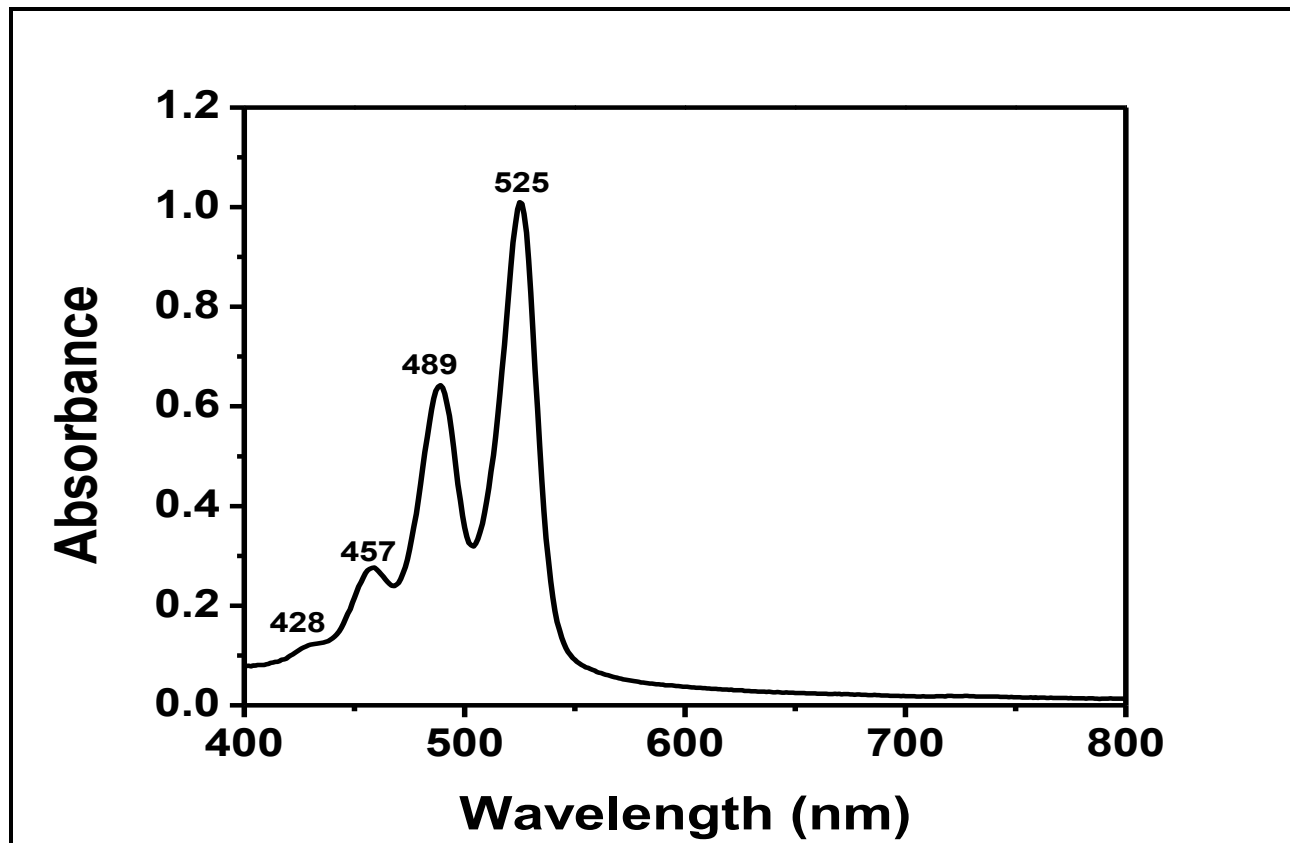


Figure 4-27: UV-vis absorption spectrum of PDI-Decanol in CHL

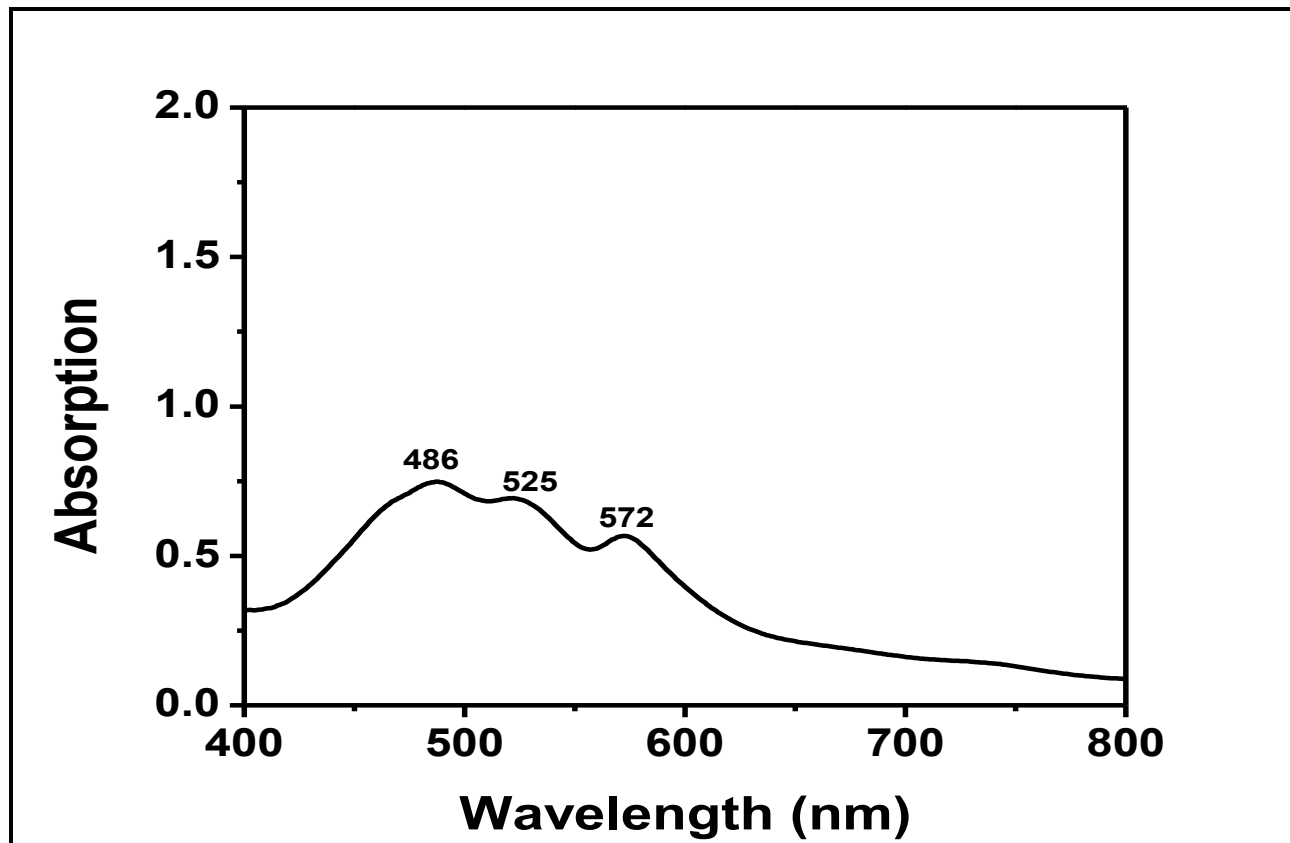


Figure 4-28: UV-vis absorption spectrum of PDI-Decanol in EtOH

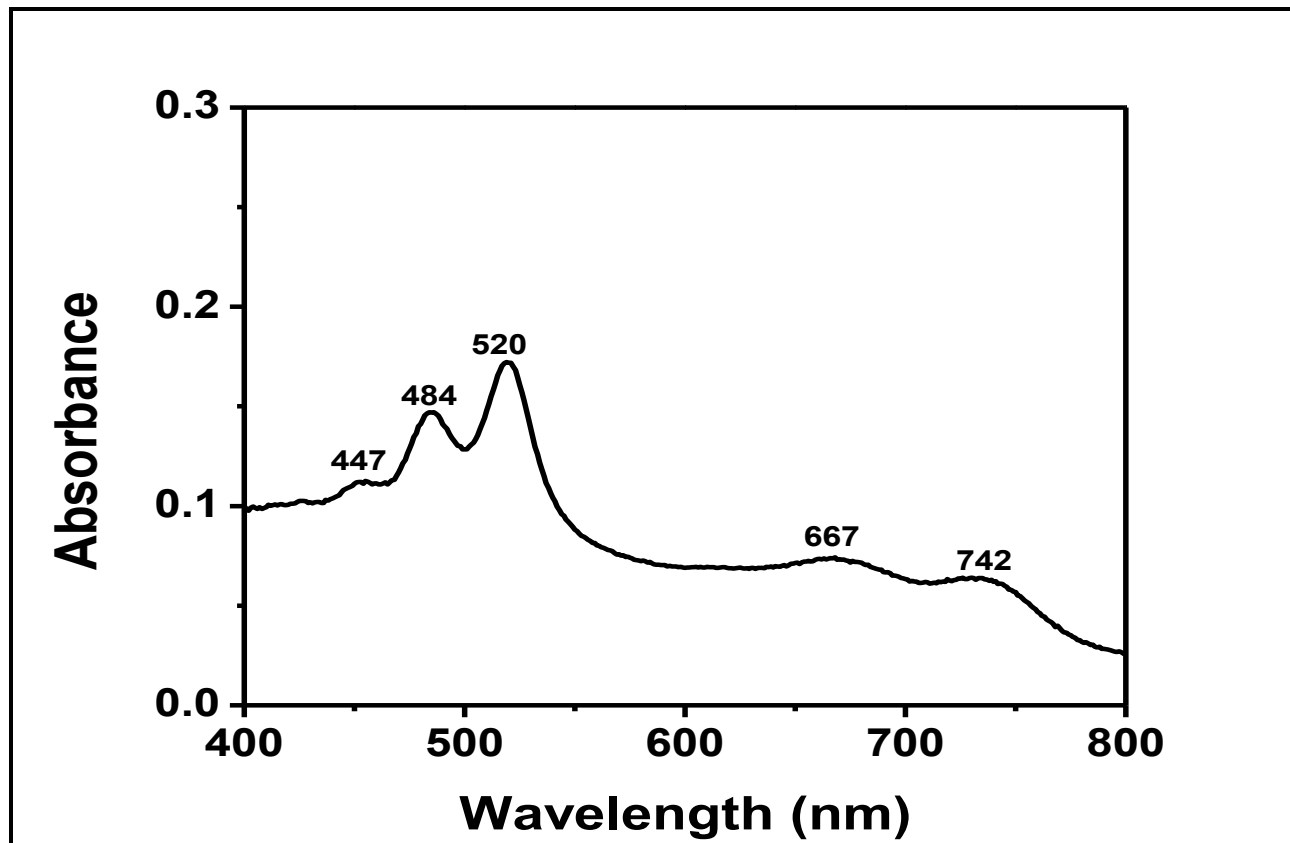


Figure 4-29: UV-vis absorption spectrum of PDI-Decanol in EtOH after Micro filtration

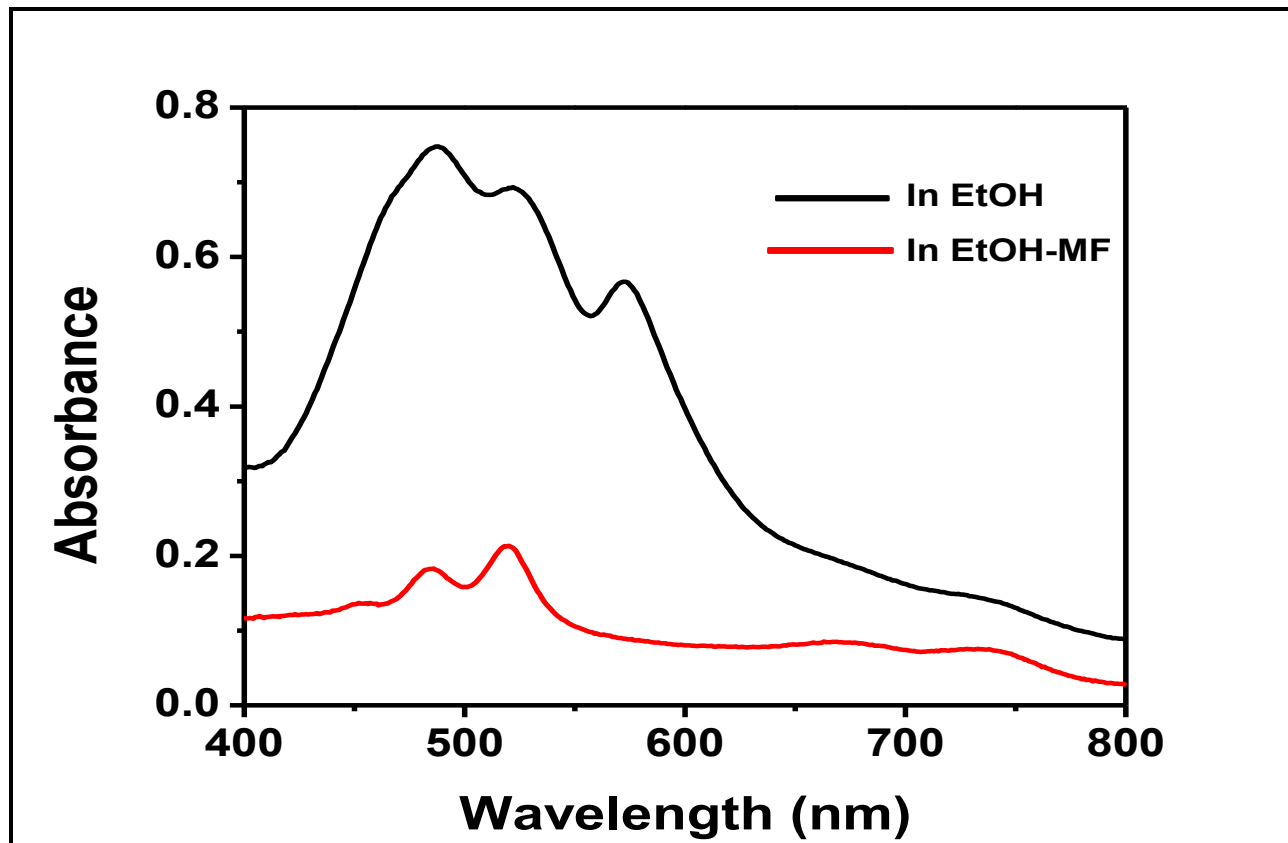


Figure 4-30: UV-vis absorption spectrum overlap of PDI-Decanol in EtOH/EtOH after Micro Filtration

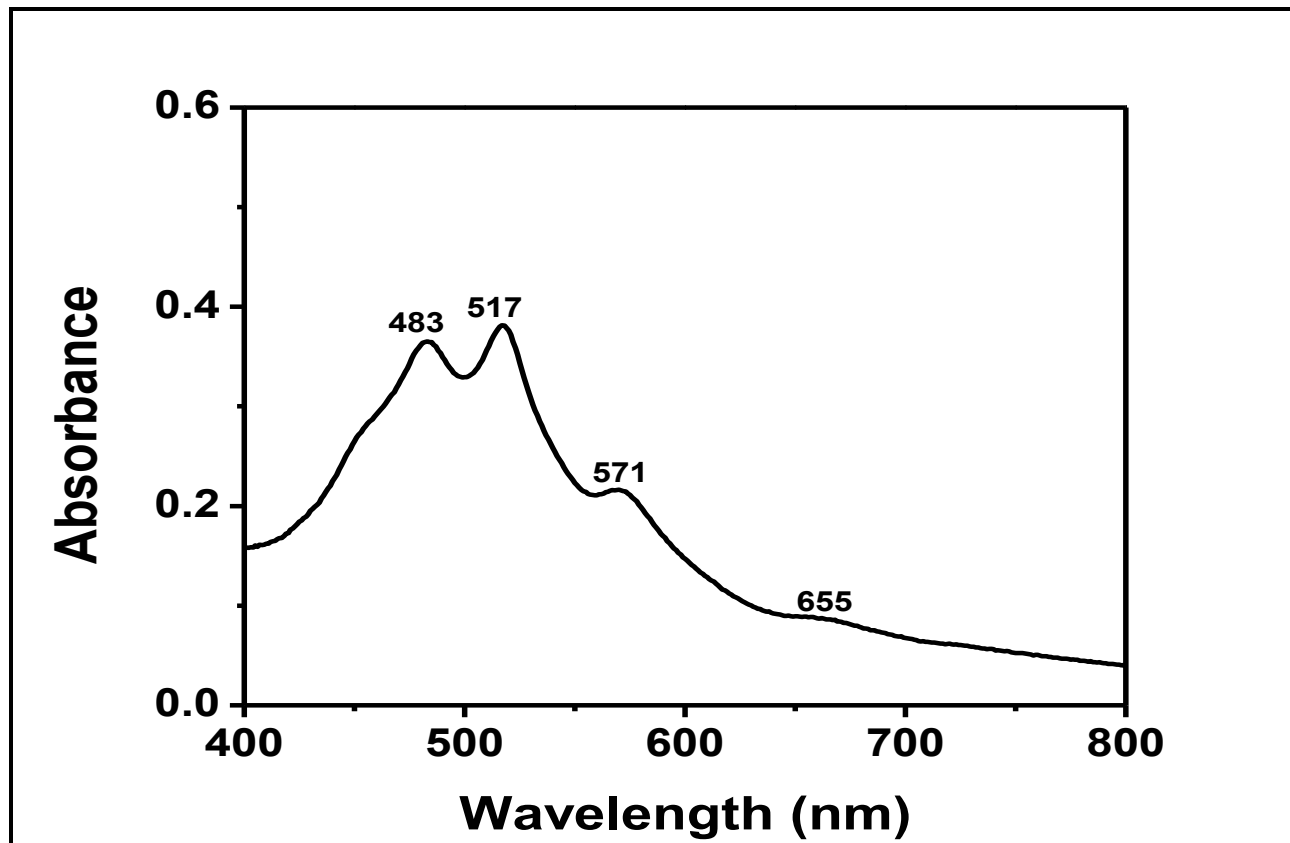


Figure 4-31: UV-Visible absorption spectrum of PDI-Decanol in Acetone

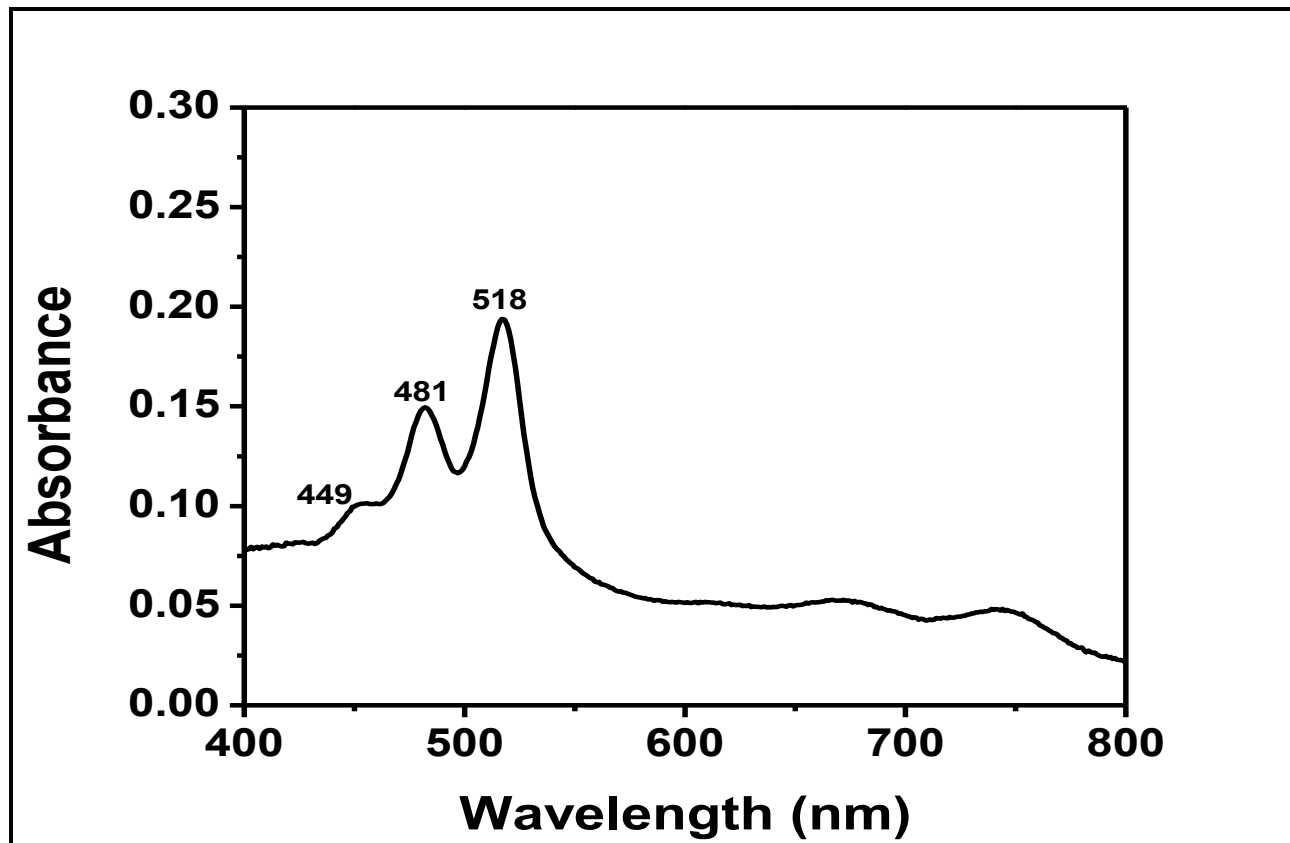


Figure 4-32: UV-Visible absorption spectrum of PDI-Decanol in Acetone after Micro Filtration

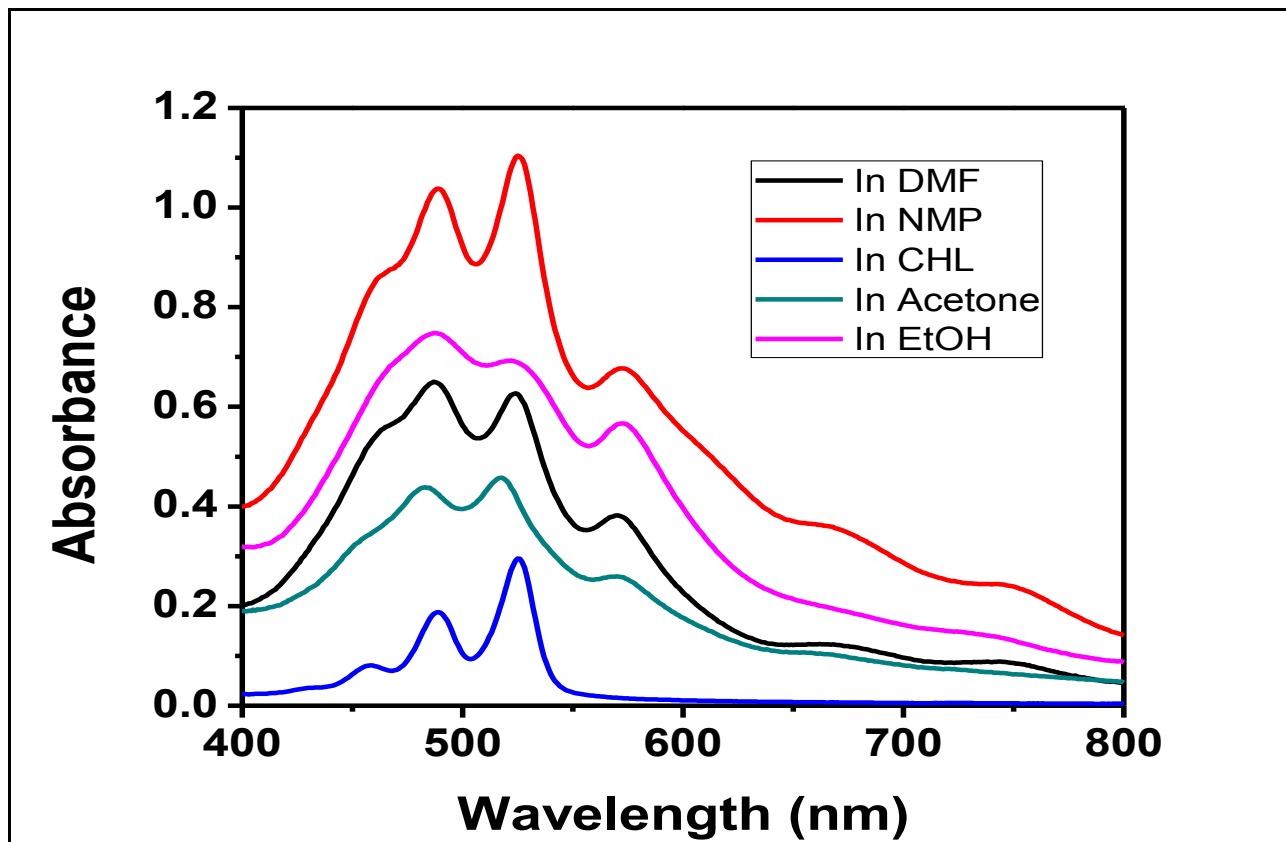


Figure 4-33: UV-Visible absorption spectrum of PDI-Decanol in DMF, NMP, CHL, EtOH AND Acetone

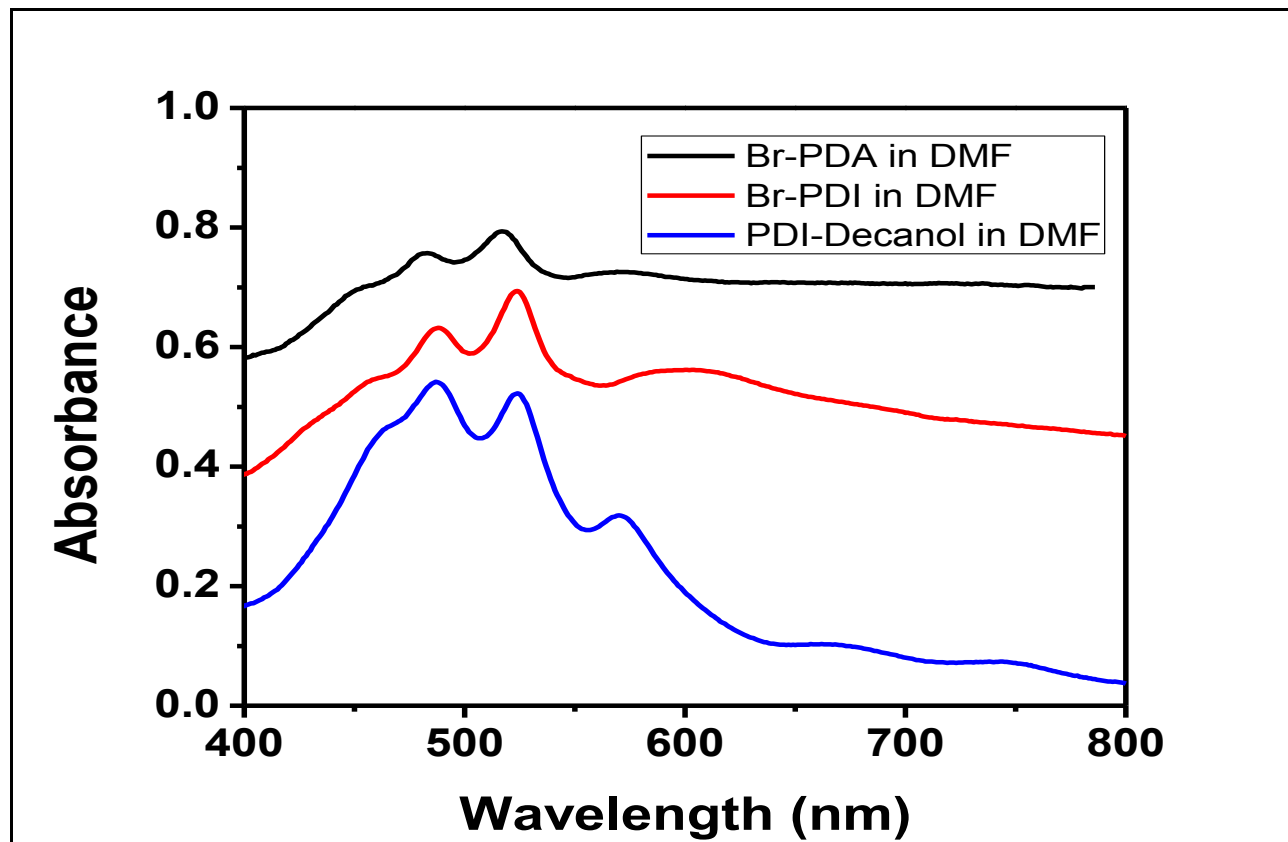


Figure 4-34: UV-Visible absorption spectrum of PDI-Decanol, BrPDI and BrPDA in DMF

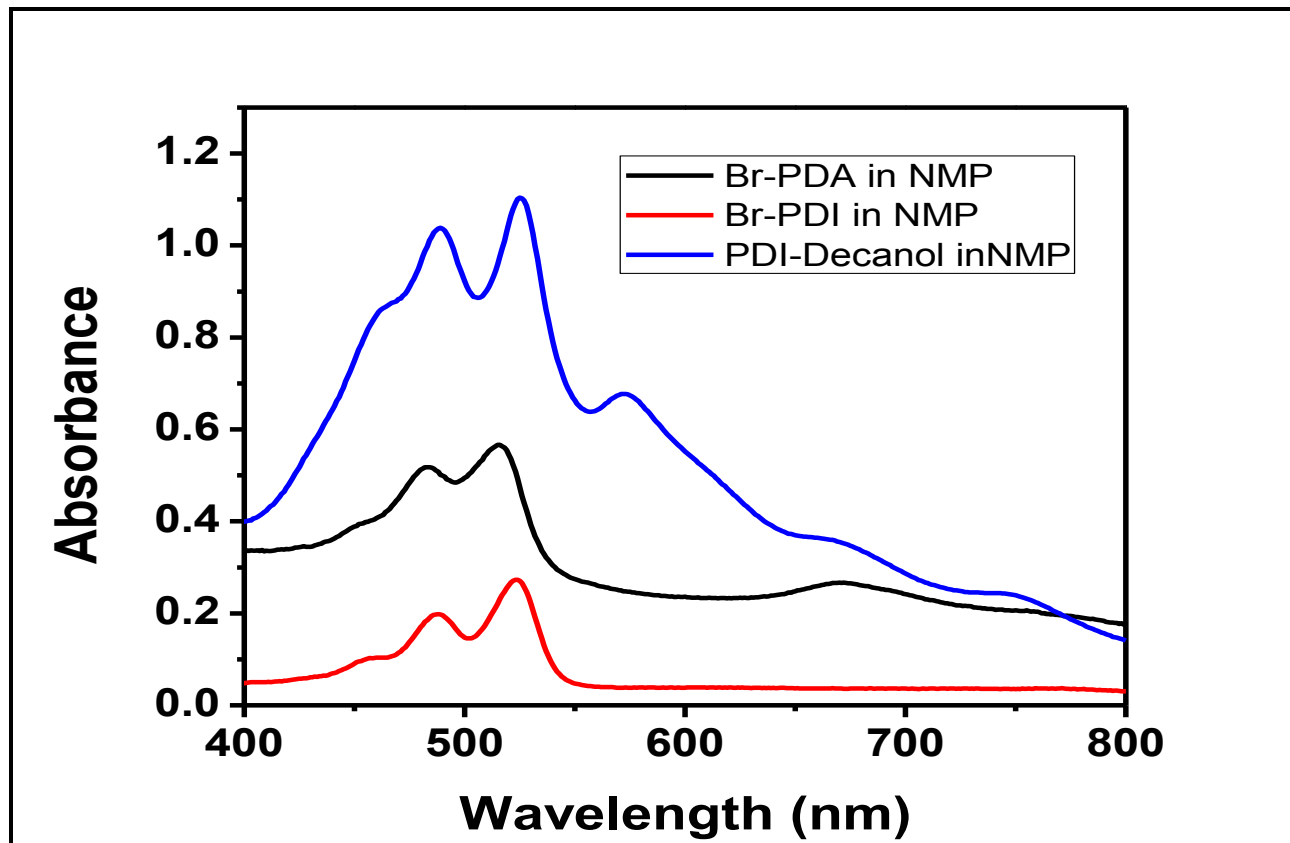


Figure 4-35: UV-Visible absorption spectrum of PDI-Decanol, BrPDI and BrPDA in NMP

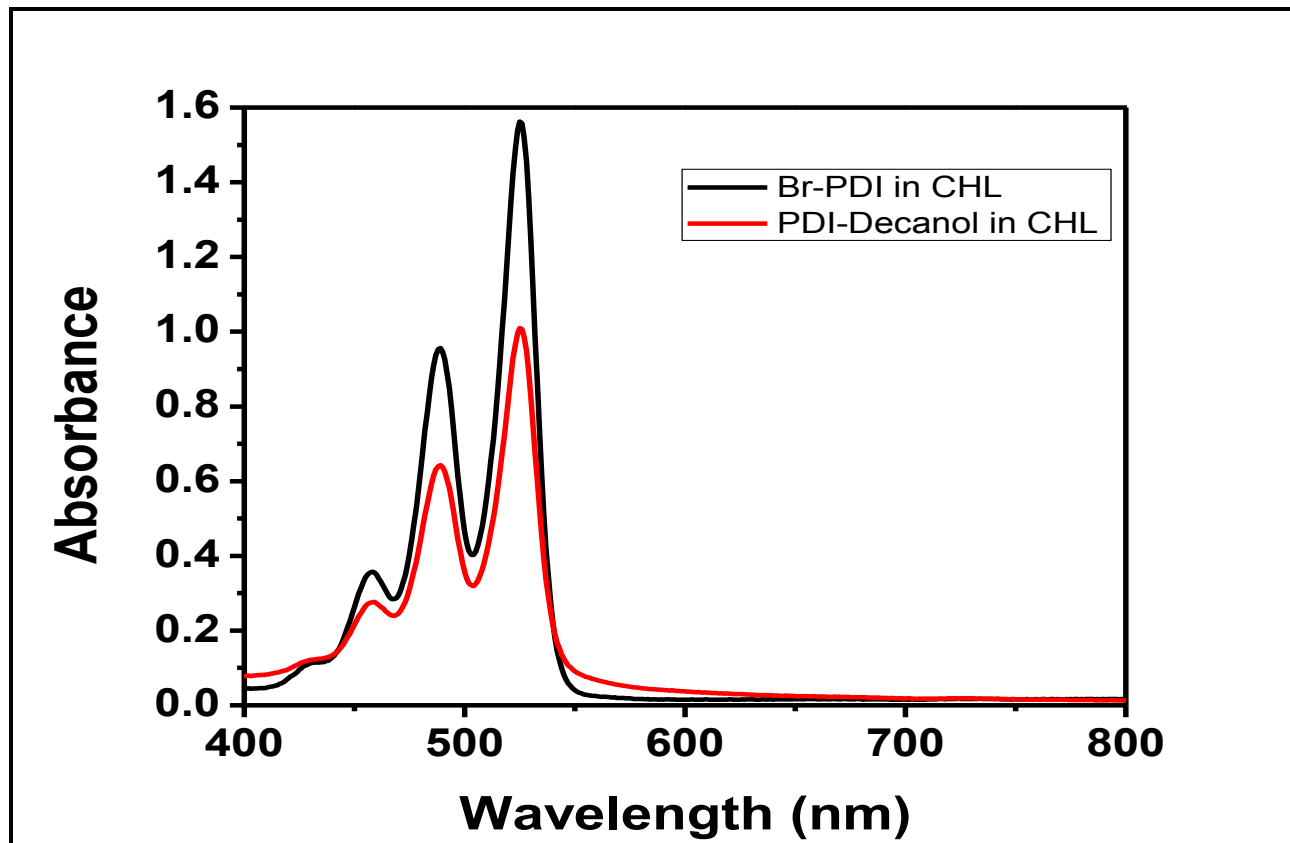


Figure 4-36: UV-Visible absorption spectrum of PDI-Decanol, BrPDI in CHL

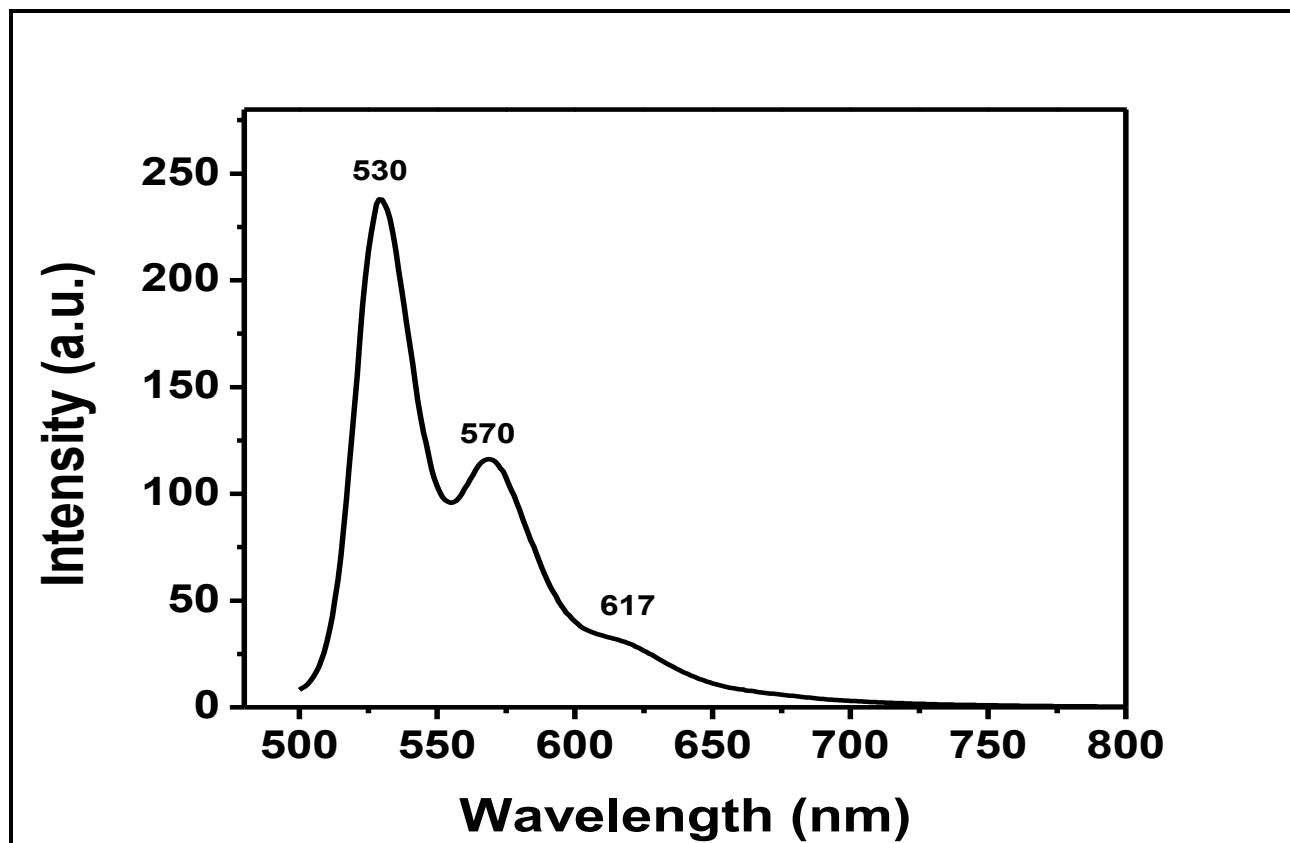


Figure 4-37: Emission spectrum ($\lambda_{exc}=485\text{nm}$) of BrPDA in DMF

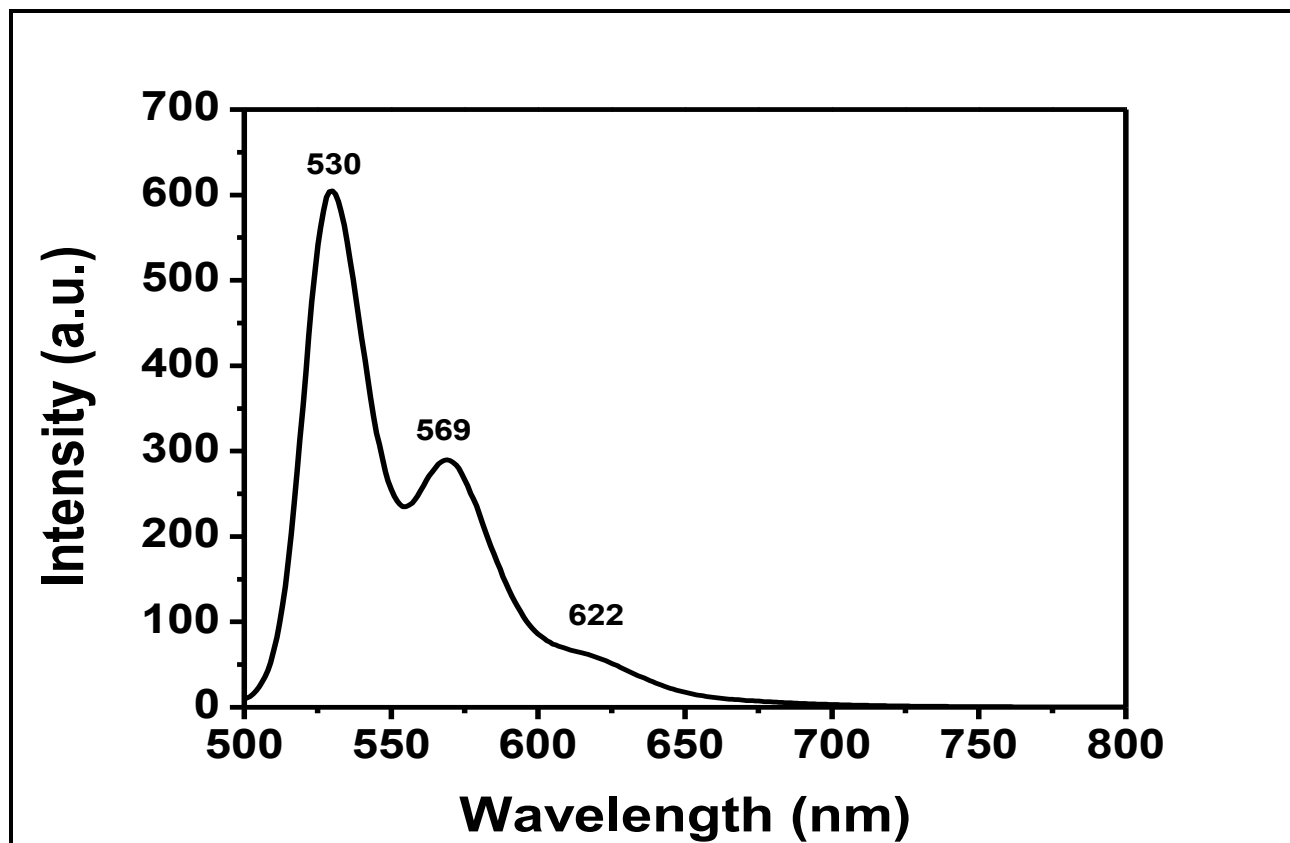


Figure 4-38: Emission spectrum ($\lambda_{exc}=485\text{nm}$) of BrPDA in DMF after micro filtration

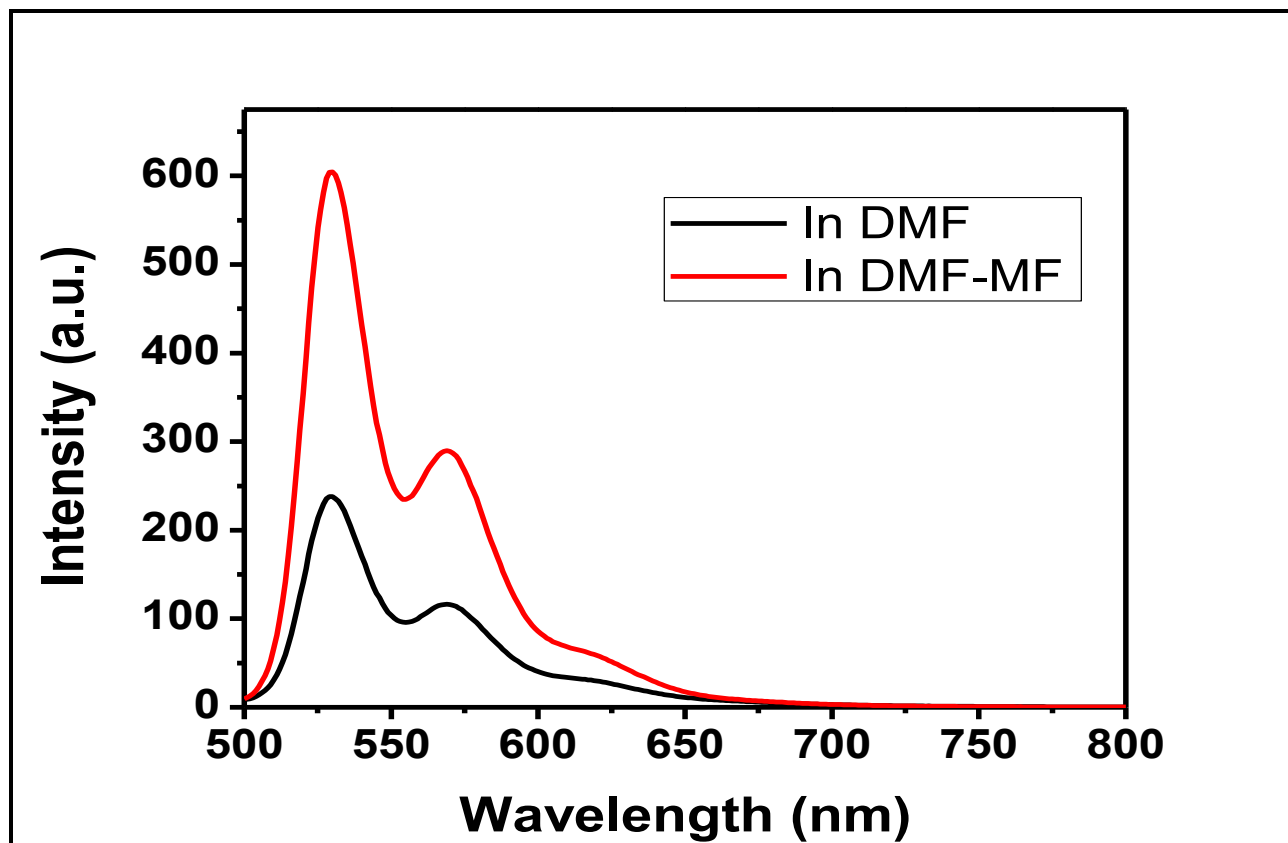


Figure 4-39: Emission spectrum ($\lambda_{exc}=485\text{nm}$) of BrPDA in DMF and in DMF after micro filtration

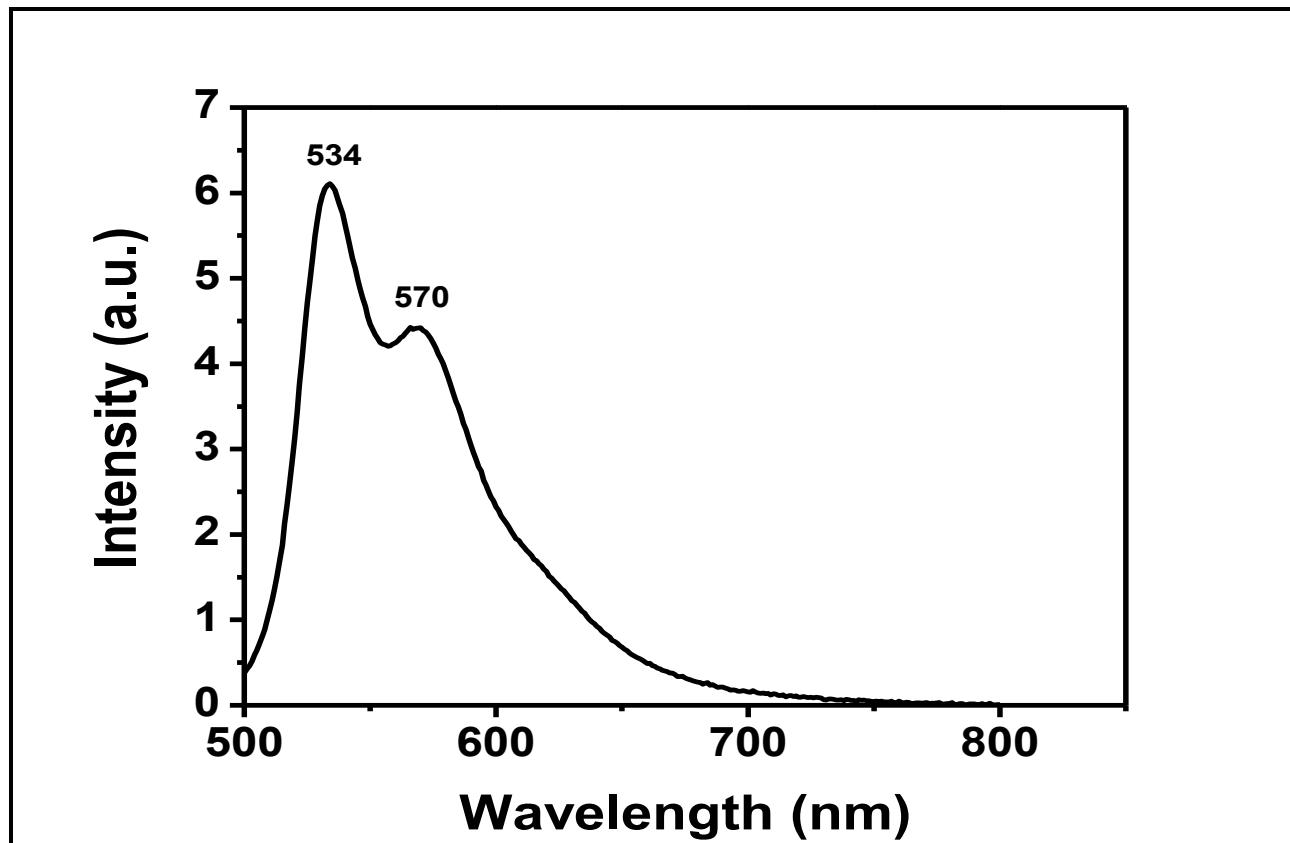


Figure 4-40: Emission spectrum ($\lambda_{exc}=485\text{nm}$) of BrPDA in NMP

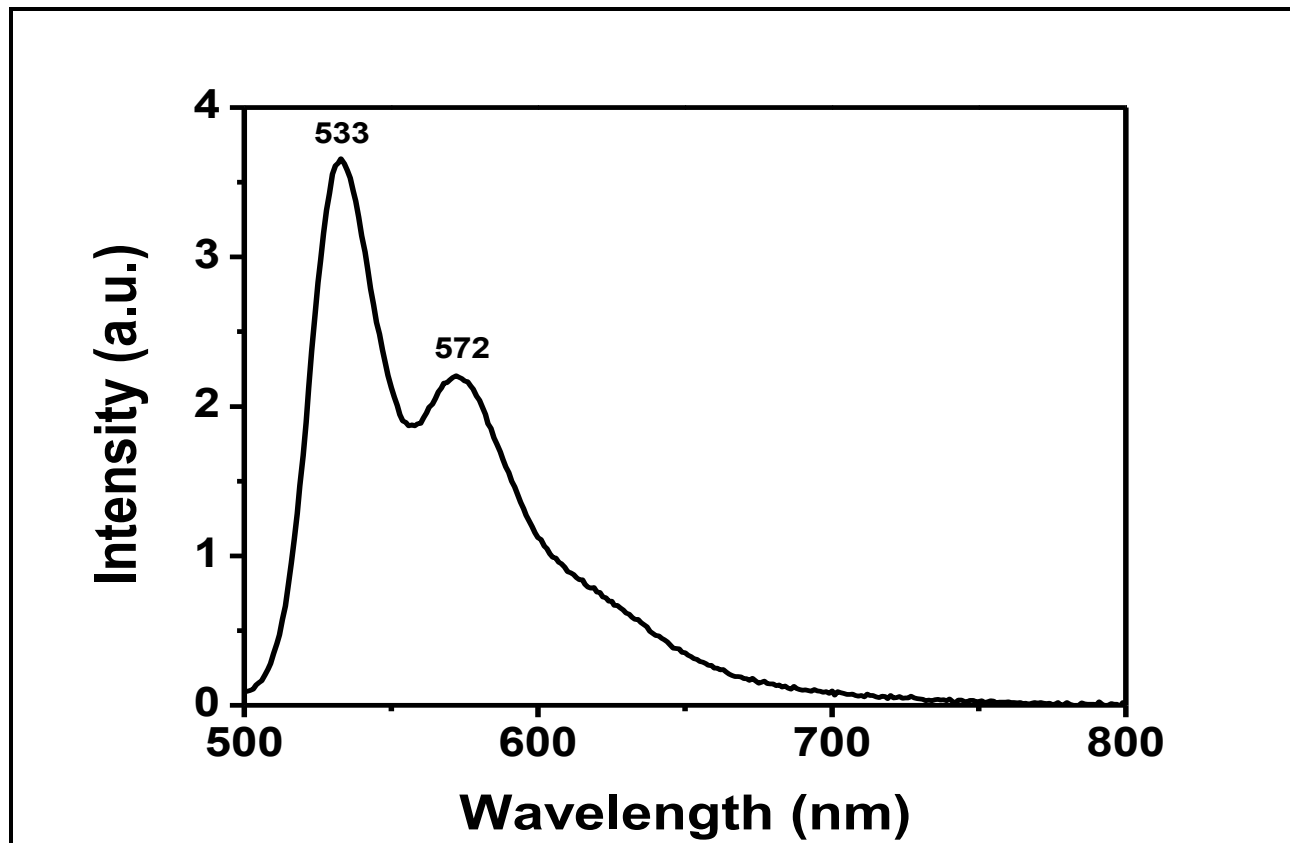


Figure 4-41: Emission spectrum ($\lambda_{exc}=485\text{nm}$) of BrPDA in NMP after micro filtration

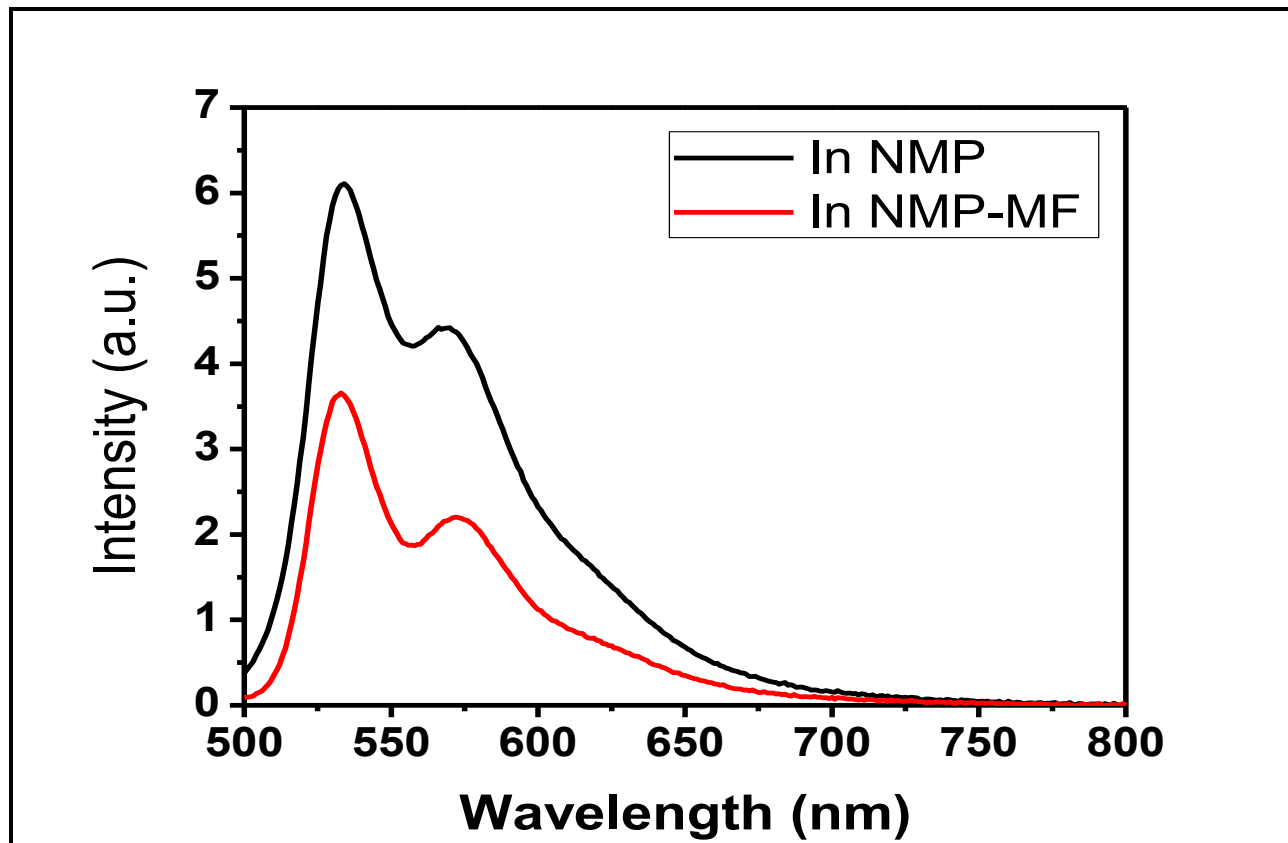


Figure 4-42: Emission spectrum ($\lambda_{exc}=485\text{nm}$) of BrPDA in NMP and in NMP after micro filtration

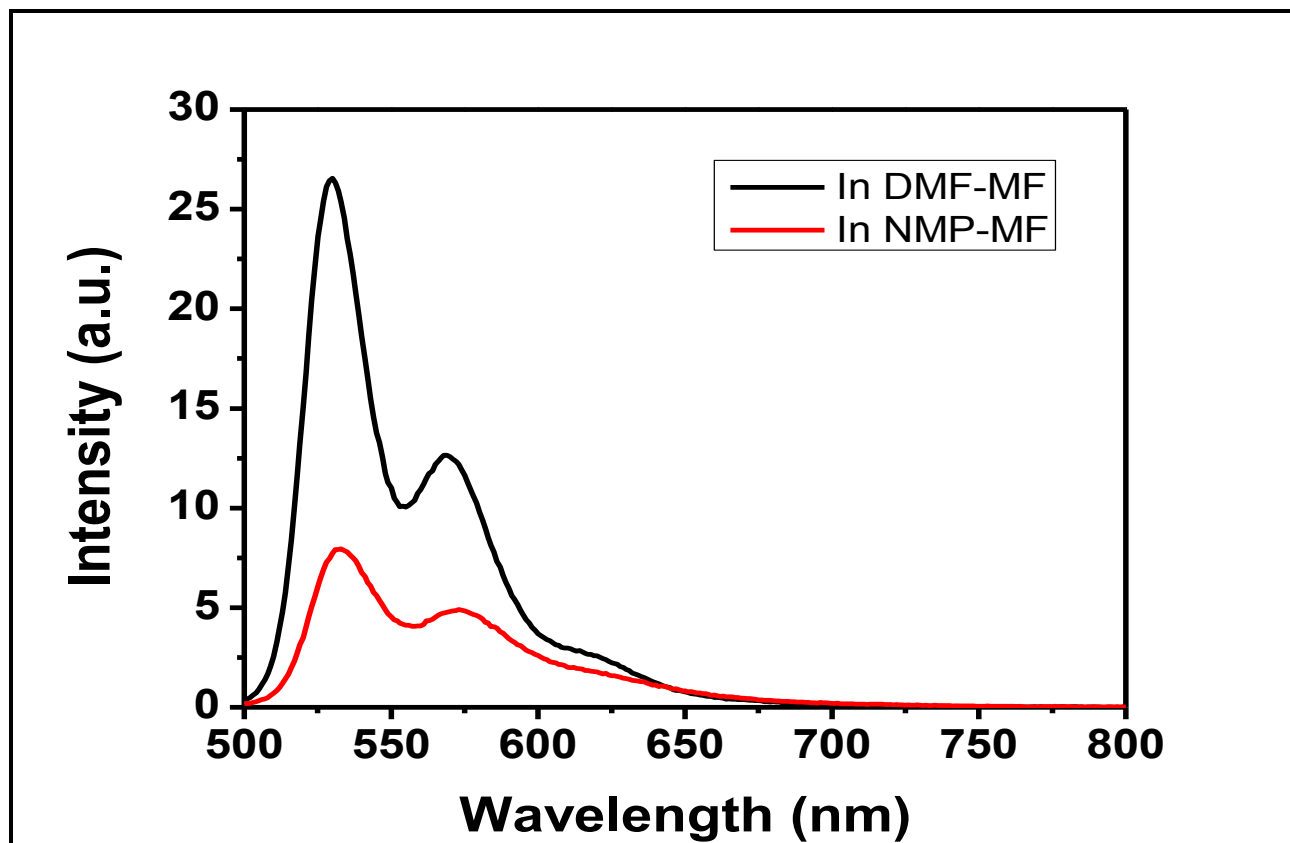


Figure 4-43: Emission spectrum ($\lambda_{exc}=485\text{nm}$) of BrPDA in NMP and in DMF

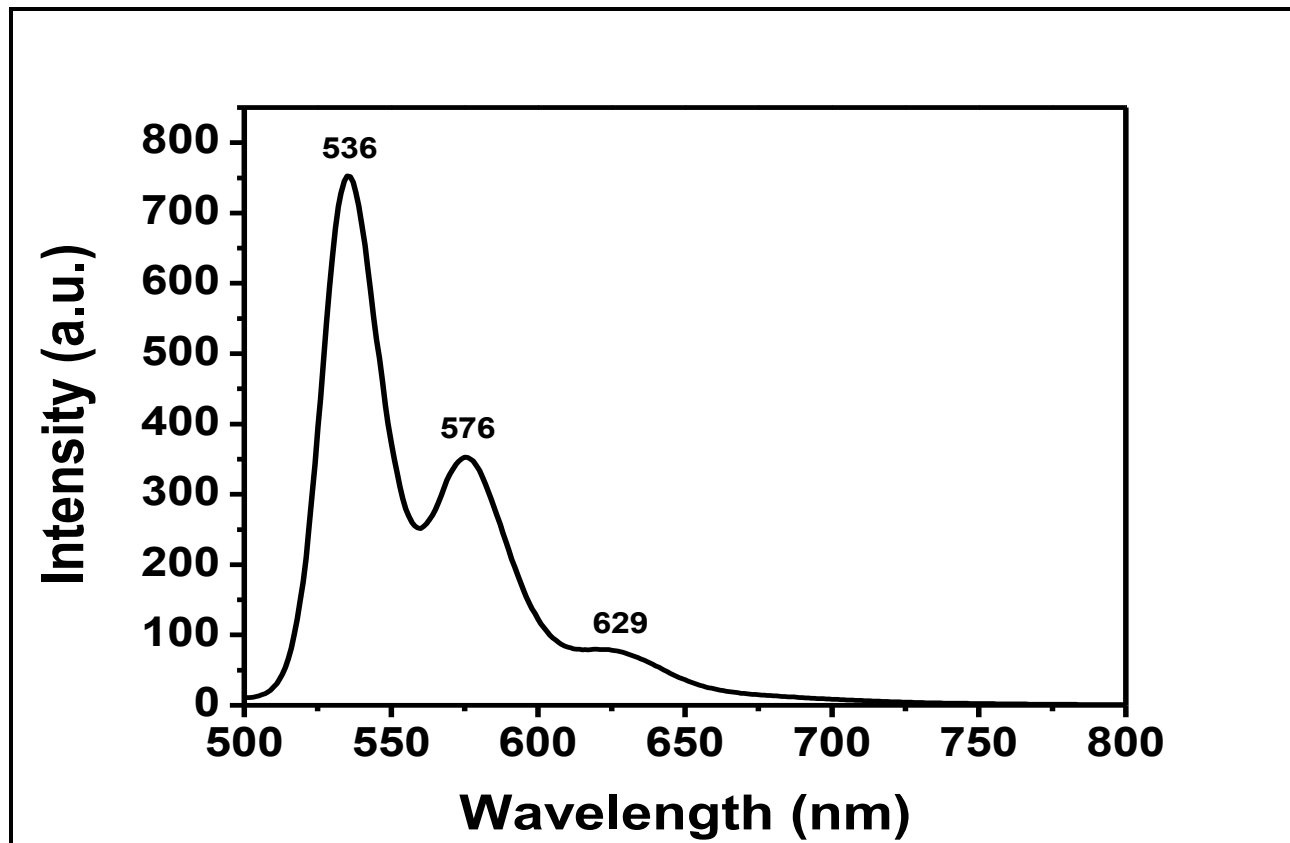


Figure 4-44: Emission spectrum ($\lambda_{exc}=485\text{nm}$) of BrPDI in DMF

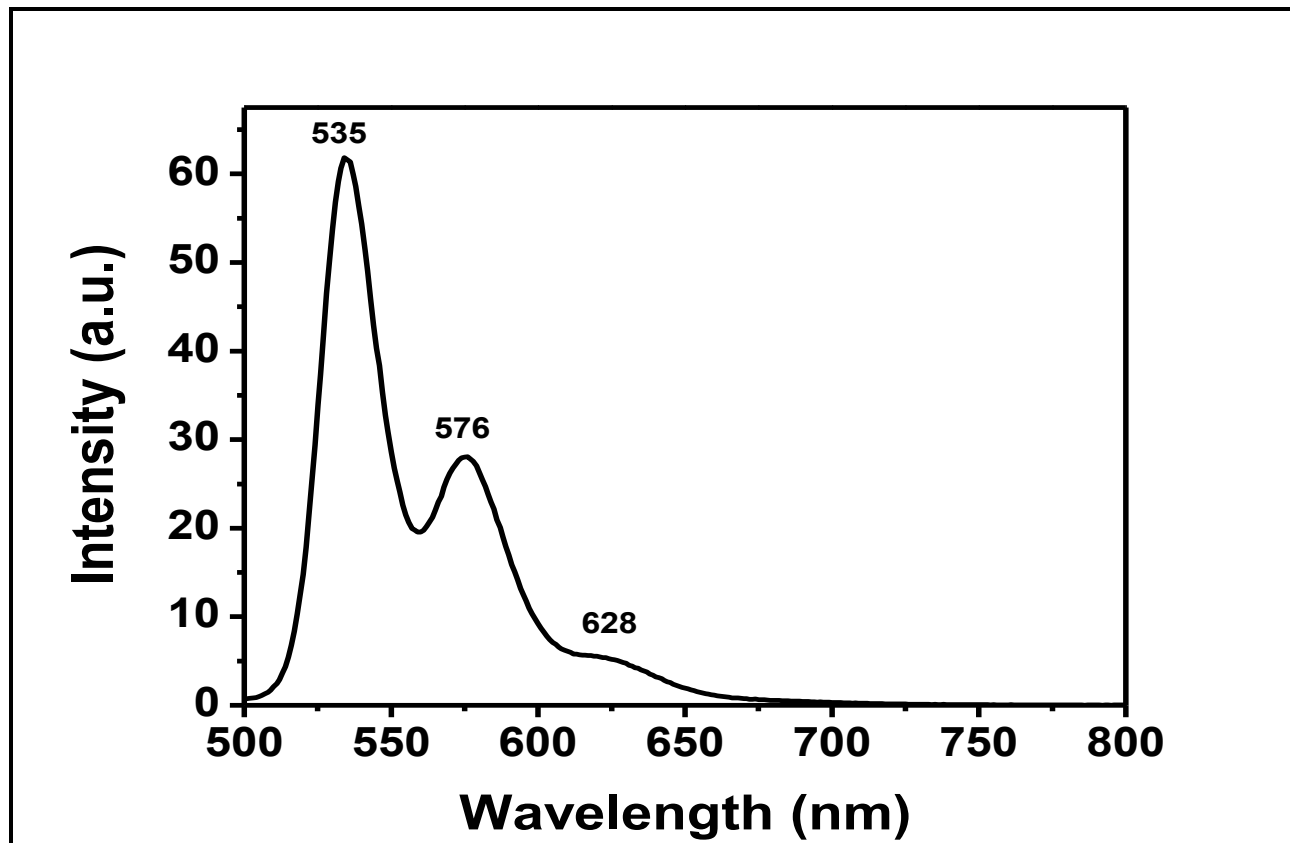


Figure 4-45: Emission spectrum ($\lambda_{exc}=485\text{nm}$) of BrPDI in DMF after micro filtration

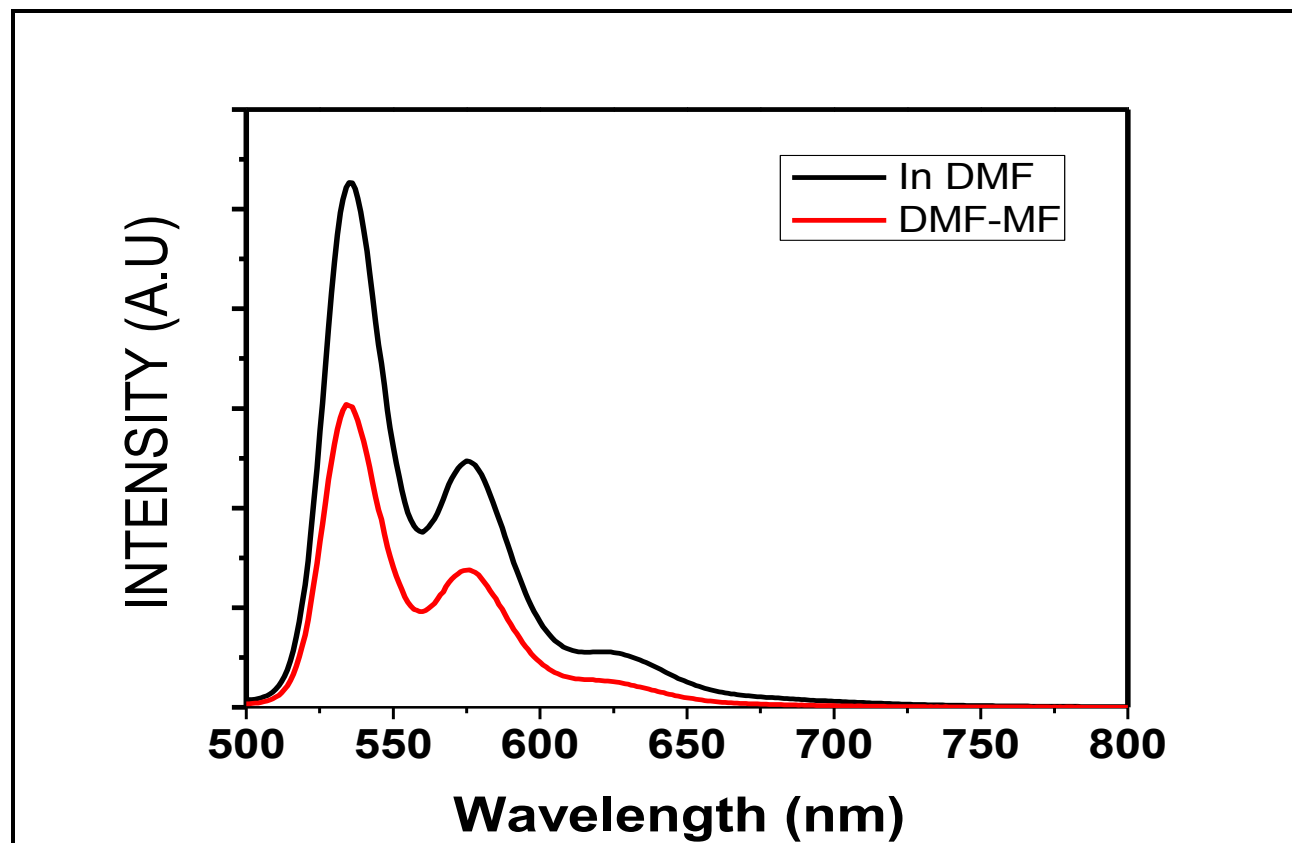


Figure 4-46: Emission spectrum ($\lambda_{exc}=485\text{nm}$) of BrPDI in DMF and in DMF after micro filtration

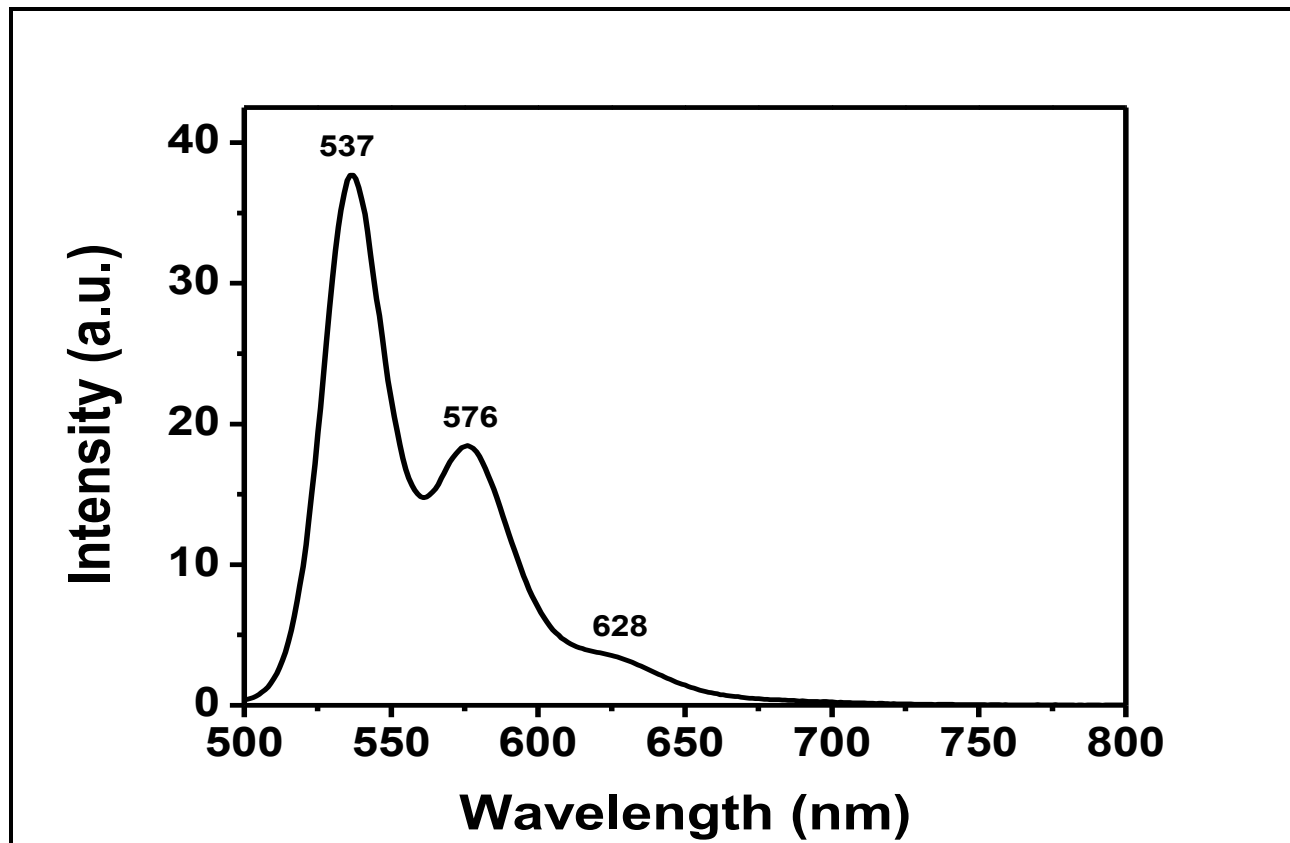


Figure 4-47: Emission spectrum ($\lambda_{exc}=485\text{nm}$) of BrPDI in NMP

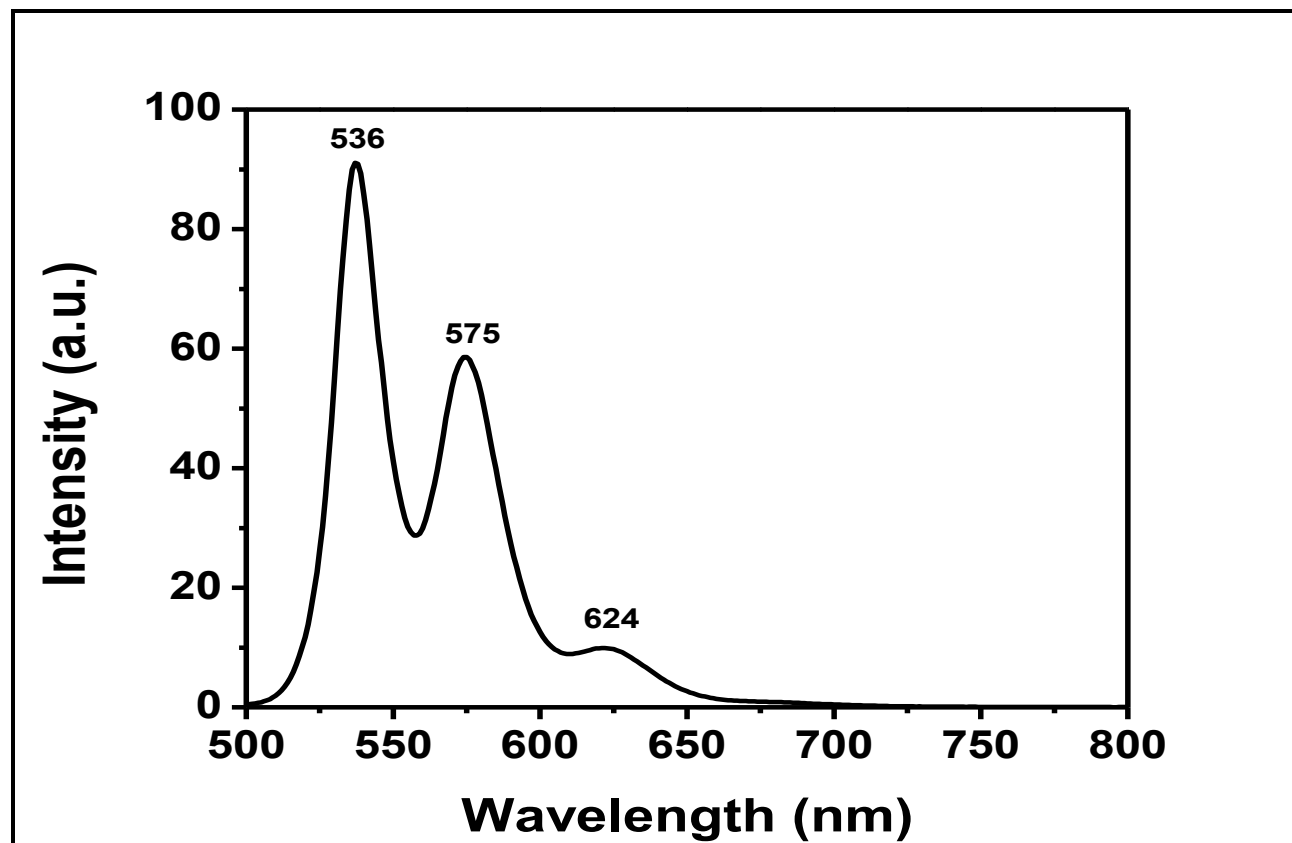


Figure 4-48: Emission spectrum ($\lambda_{exc}=485\text{nm}$) of BrPDI in CHL

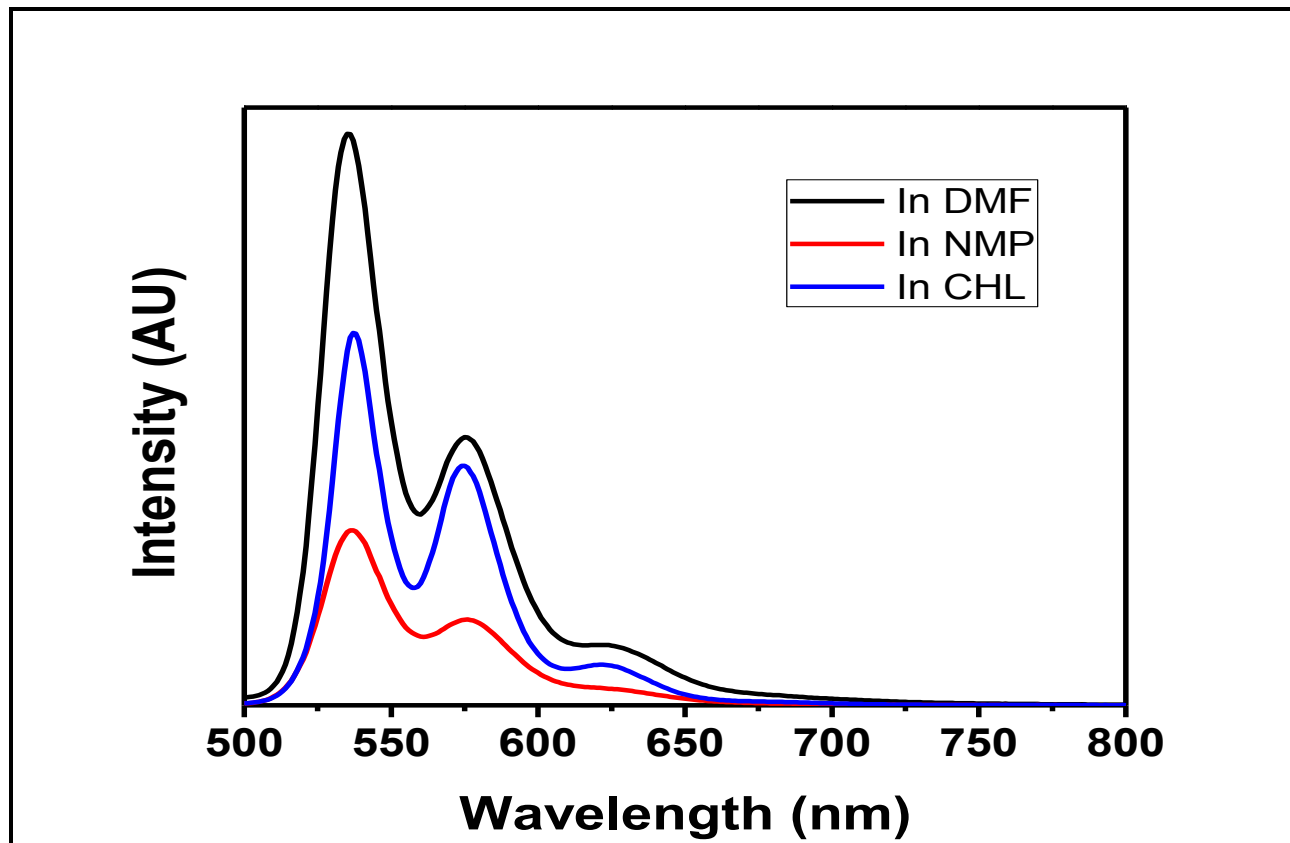


Figure 4-49: Emission spectrum ($\lambda_{exc}=485\text{nm}$) of BrPDI in DMF, NMP and CHL

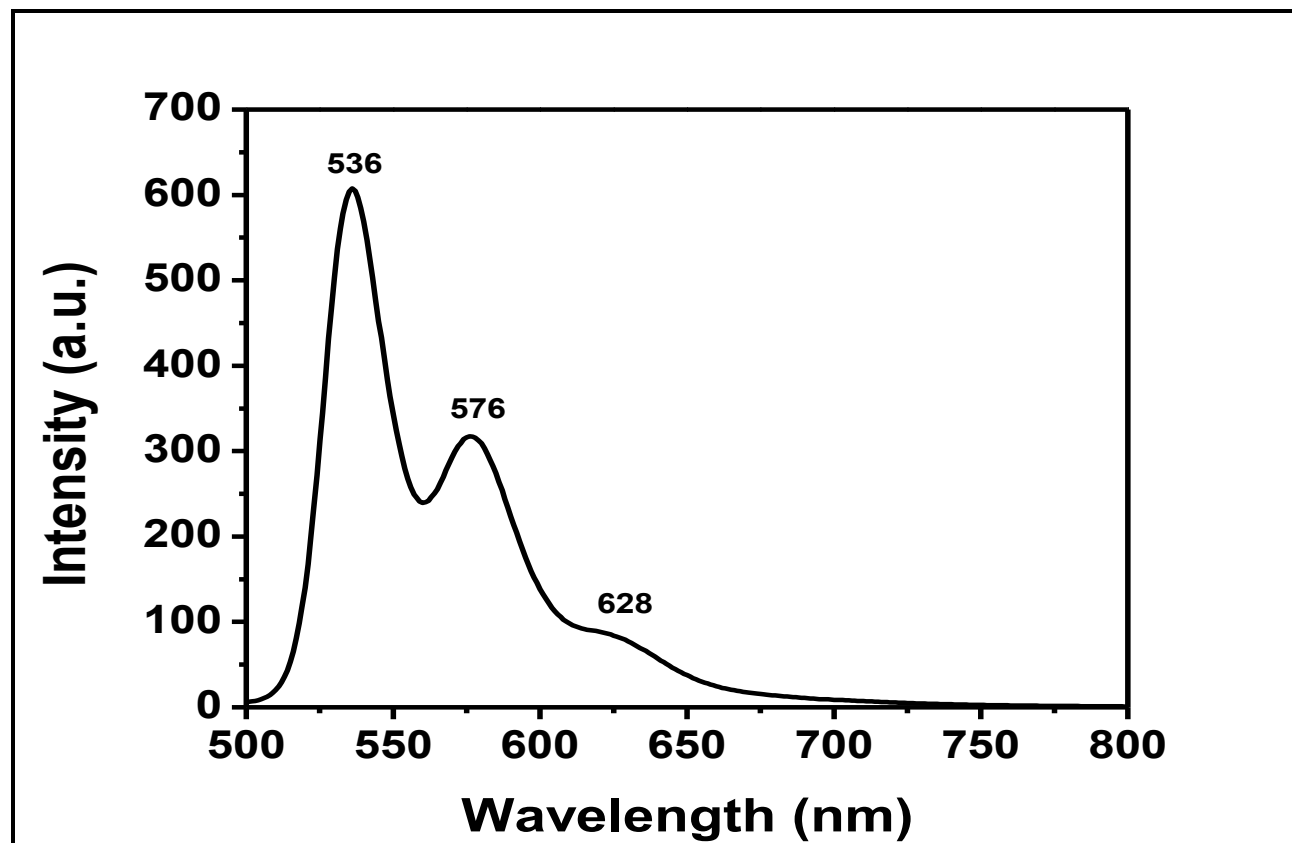


Figure 4-50: Emission spectrum ($\lambda_{exc}=485\text{nm}$) of PDI-Decanol in DMF

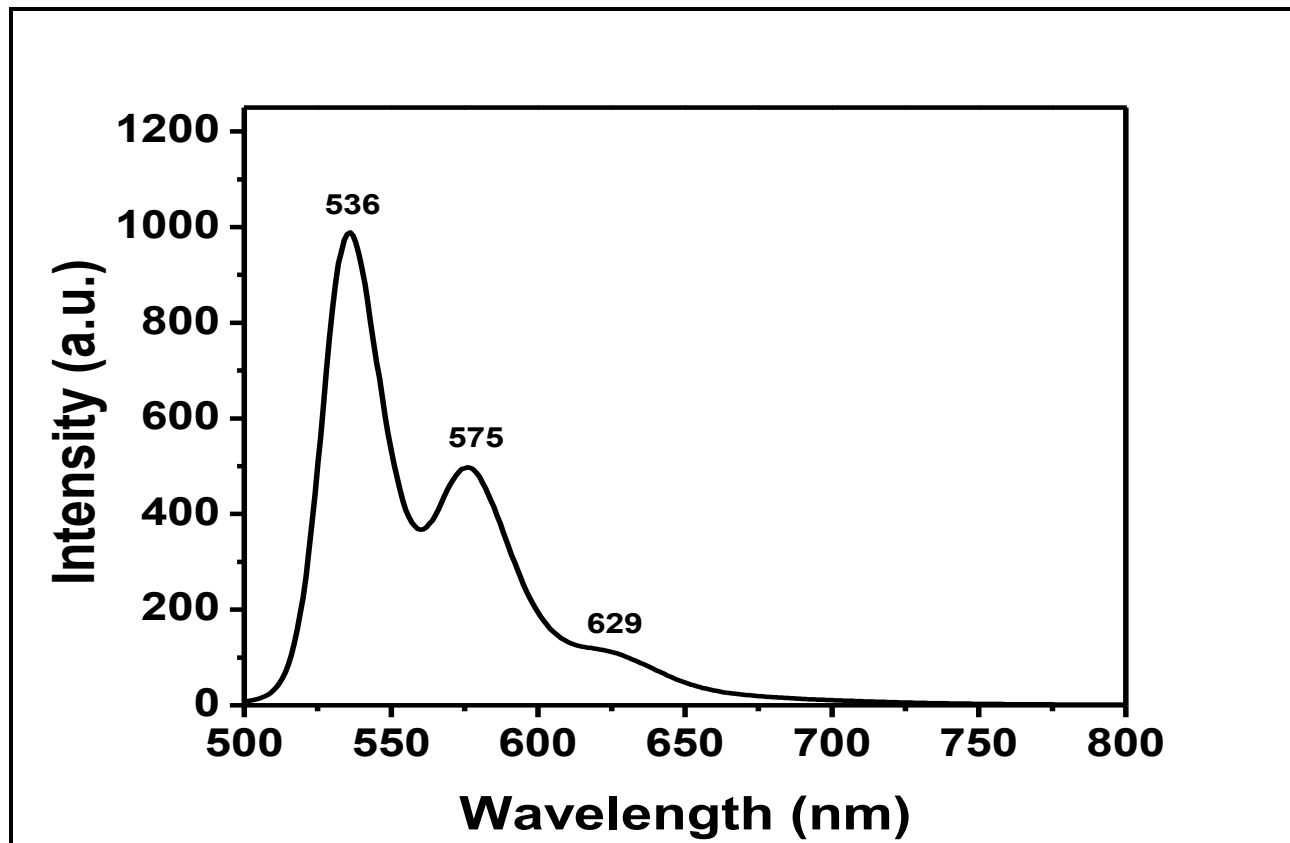


Figure 4-51: Emission spectrum ($\lambda_{exc}=485\text{nm}$) of PDI-Decanol in DMF after Micro Filtration

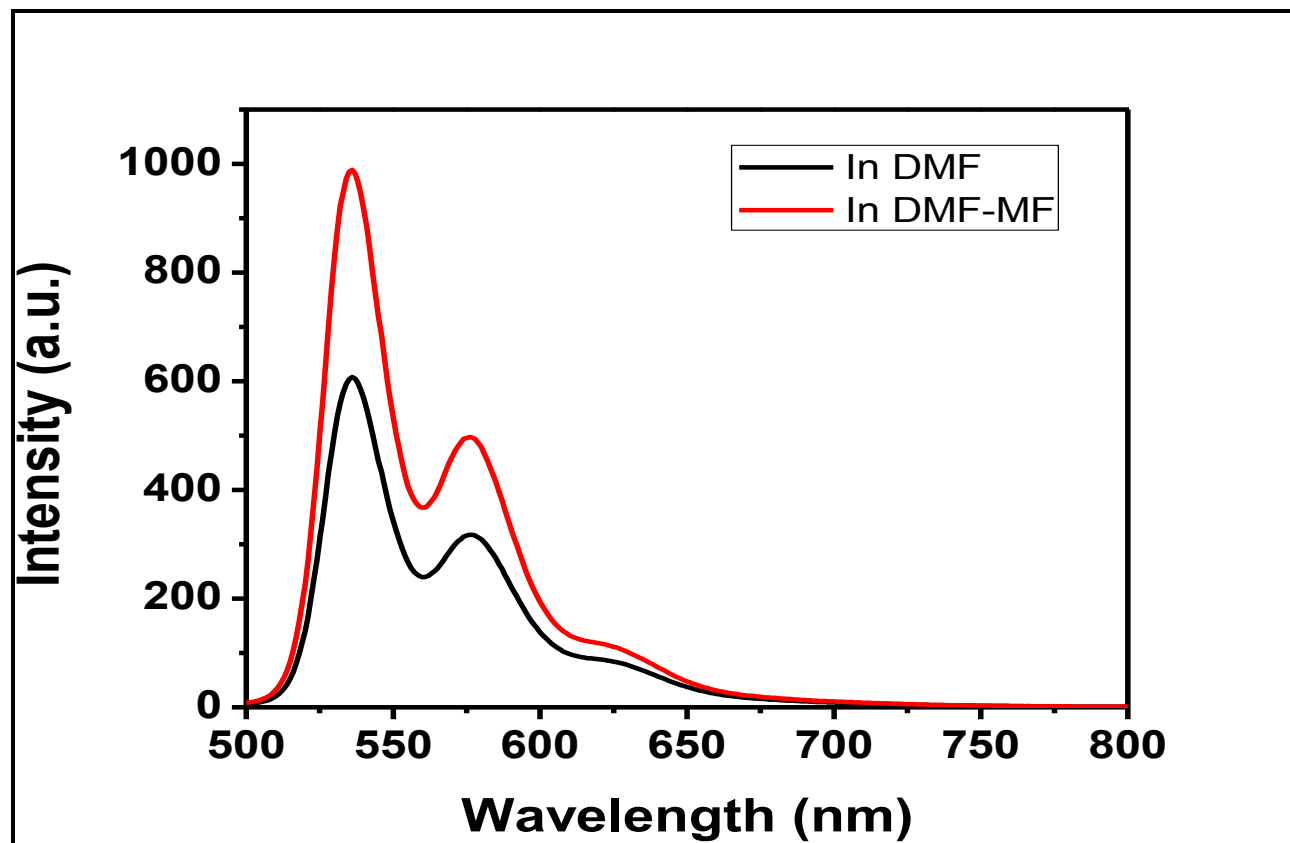


Figure 4-52: Emission spectrum ($\lambda_{exc}=485\text{nm}$) of overlap of PDI-Decanol in DMF/DMF Micro Filtration

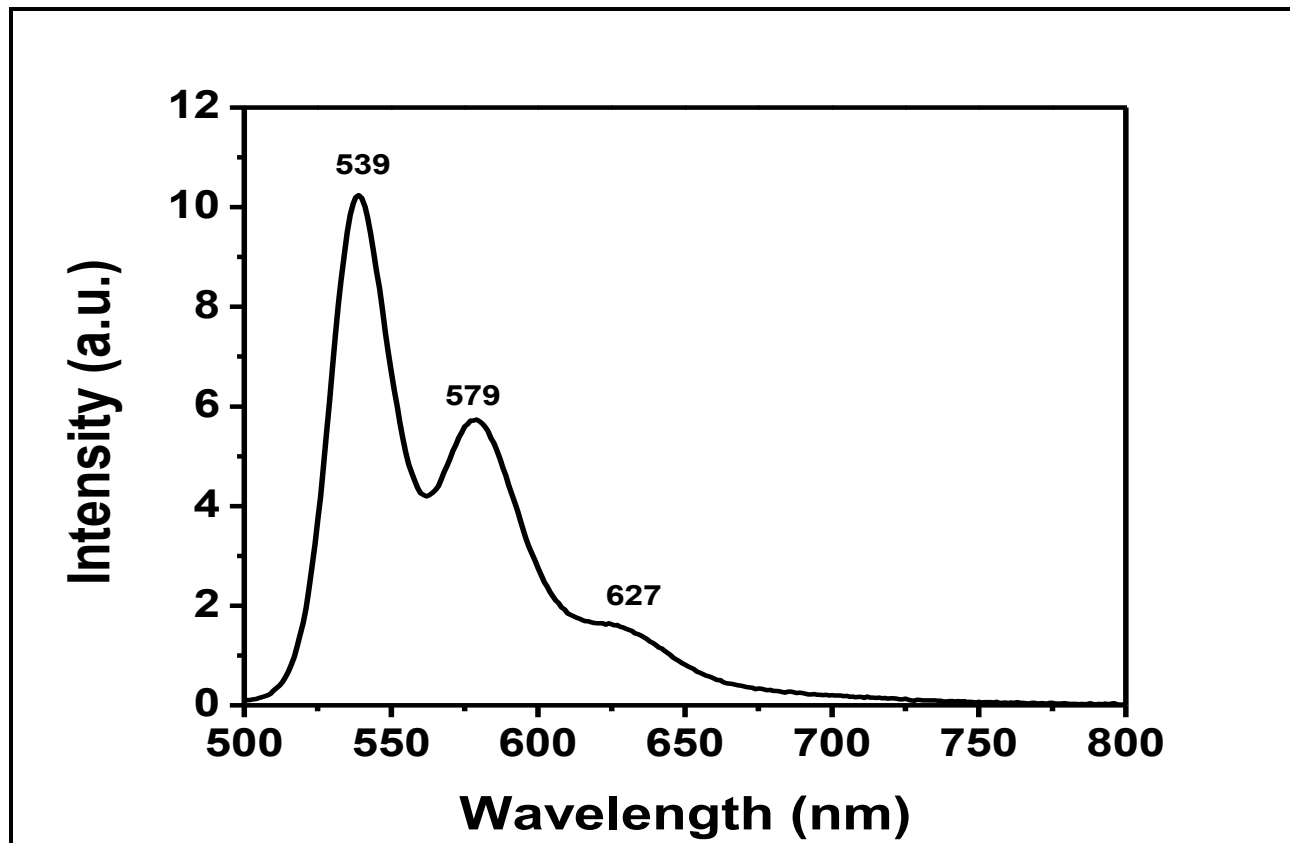


Figure 4-53: Emission spectrum ($\lambda_{exc}=485\text{nm}$) of PDI-Decanol in NMP

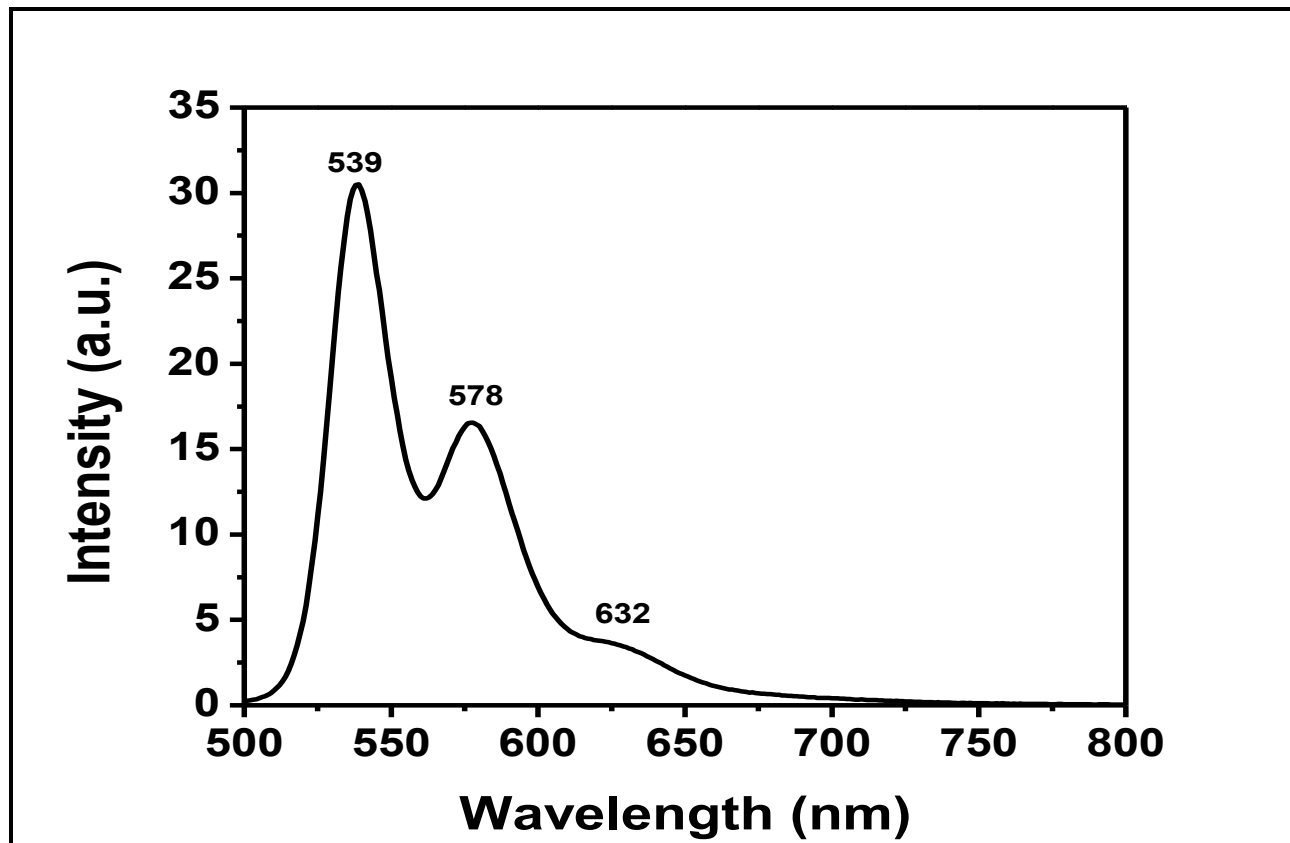


Figure 4-54: Emission spectrum ($\lambda_{exc}=485\text{nm}$) of PDI-Decanol in NMP after Micro Filtration

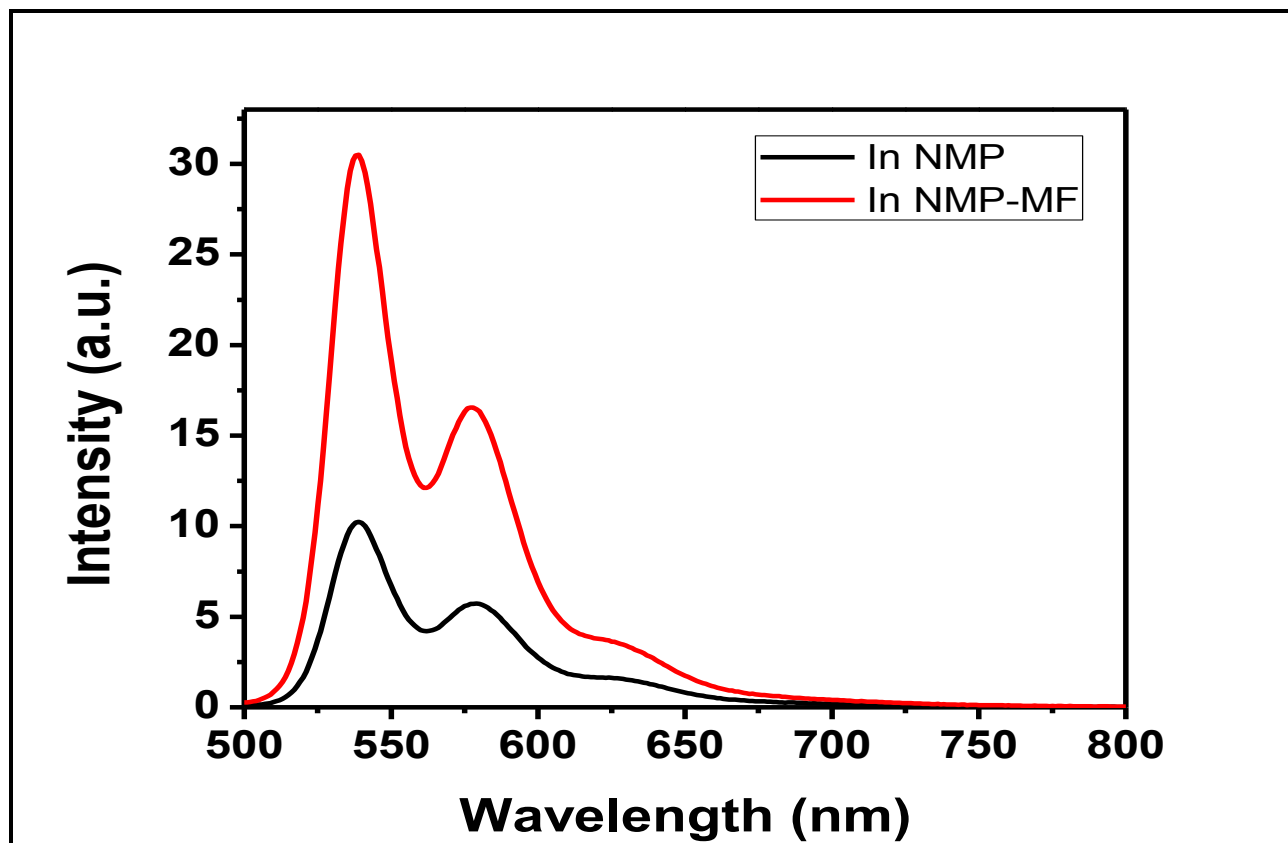


Figure 4-55: Emission spectrum ($\lambda_{exc}=485\text{nm}$) of PDI-Decanol overlap in NMP/NMP after Micro Filtration

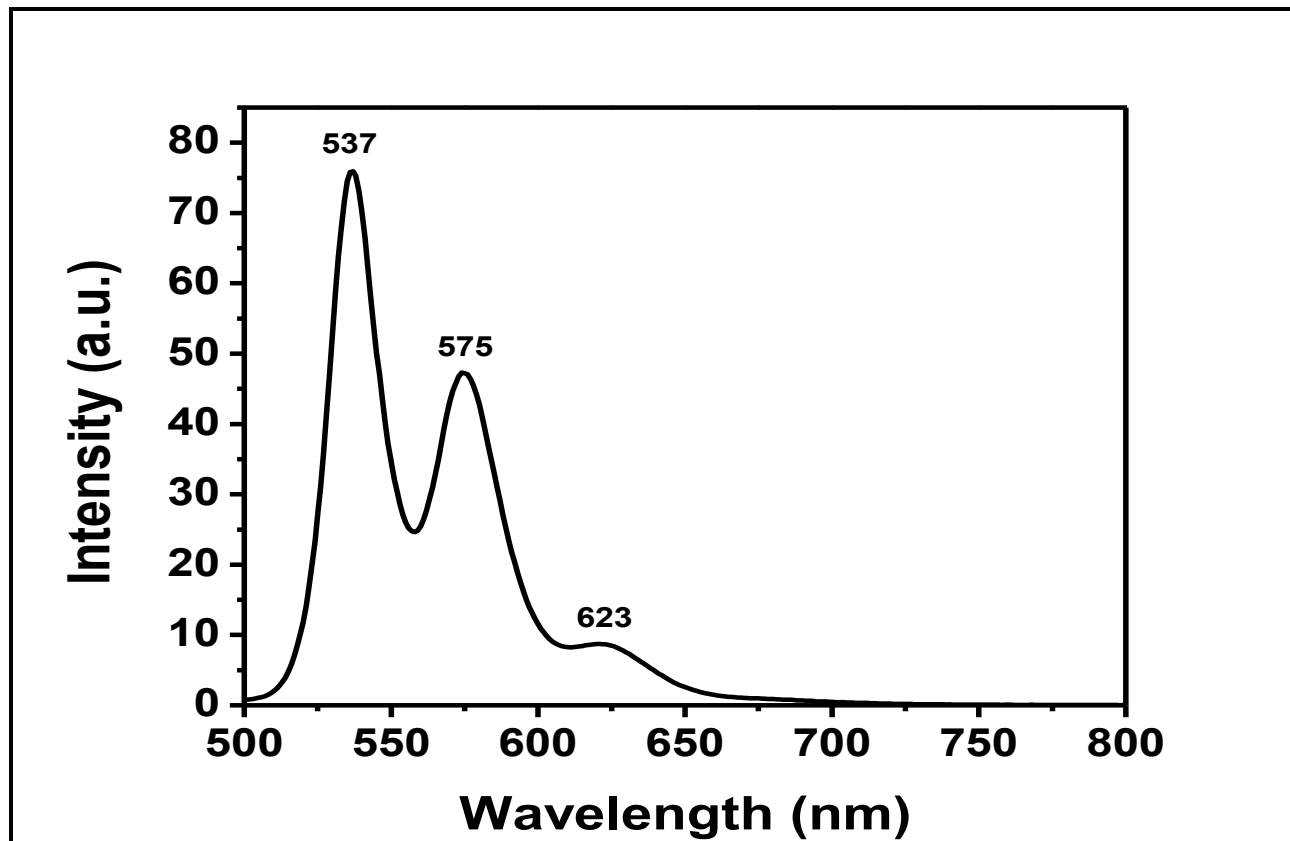


Figure 4-56: Emission spectrum ($\lambda_{exc}=485\text{nm}$) of PDI-Decanol in CHL

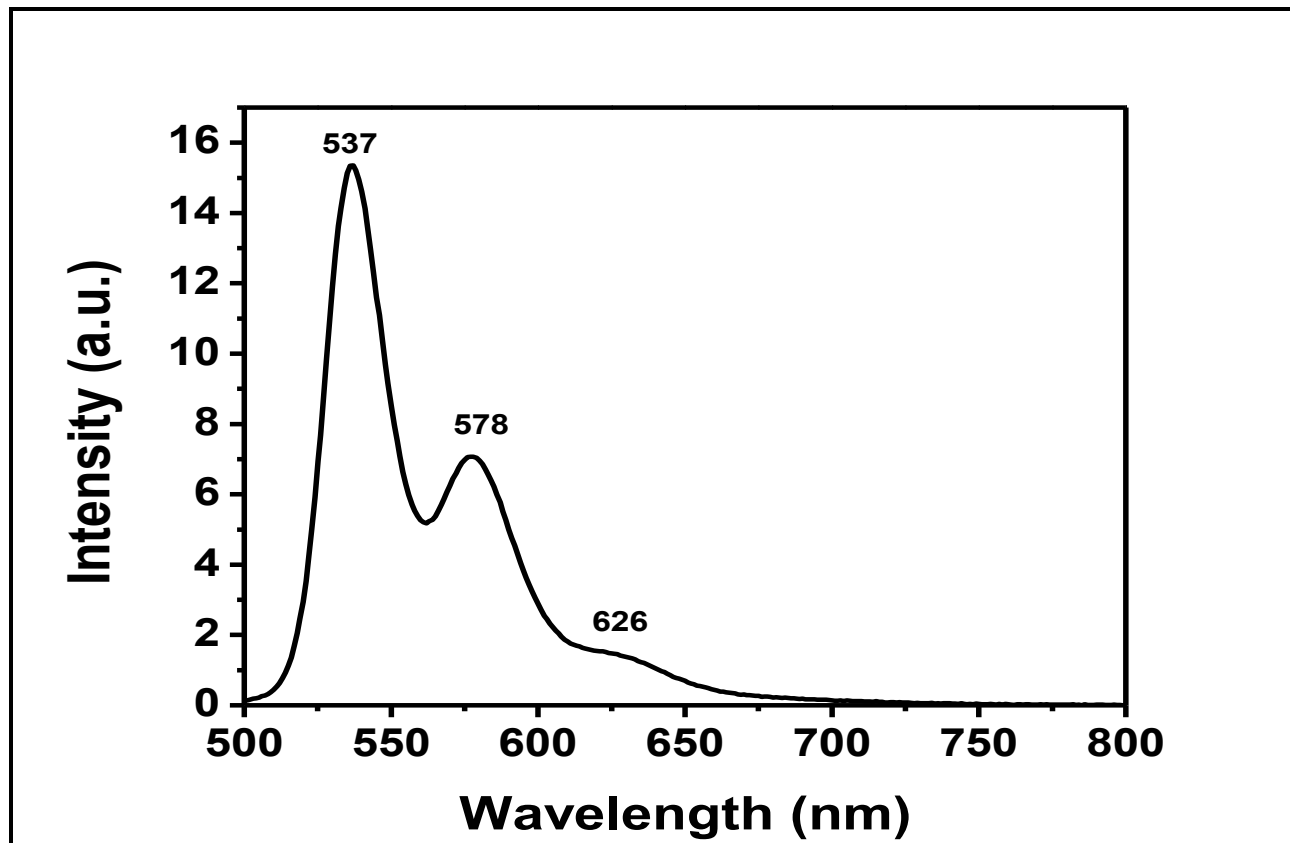


Figure 4-57: Emission spectrum ($\lambda_{exc}=485\text{nm}$) of PDI-Decanol in EtOH

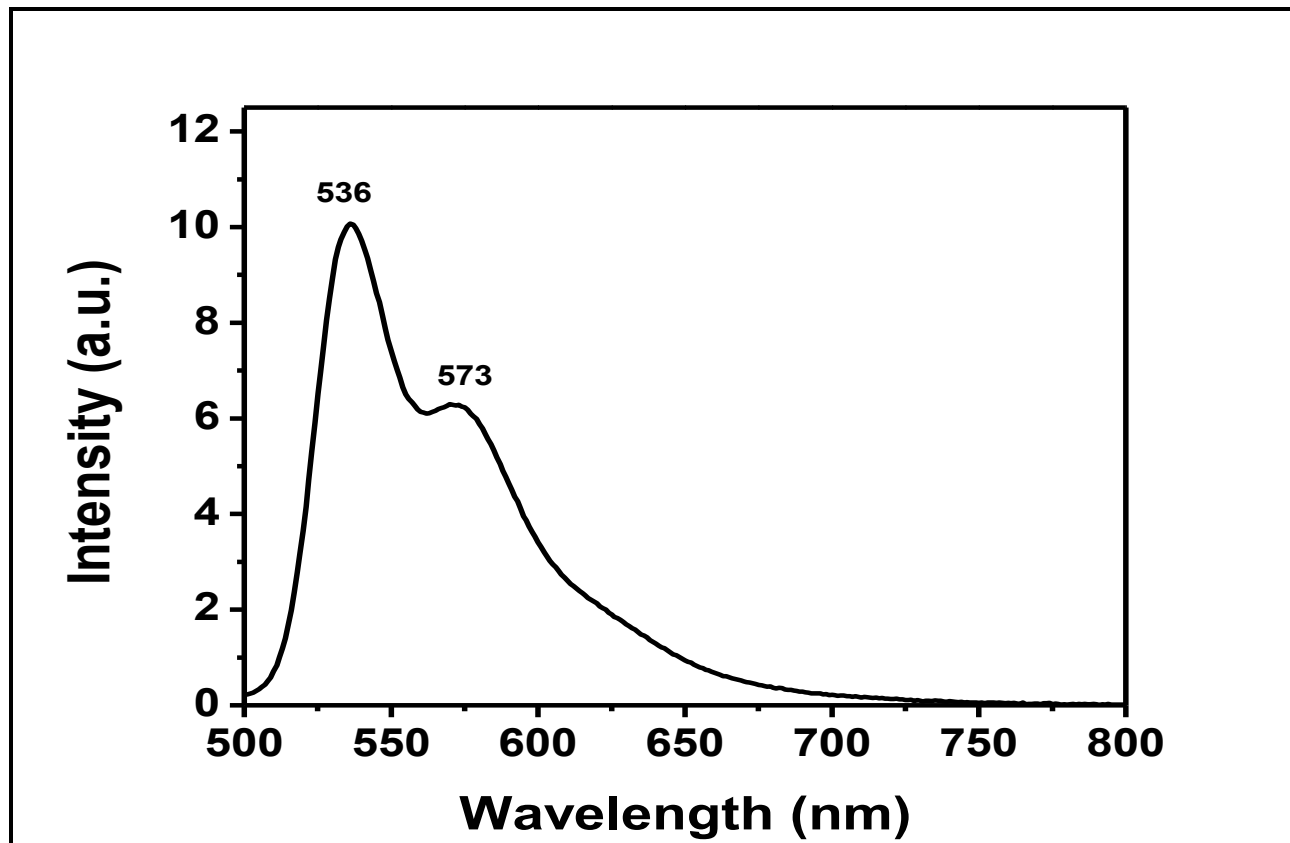


Figure 4-58: Emission spectrum ($\lambda_{exc}=485\text{nm}$) of PDI- Decanol in EtOH after Micro Filtration

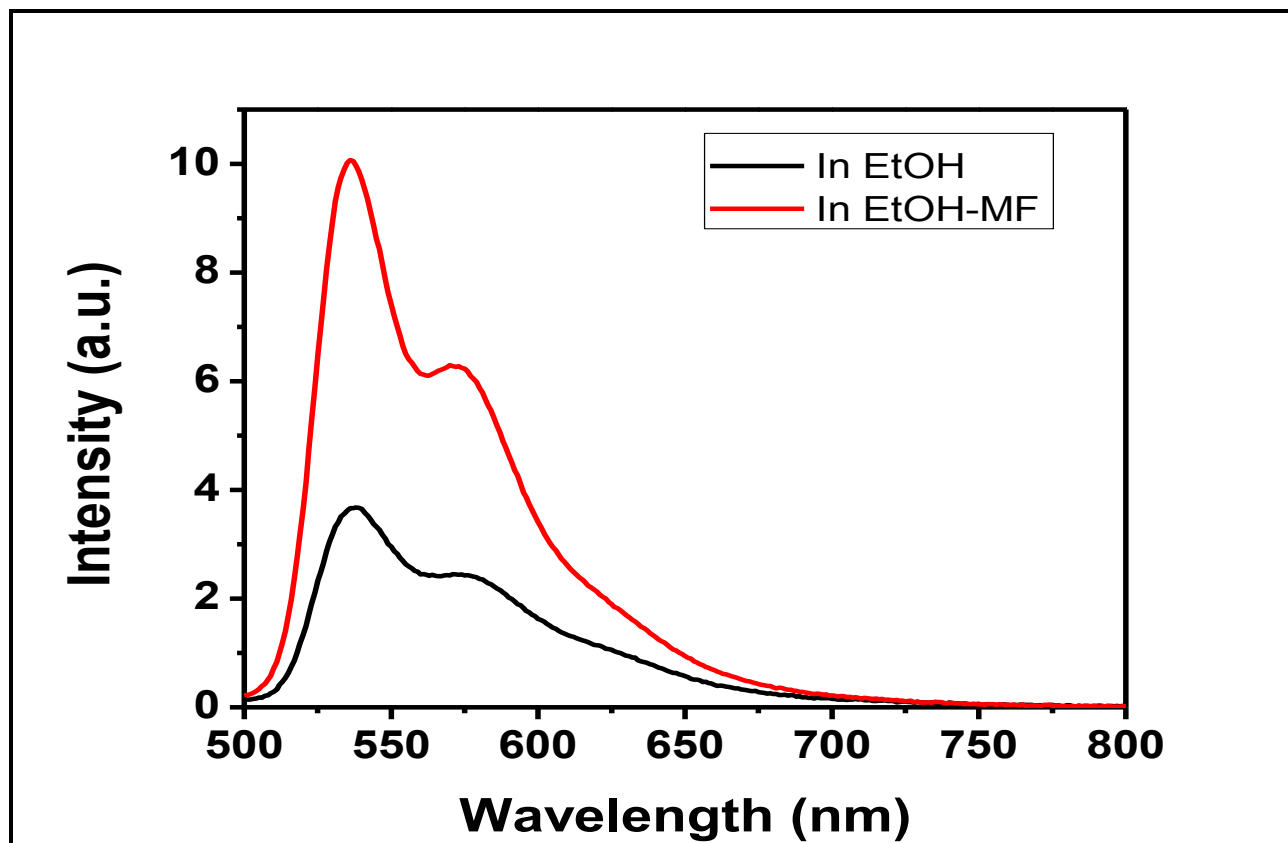


Figure 4-59: Emission spectrum ($\lambda_{exc}=485\text{nm}$) of overlap of PDI-Decanol in EtOH/EtOH after Micro Filtration

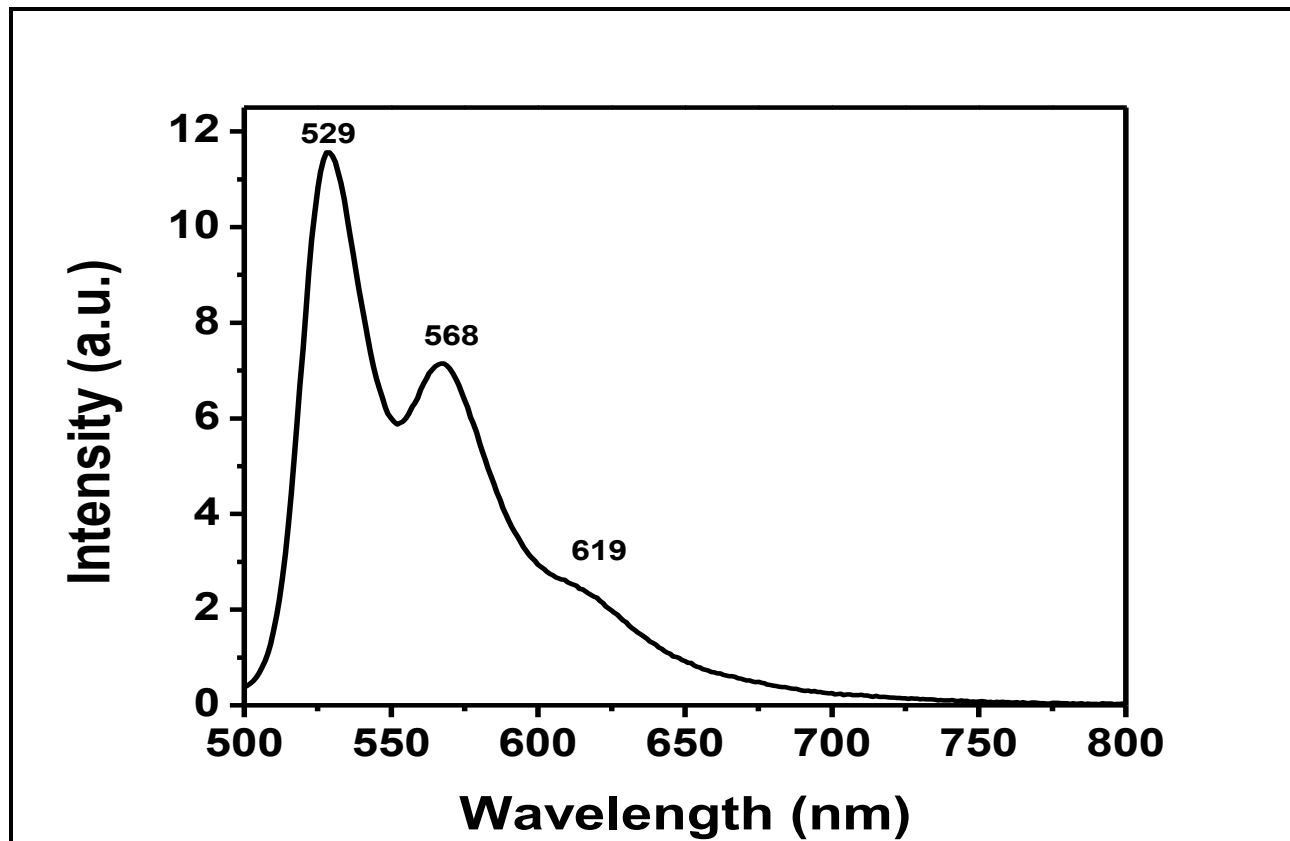


Figure 4-60: Emission spectrum ($\lambda_{exc}=485\text{nm}$) of PDI-Decanol in Acetone

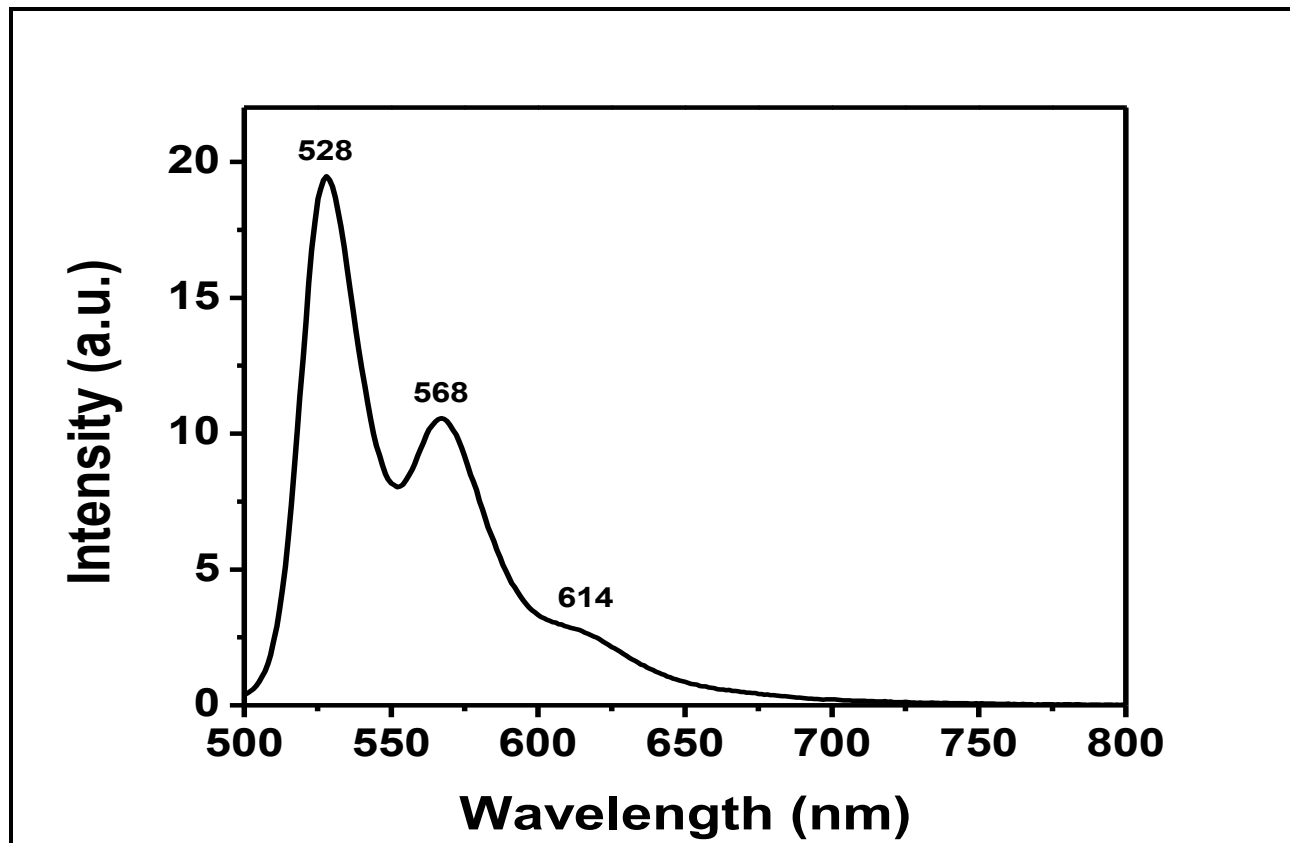


Figure 4-61: Emission spectrum ($\lambda_{exc}=485\text{nm}$) of PDI-Decanol in Acetone after Micro Filtration

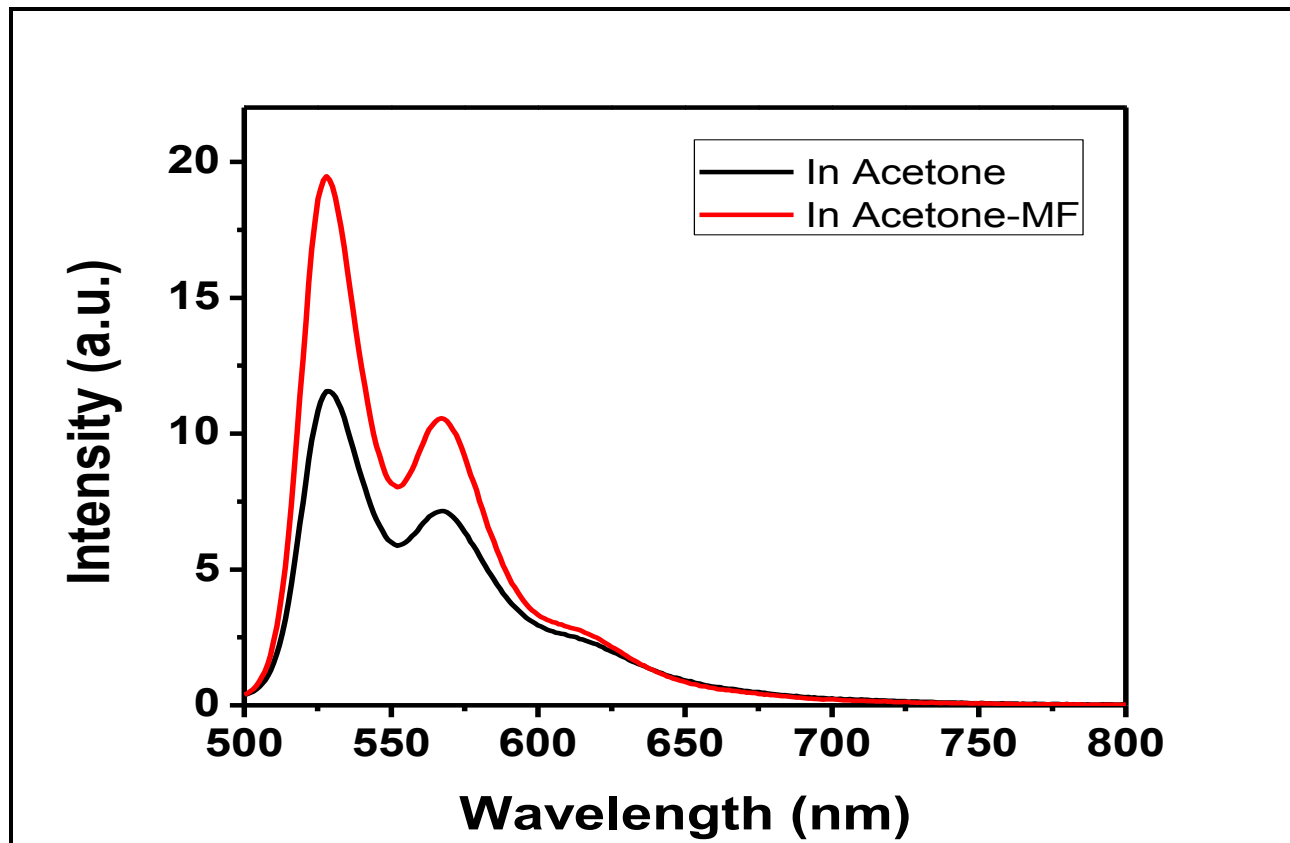


Figure 4-62: Emission spectrum ($\lambda_{exc}=485\text{nm}$) of PDI-Decanol overlap in Acetone/Acetone after Micro Filtration

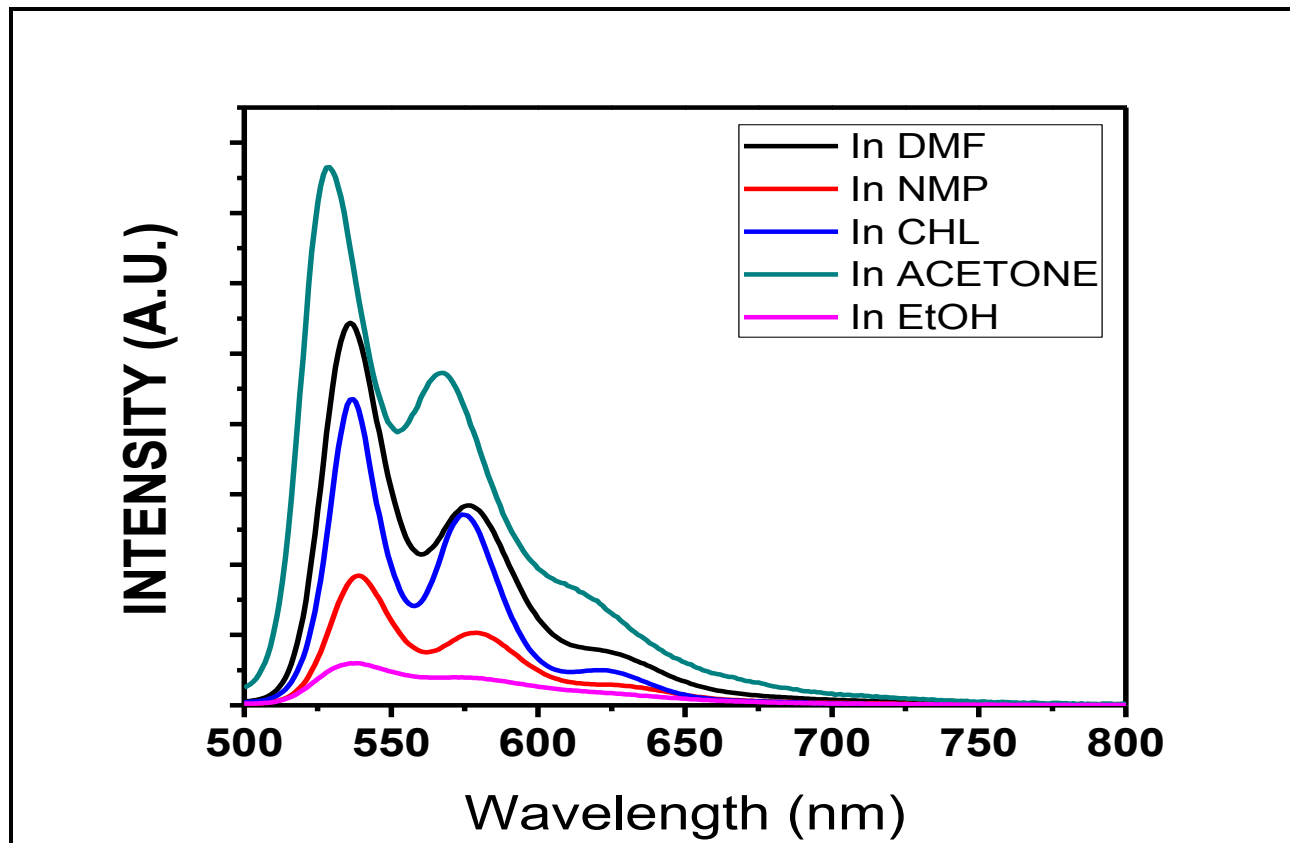


Figure 4-63: Emission spectrum ($\lambda_{exc}=485\text{nm}$) of PDI-Decanol in DMF, NMP, CHL, EtOH and Acetone

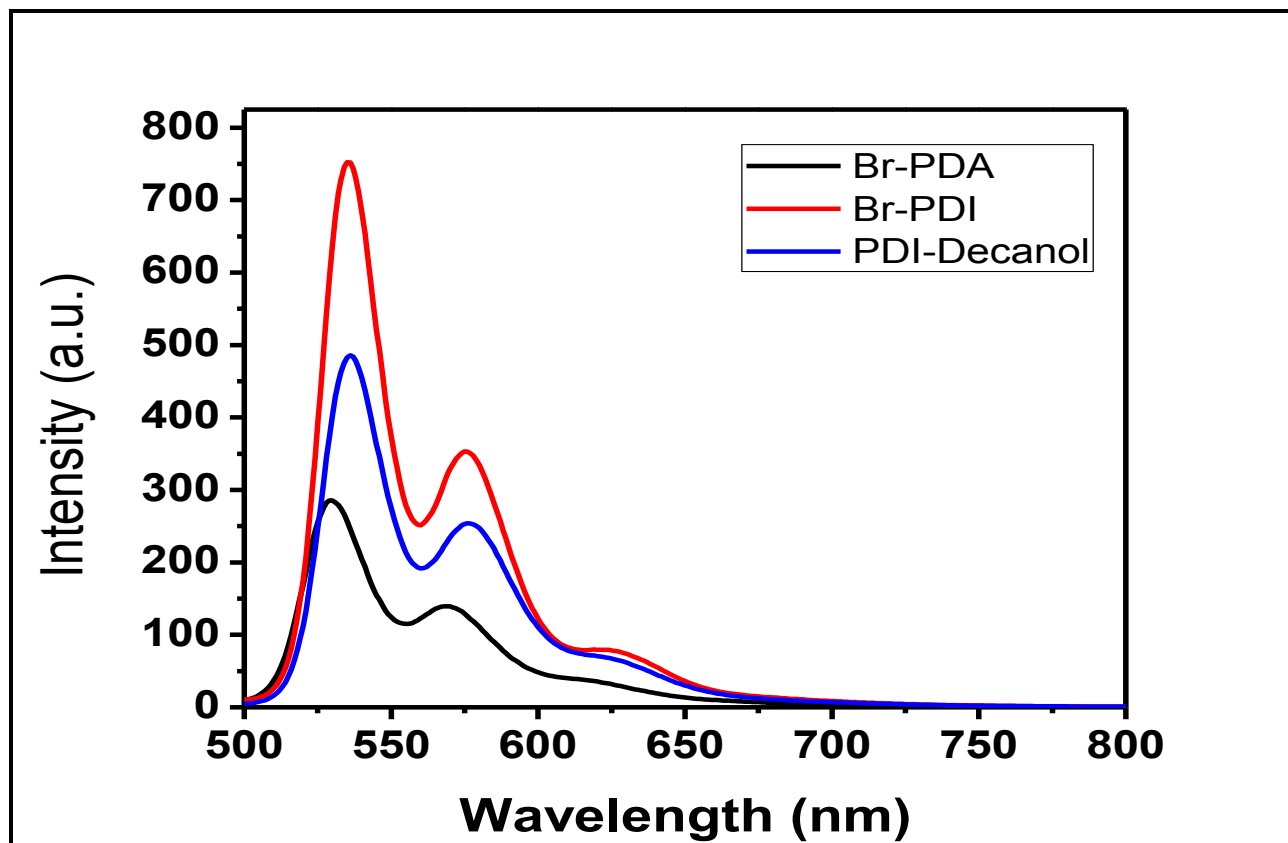


Figure 4-64: Emission spectrum ($\lambda_{exc}=485\text{nm}$) overlap of Br-PDI, Br-PDA and PDI-Decanol in DMF

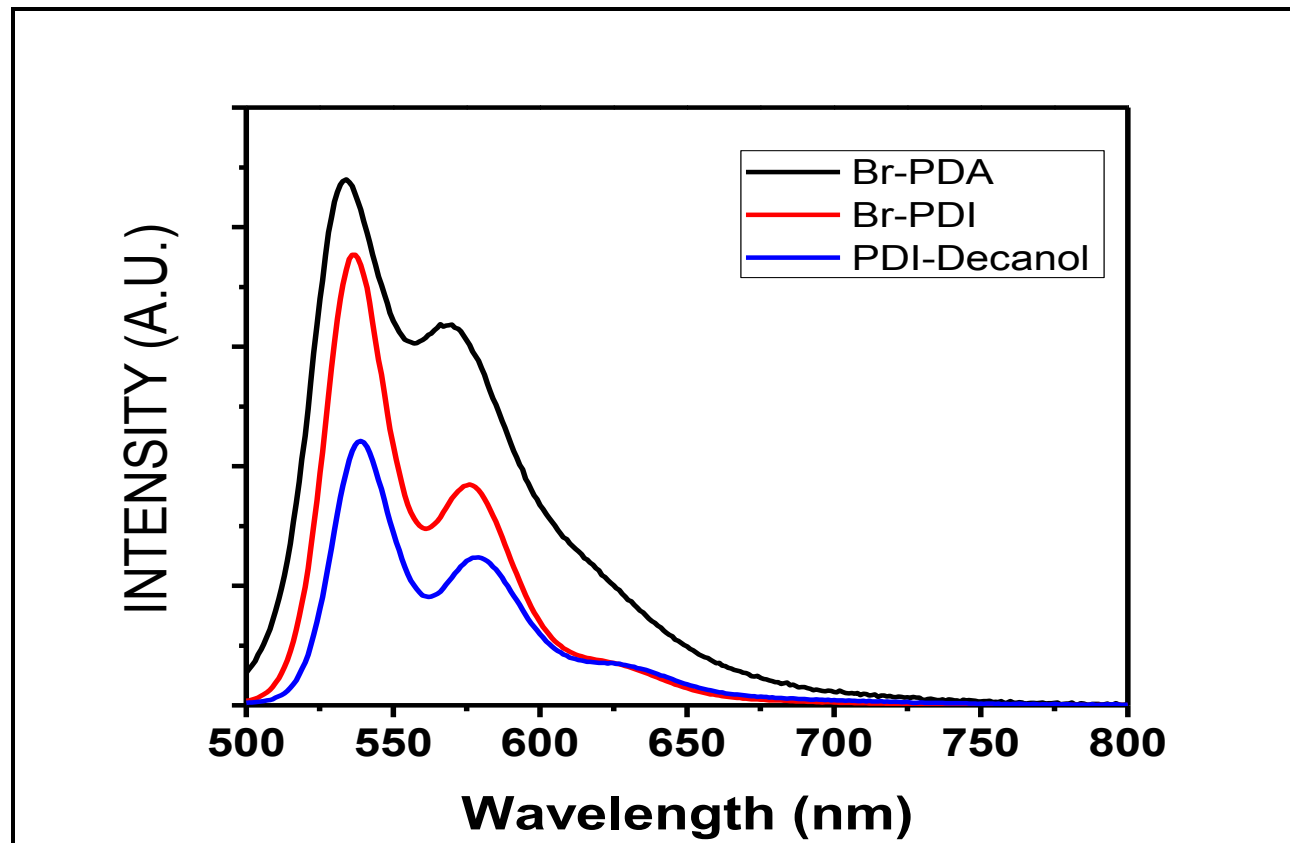


Figure 4-65: Emission spectrum ($\lambda_{exc}=485\text{nm}$) overlap of Br-PDI, Br-PDA and PDI-Decanol in NMP

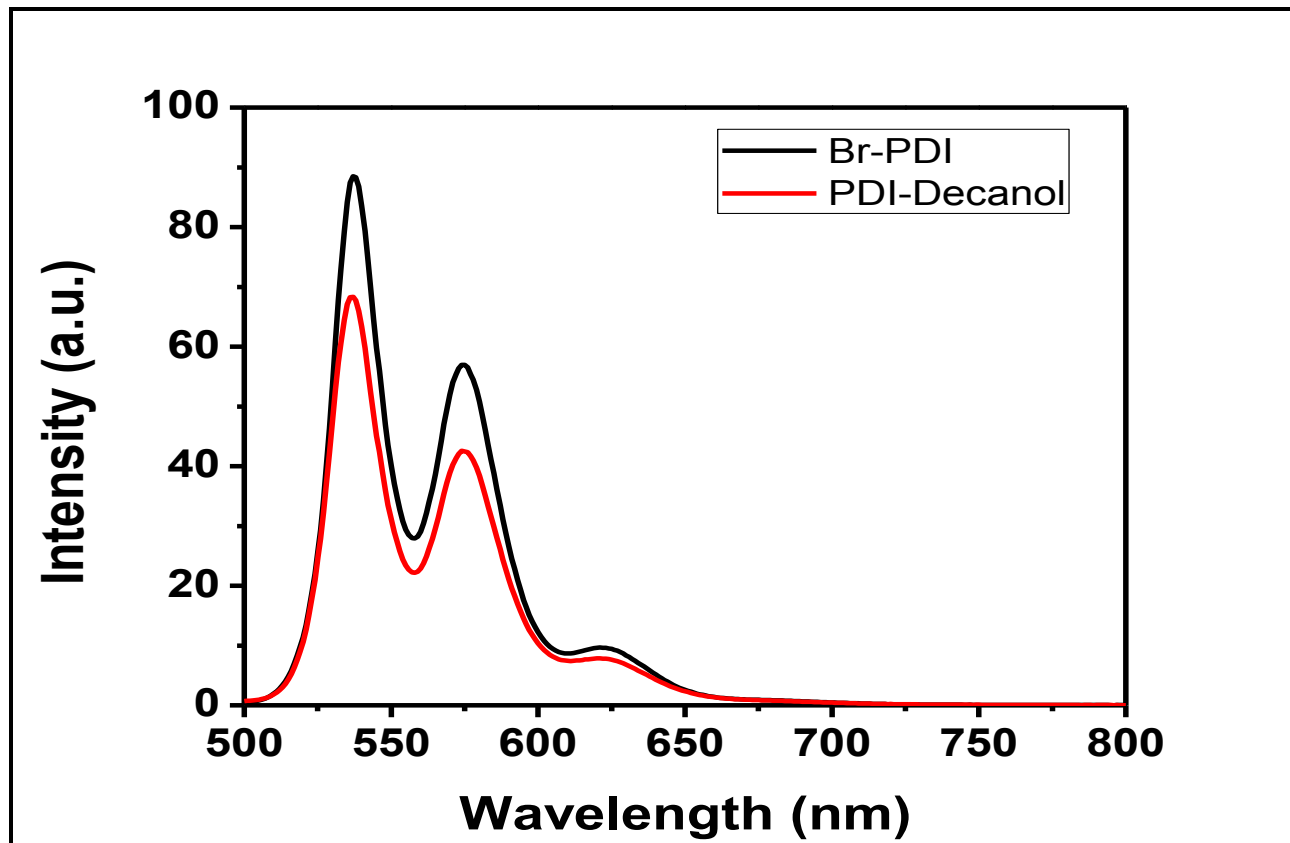


Figure 4-66: Emission spectrum ($\lambda_{exc}=485\text{nm}$) overlap of Br-PDI and PDI-Decanol in CHL

Chapter 5

RESULTS AND DISCUSSION

5.1 Synthesis of the Designed Bay-substituted Perylene Dye Derivatives

The bay-substituted perylene diimide (PDI-Decanol) was successfully synthesized in three successive steps.

a) In the first step, the reaction between raw material PDA and bromine was carried out in presence of sulfuric acid and iodine. The bromination can lead to a variety of brominated perylene derivatives and therefore care was taken to yield 1,7-dibromo perylene dianhydride in major amount [30,38]. The crude product was purified by general purification techniques.

b) In the second step, brominated (at bay-positions) perylene dianhydride (BrPDA) was reacted with the dodecyl amine to yield the perylene diimide. The imide substitution is carried out by classical condensation method. At the end of the second step, imide (at carboxylic acid dianhydride positions) and bay (at the core part of the perylene chromophore) substituted perylene diimide (BrPDI) was obtained.

c) In the final step, the product of the second step, the brominated perylene diimide (BrPDI) is reacted with the 2-decyl-1-tetradecanol to replace the bromines at

the bay positions. Consequently, the finally targeted 2-decyl-1-tetradecanol core substituted perylene diimide (PDI-Decanol) was produced. The product is purified by Soxhlet apparatus with alcoholic solvents like ethanol.

Generally, the ease in bay-substitution of perylene chromophore offers wide varieties of core-substituted perylene derivatives. Unfortunately, there is a great possibility for obtaining unwanted core substituted perylene imide compounds such as 1,6-; 1,6-,1,7-peryene dyes in minimum amounts [30,32]. Therefore, the reaction must be carefully designed with appropriate mole ratios of the reactants and should be carried out accordingly to yield 1,7-substituted perylene dyes in major amounts. The targeted 2-decyl-1-tetradecanol core substituted (1,7-substituted) perylene diimide (PDI-Decanol) was synthesized and purified accordingly.

5.2 Solubility of the Designed Bay-substituted Perylene Dye Derivatives

2-decyl-1-tetradecanol core substituted (1,7-substituted) perylene diimide (PDI-Decanol) has shown excellent solubility in nonpolar and dipolar aprotic solvents, whereas, it has shown moderate solubility in polar protic solvents like ethanol. On the other hand, BrPDI is soluble in polar solvents and comparatively, BrPDA has shown moderate solubility in dipolar aprotic solvents

Table 5-1: Solubility of the synthesized Perylene derivatives

Solvents	Br-PDA	Br-PDI	PDI-Decanol
DMF	(- +)Light red	(- +)Red	(- +)Red
NMP	(- +)Light red	(+ +)Red	(+ +)Dark red
CHL	(- -)	(+ +)Orange	(+ +)Red
ACETONE	(- -)	(- -)	(+ +)Red
EtOH	(- -)	(- -)	(- +)Red
DMSO	(- +)Red	(- -)	(+ +)Red
Dichloromethane	(- -)	(+ +)Red	(+ +) Red

Solubility test (++) soluble at room temperature; (- +) soluble on heating at 60°C; the solubility increases upon heating.

5.3 Analysis of FTIR Spectra

The spectrum of BrPDA Figure 4.4 present the following characteristic bands: aromatic C-H stretch at 3122 cm^{-1} , anhydride C=O stretches at 1765 and 1724 cm^{-1} , aromatic C=C stretch at 1595 cm^{-1} and C-Br stretch at 803 cm^{-1} .

As can be seen from the Figure 4.5, The IR spectrum of BrPDI shows the stretchings and vibrations of all functional groups present in the structure. Importantly, the long dodecyl alkyl chains present at the imide positions of perylene chromophore can be seen at 2919 cm^{-1} (aliphatic C-H stretch), 1377 cm^{-1} (aliphatic C-H bending), 1344 cm^{-1} (C-N stretch), respectively. The aromatic functional groups can be seen at 3050 cm^{-1} (aromatic C-H stretch), 1599 cm^{-1} (aromatic C=C), respectively. The major imide functional groups can be observed at 1697 and 1656 cm^{-1} , respectively.

As can be seen from the Figure 4.6, The IR spectrum of PDI-Decanol shows the stretchings and vibrations of all functional groups present in the structure. Importantly, the long dodecyl alkyl chains present at the imide positions as well as bay positions of perylene chromophore can be seen at $2923, 2852\text{ cm}^{-1}$ (aliphatic C-H stretch), $1466, 1438\text{ cm}^{-1}$ (aliphatic C-H bending), 1345 cm^{-1} (C-N stretch), respectively. The aromatic functional groups can be seen at 3050 cm^{-1} (aromatic C-H stretch), 1598 cm^{-1} (aromatic C=C), respectively. The major imide functional groups can be observed at 1697 and 1657 cm^{-1} , respectively. Clearly, the strong absorption at $1438 - 1466$ regions (which is different for BrPDI) shows increase in aliphatic character due to the substitutions of long alkyl chains both at imide and bay-positions of the perylene chromophore.

5.4 Interpretation of UV-vis Spectra

The research on perylene dyes for various interesting electronic and photonic properties reveal that bay-substitution can greatly alter the electronic structure of perylene chromophore and could result in narrow band gaps and excellent HOMO, LUMO properties[32]. Additionally, interesting optical properties can be achieved via substitution at imide positions of the perylene core with designed long/bulky chains.

In order to use perylene dyes in solar cell applications, the potential of these dyes must be expanded with great optical and electronic properties. The optical properties are investigated through absorption and emission spectra and the results are discussed in detail.

The UV-vis absorption of brominated perylene dianhydride was shown in (Figure 4.7). The spectrum shows three major peaks at 452, 479, and 516 nm respectively in dipolar aprotic solvent, DMF. The peaks are characterized as characteristic absorption peaks of perylene chromophore responsible for strong π - π electronic transitions representing $0 \rightarrow 2$, $0 \rightarrow 1$, and $0 \rightarrow 0$ transitions, respectively.

The UV-vis absorptions of core bromine substituted perylene dianhydride in NMP before and after microfiltration from Figures 4.9 and 4.10 show that before microfiltration, there are two dominant absorption peaks at 481 and 515 nm in addition to the weak shoulder absorption band at 673 nm. This can be attributed to strong solvent and solute interactions. The additional shoulder band at 672 nm after microfiltration suggests that the band is not aroused due to aggregation. Moreover,

the classical absorption bands of perylene are better resolved into three absorption peaks after microfiltration.

The UV-vis absorptions of core bromine substituted perylene dodecyl diimide (BrPDI) in dipolar aprotic DMF from Figures 4.14 – 4. The broad absorption shows that the compound has great tend of absorbing the light in dipolar aprotic media. The broad absorption also includes the three typical perylene electronic transition peaks at 457, 486 and 522 nm followed by a broad absorption shoulder band at 610 nm, respectively (Figure 4.14). Interestingly, upon micro filtering the solution, the additional shoulder band at longer wavelengths is vanished which shows that a kind of aggregation is present in the solution at high concentrations (Figure 4.15).

The UV-vis absorptions of core bromine substituted perylene dodecyl diimide (BrPDI) in dipolar aprotic NMP from (Figure 4.16) shows no signs of aggregation like in DMF. The absorption indicates the three classic perylene core absorptions at 457, 488, and 523 nm, respectively.

The UV-vis absorptions of core bromine substituted perylene dodecyl diimide (BrPDI) in nonpolar chloroform from (Figure 4.17) shows the three typical perylene absorption peaks at 457, 488, and 525 nm, respectively. There is no aggregation noticed similar to the absorption spectra noticed for brominated BrPDI in NMP.

The UV-vis absorption of core 2-decyl-1-tetradecanol substituted perylene dodecyl diimide (PDI-Decanol) in DMF from (Figure 4.20) shows three major peaks at 462, 486, and 522 nm, respectively, which are responsible for perylene chromophore absorptions. Interestingly, 0→2 electron transition peak at 462 nm is not like the

traditional perylene absorption peaks and is more like a shoulder band. Subsequently, 0→1 electron transition peak at 486 nm is higher in absorption intensity. Generally, the characteristic perylene dye absorption peaks show gradual increase in absorption intensity from 0→2 to 0→0 electronic transitions and therefore the highest absorption intensity will be remained for 0→0 transition. On the other hand, PDI-Decanol shows the highest intensity at 0→1 electron transition. The absorption intensity reversal is due to the extended long aliphatic chains at both imide and bay positions [13]. Moreover, the absorption is broad and additional weak multiple shoulder absorption bands were noticed at 571, 674, and 742 nm, respectively. This absorption intensity reversal indicates the self-assembly of perylene dye molecules in solution. Upon microfiltration of the same PDI-Decanol solution in DMF,(Figure 4.25) shows characteristic perylene absorption peaks instead of the absorption intensity reversal that was noticed in the absorption spectrum before microfiltration. This behavior strongly supports the occurrence of self-assembly before microfiltration. Interestingly, the additional shoulder bands at 570, 672, 747 nm were unchanged and is probably due to the presence of long alkyl chains at both imide and bay positions.

The UV-vis absorption of core 2-decyl-1-tetradecanol substituted perylene dodecyl diimide (PDI-Decanol) in NMP before and after microfiltration from (Figures 4.21 – 4.22) reveals the similar results that were noticed for PDI-Decanol in DMF. Before Microfiltration, in NMP, PDI-Decanol shows a broad absorption along with the multiple shoulder bands. Upon microfiltration, the absorption is a typical of perylene dye absorption with three characteristic peaks. However, like in DMF, the additional shoulder bands were remained after microfiltering the PDI-Decanol solution.

The UV-vis absorption of core 2-decyl-1-tetradecanol substituted perylene dodecyl diimide (PDI-Decanol) in nonpolar solvents such as chloroform and acetone before and after microfiltration from (Figures 4.27, 4.31 and 4.32) reveal that the absorption peaks are traditional perylene absorption peaks. There are signs of neither absorption intensity reversal nor the additional shoulder bands unlike the broad absorption of PDI-Decanol in DMF and NMP (before microfiltration). This is due to the fact that PDI-Decanol can better polarize in strong dipolar aprotic solvents when compared to the nonpolar solvents.

Interestingly, the UV-vis absorption of core 2-decyl-1-tetradecanol substituted perylene dodecyl diimide (PDI-Decanol) in polar protic MeOH before and after microfiltration from Figures 4.28– 4.29 reveal the similar results that were noticed for PDI-Decanol in DMF and NMP. Before Microfiltration, in EtOH, PDI-Decanol shows a broad absorption along with the weak shoulder band at 572 nm. Upon microfiltration, the absorption is a typical of perylene dye absorption with three characteristic peaks.

5.5 Interpretation of Emission Spectra

The emission spectra of BrPDA from Figures 4.37 and 4.38 show three typical perylene chromophoric emission peaks at 530, 569, and 622 nm respectively in dipolar aprotic solvent, DMF. The three emission peaks represent the $0 \rightarrow 0$, $0 \rightarrow 1$, and $0 \rightarrow 2$ electronic transitions of perylene chromophore which were unchanged before and after microfiltration unlike their absorption spectra.

The emission spectra of BrPDA from Figures 4.40 and 4.41 show three traditional perylene chromophoric emission peaks (which were mostly mirror images of their absorption spectra) at around 532, 570 nm in dipolar aprotic solvent, NMP. The three characteristic peaks were slightly changed after microfiltering the solution. Before microfiltration, the peaks were broader, whereas, after microfiltration, the peaks were better resolved. Interestingly, the additional peaks found in absorption spectra of the dye in the same solvent have no significance on the emission of the core substituted perylene dye.

The emission spectra of BrPDI from Figures 4.44 and 4.45 show three classic perylene chromophoric emission peaks (which were mostly mirror images of their absorption spectra) at around 535, 576, and 628 nm, respectively, in dipolar aprotic solvent, DMF. The three characteristic peaks were unchanged after microfiltering the solution. Interestingly, the additional peaks found in absorption spectra of the dye in the same solvent have no significance on the emission of the core substituted perylene dye.

The emission spectra of BrPDI from (Figure 4.47) show three typical perylene chromophoric emission peaks (which were mirror images of their absorption spectra)

at around 536, 575, and 632 nm, respectively in dipolar aprotic solvent, NMP. Interestingly, the additional peaks found in absorption spectra of the dye in the same solvent have no significance on their corresponding emission of the perylene derivative.

The emission spectrum of brominated perylene diimide (Figure 4.48) show three characteristic perylene emission peaks (which were mirror images of their absorption spectra) at around 536, 575, and 624 nm, respectively in nonpolar aprotic solvent, chloroform.

The emission spectra of core 2-decyl-1-tetradecanol substituted perylene dodecyl diimide (PDI-Decanol) in DMF before and after microfiltration were shown in (Figures 4.50 and 4.51). The figures indicate no differences in their emission spectra in terms of spectral shapes and peak positions. The spectra indicate classic three perylene core emission peaks of electronic transitions ($0 \rightarrow 0$, $0 \rightarrow 1$, and $0 \rightarrow 2$). The spectrum is a mirror image of its corresponding absorption spectrum that was recorded upon microfiltration.

The emission spectra of core 2-decyl-1-tetradecanol substituted perylene dodecyl diimide (PDI-Decanol) in NMP before and after microfiltration were shown in (Figures 4.53 and 4.54). The figures indicate no differences in their emission spectra in terms of spectral shapes and peak positions. The spectra indicate classic three perylene core emission peaks of electronic transitions ($0 \rightarrow 0$, $0 \rightarrow 1$, and $0 \rightarrow 2$). The spectrum is a mirror image of its corresponding absorption spectrum that was recorded after microfiltration.

The emission spectra of core 2-decyl-1-tetradecanol substituted perylene dodecyl diimide (PDI-Decanol) in nonpolar chloroform before and after microfiltration were shown in Figure 4.56. The figures indicate no differences in their emission spectra in terms of spectral shapes and peak positions. The spectra indicate classic three perylene core emission peaks of electronic transitions ($0 \rightarrow 0$, $0 \rightarrow 1$, and $0 \rightarrow 2$). The emission spectrum is a mirror image of its corresponding absorption spectrum.

The emission spectra of core 2-decyl-1-tetradecanol substituted perylene dodecyl diimide (PDI-Decanol) in polar protic ethanol before and after microfiltration were shown in Figures 4.57 and 4.58. The figures indicate no differences in their emission spectra in terms of spectral shapes and peak positions. The spectrum is broader when compared to the emission spectra of PDI-Decanol in other nonpolar and dipolar aprotic solvents. This could be attributed to the possible hydrogen bonding of PDI-Decanol in ethanol.

The emission spectra of core 2-decyl-1-tetradecanol substituted perylene dodecyl diimide (PDI-Decanol) in nonpolar acetone before and after microfiltration were shown in (Figures 4.60 and 4.61). The figures indicate no differences in their emission spectra in terms of spectral shapes and peak positions. The spectra indicate classic three perylene core emission peaks of electronic transitions ($0 \rightarrow 0$, $0 \rightarrow 1$, and $0 \rightarrow 2$). The emission spectrum is a mirror image of its corresponding absorption spectrum.

Chapter 6

CONCLUSION

The bay-substituted (with 2-decyl-1-tetradecanol) perylene dodecyl diimide (PDI-Decanol) was synthesized successfully in three steps. In the first step, bromination at the bay area (at 1,7-positions) of perylene chromophore was carried out by the reaction between perylene dianhydride and bromine to result in brominated dianhydride (BrPDA). In the next step, imidization of anhydride groups of BrPDA was carried out with dodecyl amine to yield brominated perylene diimide (BrPDI). Subsequently, in the final step, the targeted bay-substituted perylene diimide (PDI-Decanol) was synthesized upon substituting 2-decyl-1-tetradecanol at the core positions (1,7-positions) of perylene core.

The final compound was purified and the resulting PDI-Decanol was characterized by FTIR to confirm the functional groups present in the structure. The optical properties of PDI-Decanol were studied through UV-vis and fluorescence measurements. For comparison, photophysics of the intermediate products were studied.

The core substituted PDI-Decanol has shown excellent solubility in most of the commercial organic solvents. This result is attributed to the branched aliphatic chains in the bay-position of the perylene core.

The optical properties of the PDI-Decanol are quite interesting as the bay-substituted diimide has shown weak additional absorption shoulder bands at higher wavelengths in dipolar aprotic (DMF and NMP) and protic solvents (methanol). The additional bands were remained after microfiltering the solution (by 0.2 μm filter) suggesting the absence of aggregation but existence of possible self-assembly due to long and branched alkyl chains at the imide and bay-positions of perylene core, respectively. However, UV-vis absorption spectra of the three synthesized perylene derivatives in nonpolar aprotic solvents show regular characteristic π - π^* absorption bands. Absorption of BrPDA in NMP and BrPDI in DMF show similar (like for PDI-Decanol in DMF and NMP) weak additional shoulder bands at higher wavelengths

Interestingly, the emission spectra of the three perylene derivatives (BrPDA, BrPDI and PDI-Decanol) have shown traditional three characteristic emission peaks in all of the reported organic solvents and were not influenced by additional weak absorption bands.

The future work includes the thermal and electrochemical studies of the synthesized derivatives and their potential toward solar cell applications.

REFERENCES

- 1-Frank Würthner, 2006, Bay-substituted perylene bisimides: Twisted fluorophores for supramolecular chemistry, Universität Würzburg, Institut für Organische Chemie, Am Hubland, 97074 Würzburg, Germany. *Pure Appl. Chem.*, Vol. 78, No. 12, pp. 2341–2349.
- 2- Balakrishnan, K., Datar, A., Naddo, T., Huang, J., Oitker, R., Yen, M., Zhao, J., & Zang, L. (2006). Effect of Side-Chain Substituents on Self-Assembly of Perylene Diimide Molecules: Morphology Control. *J. Am. Chem. Soc.* 128: 7390-7398.
- 3- Brunetti, F. G., Kumar, R., & Wudl, F. (2010). Organic Electronics from Perylene to Organic Photovoltaics: Painting a Brief History with a Broad Brush. *J. Mater. Chem.* 20: 2934-2948.
- 4- Kim, J. Y., Lee, K., Coates, N. E., Moses, D., Nguyen, T. -Q., Dante, M., & Heeger, A. J. (2007). Efficient tandem polymer solar cells fabricated by all-solution processing. *Science*. 317: 222.
- 5- Weil, T., Vosch, T., Hofkens, J., Peneva, K., & Müllen, K. (2010). The Rylene Colorant Family—Tailored Nanoemitters for Photonics Research and Applications. *Angewandte.Chem. Int. Ed.* 49: 9068-9093.
- 6- Albinsson, B., & Martensson, J. (2010). Excitation Energy Transfer in Donor-Bridge-Acceptor Systems. *Phys. Chem. Chem. Phys.* 12: 7338-7351.

- 7- Beckers, E. H. A., Meskers, S. C. J., Schenning, A. P. H. J., Chen, Z., Würthner, F., Marsal, P., Beljonne, D., Cornil, J., & Janssens, R. A. J. (2006). Influence of Intermolecular Orientation on the Photoinduced Charge Transfer Kinetics in Self-Assembled Aggregates of Donor-Acceptor Arrays. *J. Am. Chem. Soc.* 128: 649-657.207
- 8- E.B.Faulkner, & R.J.Schwartz, 2009, High performance pigments, Second revised and expanded ed., Wiley-VCH, Weinheim.
- 9- Wöhrle, D., Kreienhoop, L., Schnurpfeil, G., Elbe, J., Tennigkeit, B., Hiller, S., & Schlettwein, D. (1995). Investigations of n/p-Junction Photovoltaic Cells of Perylene-tetracarboxylic Acid Diimides and Phthalocyanines. *J. Mater. Chem.* 5 : 1819-1829.
- 10- Quante, H., Geerts, Y., & Müllen, K. (1997). Synthesis of Soluble Perylenebisimidine derivatives. Novel Long-Wavelength Absorbing and Fluorescent Dyes. *Chemistry of Materials.* 9: 495-500.202
- 11- Shibano, Y., Umeyama, T., Matano, Y., & Imahori, H. (2007). Electron-Donating Perylene Tetracarboxylic Acids for Dye-Sensitized Solar Cells. *Organic Letters.* 9: 1971-1974.
- 12- Wang, W., Han, J. J., Wang, L. -Q., Li, L. -S., Shaw, W. J. & Li, A. D. Q. (2003). Dynamic π - π Stacked Molecular Assemblies Emit from Green to Red Colors. *Nano Letters.* 3: 455-458.

- 13- Bodapati, J. B., & Icil, H. (2008). Highly Soluble Perylene Diimide and Oligomeric Diimide Dyes Combining Perylene and Hexa(ethylene glycol) Units: Synthesis, Characterization, Optical and Electrochemical Properties. *Dyes and Pigments*. 79: 224-235.
- 14- Bodapati, J. B., & Icil, H. (2006). A New Tunable Light-Emitting and π -Stacked Naphthalene Oligomer: Synthesis, Photophysics and Electrochemical Properties. *Photochemical and Photobiological Sciences*.
- 15- Pasaogullari, N., Icil, H., & Demuth, M. (2006). Symmetrical and Unsymmetrical Perylene Diimides: Their Synthesis, Photophysical and Electrochemical Properties. *Dyes and Pigments*. 69: 118-127.
- 16- Yoney, K., & Icil, H. (2007). Symmetrical and Unsymmetrical Perylene Diimides: Their Synthesis, Photochemical, and Electrochemical Properties of Naphthalene-1,4,5,8-tetracarboxylic acid bis(N,N-bis(2,2,4(2,4,4)-trimethylhexyl)polyimide) and Poly(N,N-bis(2,2,4(2,4,4)-trimethylhexyl)-6,20,3,4,9,10-perylene-tetracarboxydiimide. *European Polymer Journal*. 43: 2308-2320.
- 17- Amiralaei, S., Uzun, D., & Icil, H. (2008). Chiral Substituent Containing Perylene Monoanhydride Monoimide and its Highly Soluble Symmetrical Diimide: Synthesis, Photophysics and Electrochemistry from Dilute Solution to Solid State. *Photochemical and Photobiological Sciences*. 7: 936-947.

- 18- Asir, S., Demir, A. S., & Icil, H. (2009). The Synthesis of Novel, Unsymmetrically Substituted, Chiral Naphthalene and Perylene Diimides: Photophysical, Electrochemical, Chiroptical and Intramolecular Charge Transfer Properties. *Dyes and Pigments*. 84: 1-14.
- 19- Antonello, M., Franceschin, C., Cefaro, S., Borioni, G., Ortaggi, A., & Bianco, 2007, synthesis and optical properties of highly water-soluble perylene derivatives, universita di roma, la sapienza, roma Italy.
- 20- Nwanya, A. C., Ezema, F.I., and Ejikeme, P.M., 2011, dyed sensitized solar cells: A technically and economically alternative concept to p-n junction photovoltaic devices, university of Nigeria mnsukka, Nigeria.
- 21- Frank, V., Stepanenko, Z., Chen, C., R. Saha-Moller, N., Kocher, & D., Stalke, 2004, preparation and characterization of regioisomerically pure 1,7-disubstituted perylene bisimide dyes, university of Wurzburg, Germany.
- 22- Yamashita, Y. (2009). Organic Semiconductors for Organic Field-Effect Transistors. *Science and Technology of Advanced Materials*. 10: 024313.
- 23- Ahrens, M. J., Fuller, M. J., & Wasielewski, M. R. (2003). Cyanated Perylene-3,4-dicarboximides and Perylene-3,4,9,10-bis(dicarboximide): facile Chromophoric Oxidants for Organic Photonics and Electronics. *Chemistry of Materials*. 15: 2684-2686.

- 24- Würthner, F. (2004). Perylene Bisimide Dyes as Versatile Building Blocks for Functional Supramolecular Architectures. *Chemical Communications*.:1564-1579.204
- 25- Qu, J., Zhang, J., Grimsdale, A. C., Millen, K., Jaiser, F., Yang, X., & Neher, D. (2004). Dendronized Perylene Diimide Emitters: Synthesis, Luminescence, and Electron and Energy Transfer Studies. *Macromolecules*.37: 8297-8306. Ph. Sonnet, L. Stauffer, S. Nagarajan, A. Gourdon, Physical Chemistry Chemical Physics 14 (2012) 1700–1705.
- 26- Lee, S., Miller, A. M., Al-Kaysi, R., & Bardeen, C. J. (2006). Using Perylene-Doped Polyme Nanotubes as Fluorescence Sensors. *Nano Letters*. 6: 1420-1424.
- 27- Anthony, J. E., Facchetti, A., Heeney, M., Marder, S. R., & Zhan, X. (2010). *n*-Type Organic Semiconductors in Organic Electronics. *Adv. Mater.* 22: 3876-3892.
- 28- Bevers, S., Schuttle, S., & McLaughlin, L. W. (2000). Naphthalene- and Perylene-Based Linkers for the Stabilization of Hairpin Triplexes. *J. Am. Chem. Soc.* 122:5905-5915.
- 29- Ofir, Y., Zelichenok, A., & Yitzchaik, S. (2006). 1,4;5.8-Naphthalene-tetracarboxylic Diimide Derivatives as Model Compounds for Molecular Layer Epitaxy. *J. Mater. Chem.* 16: 2142-2149.
- 30- Tomizaki, K. -Y., Loewe, R. S., Kirmaier, C., Schwartz, J. K., Retsek, J. L., Bocian, D. F., Holten, D., & Lindsey, J. S. (2002). Synthesis and Photophysical Properties of Light-Harvesting Arrays Comprised of a Porphyrin Bearing Multiple Perylene-Monoimide Accessory Pigments. *J. Org. Chem.* 67:6519-6534.206

- 31- Jones, B. A., Facchetti, A., Wasielewski, M. R., & Marks, T. J. (2007). Tuning Orbital Energetics in Arylene Diimide Semiconductors. Materials Design for Ambient Stability of *n*-type Charge Transport. *J. Am. Chem. Soc.* 129: 15259-15278.
- 32- Fukaminato, T., Tanaka, M., Doi, T., Tamaoki, N., Katayama, T., Mallick, A., Ishibashi, Y., Miyasaka, H., & Irie, M. (2010). Fluorescence Photoswitching of a Diarylethene-Perylenebisimide Dyad Based on Intramolecular Electron Transfer. *Photochemical and Photobiological Sciences.* 9: 181-187.205
- 33- Thelakkat, M., Schmitz, C., & Schmidt, H. -W. (2002). Fully Vapor-Deposited Thin-Layer Titanium Dioxide Solar Cells. *Adv. Mater.* 14: 577.
- 34- Pandey, A. K., Unni, K. N. N., & Nunzi, J. -M. (2006). Pentacene/Perylene Co-Deposited Solar Cells. *Thin Solid Films.* 511-512: 529-532.
- 35- Breeze, A. J., Salomon, A., Ginley, D. S., Gregg, B. A., Tillmann, H., & Hörhold, H. -H. (2002). Polymer-Perylene Diimide Heterojunction Solar Cells. *Applied Physics Letters.* 81: 3085-3087.
- 36- Nakamura, J. -I., Yokoe, C., Murata, K., & Takahashi, K. (2004). Efficient Organic Solar Cells by Penetration of Conjugated Polymers into Perylene Pigments. *J. App. Phys.* 96: 6878-6883.

- 37- Foster, S., Finlayson, C. E., Keivaanidis, P. E., Huang, Y. -S., Hwang, I., Friend, R. H., Otten, M. B. J., Lu, L. -P., Schwartz, E., Nolte, R. J. M., & Rowan, A. E. (2009). Improved Performance of Perylene-Based Photovoltaic Cells Using Polyisocyanopeptide Arrays. *Macromolecules*. 42: 2023-2030.
- 38- Tomizaki, K. -Y., Loewe, R. S., Kirmaier, C., Schwartz, J. K., Retsek, J. L., Bocian, D. F., Holten, D., & Lindsey, J. S. (2002). Synthesis and Photophysical Properties of Light-Harvesting Arrays Comprised of a Porphyrin Bearing Multiple Perylene-Monoimide Accessory Pigments. *J. Org. Chem.* 67:6519-6534.206
- 39- Qu, J., Zhang, J., Grimsdale, A. C., Mllen, K., Jaiser, F., Yang, X., & Neher, D. (2004). Dendronized Perylene Diimide Emitters: Synthesis, Luminescence, and Electron and Energy Transfer Studies. *Macromolecules*. 37: 8297-8306.
- 40- Ofir, Y., Zelichenok, A., & Yitzchaik, S. (2006). 1,4;5.8-Naphthalene-tetracarboxylic Diimide Derivatives as Model Compounds for Molecular Layer Epitaxy. *J. Mater. Chem.* 16: 2142-2149.
- 41- Ishi-i, T., Murakami, K. -I., Imai, Y., & Mataka, S. (2005). Light-Harvesting and Energy Transfer System Based on Self-Assembling Perylene Diimide-Appended Hexaazatriphenylene. *Org. Lett.* 7: 3175-3178.
- 42- Sermet K.,Mahmut K.,& Seraftin D.(2007).electrochemical and optical properties of novel donor-acceptor thiophene-perylene-thiophene polymers, wiely interscience, *department of chemistry faculty of art and science,mugla university ,48000,mugla,turkey*

43- Edvinsson, T., Li, C., Pschirer, N., Schneboom, J., Eickemeyer, F., Sens, R., Boschloo, G., Herrmann, A., Mllen, K., & Hagfeldt, A. (2007). Intramolecular Charge-Transfer Tuning of Perylenes: Spectroscopic Features and Performance in Dye- Sensitized Solar Cells. *The Journal of Physical Chemistry C*. 111: 15137-15140.

44- Sautter, A., Kaleta, B. K., Schmid, D. G, Dobrawa, R., Zimine, M., Jung, G., Stokkum, I. H. M. V., Cola, L. D., Williams, R. M., & Würthner, F. (2005). Ultrafast Energy-Electron Transfer Cascade in a Multichromophoric Light-Harvesting Molecular Square. *J. Am. Chem.Soc.* 127: 6719-6729.

45- Mishra A, Fischer MKR, & Bauerle P, 2009. Metal-free organic dyes for dye-sensitized solar cells: from structure: property relationships to design rules. *Angewandte Chemie-International Edition*; 48(14): 2474–99.

46- Jiawei, J .Liang, & K.Sumathy, 2012, Review on dye sensitized solar cells (DSSCs): Fundamental concepts and novel materials, North Dakota State University, Fargo, USA.